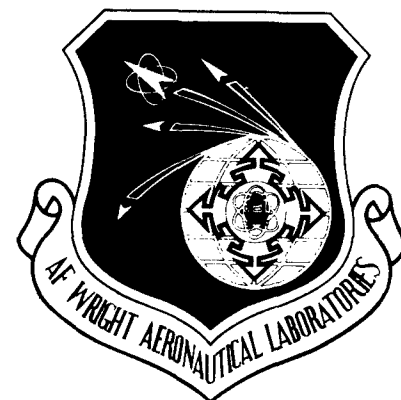


AFWAL-TR-88-4201

ADA201225

A COMPUTATIONAL STUDY OF THE TENSILE AND COMPRESSIVE  
PROPERTIES OF ORDERED POLYMERS VIA THE AUSTIN MODEL 1  
(AM1) SEMI-EMPIRICAL MOLECULAR ORBITAL METHOD



Scott G. Wierschke, 1 Lt, USAF

Polymer Branch  
Nonmetallic Materials Division

October 1988

Final Report for Period April 1987 - March 1988

Approved for Public Release; Distribution Unlimited

MATERIALS LABORATORY  
AIR FORCE WRIGHT AERONAUTICAL LABORATORY  
AIR FORCE SYSTEMS COMMAND  
WRIGHT-PATTERSON AIR FORCE BASE, OHIO 45433-6533

20040219159

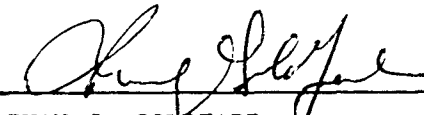
BEST AVAILABLE COPY

## NOTICE

When Government drawings, specifications, or other data are used for any purpose other than in connection with a definitely Government-related procurement, the United States Government incurs no responsibility or any obligation whatsoever. The fact that the Government may have formulated or in any way supplied the said drawings, specifications, or other data, is not to be regarded by implication, or otherwise in any manner construed, as licensing the holder, or any other person or corporation; or as conveying any rights or permission to manufacture, use, or sell any patented invention that may in any way be related thereto.

This report has been reviewed by the Office of Public Affairs (ASD/PA) and is releasable to the National Technical Information Service (NTIS). At NTIS, it will be available to the general public including foreign nations.

This technical report has been reviewed and is approved for publication.

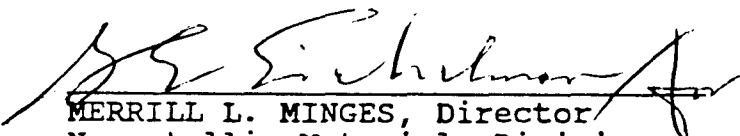


IVAN J. GOLDFARB  
Project Scientist  
Nonmetallic Materials Division



R. L. VAN DEUSEN, Chief  
Polymer Branch  
Nonmetallic Materials Division

FOR THE COMMANDER



MERRILL L. MINGES, Director  
Nonmetallic Materials Division

If your address has changed, if you wish to be removed from our mailing list, or if the addressee is no longer employed by your organization, please notify AFWAL/MLBP, Wright-Patterson AFB, OH 45433-6533, to help us maintain a current mailing list.

Copies of this report should not be returned unless return is required by security considerations, contractual obligations, or notice on a specific document.

# REPORT DOCUMENTATION PAGE

Form Approved  
OMB No. 0704-0188

1a. REPORT SECURITY CLASSIFICATION Unclassified			1b. RESTRICTIVE MARKINGS	
2a. SECURITY CLASSIFICATION AUTHORITY			3. DISTRIBUTION/AVAILABILITY OF REPORT Approved for public release; distribution unlimited	
2b. DECLASSIFICATION/DOWNGRADING SCHEDULE				
4. PERFORMING ORGANIZATION REPORT NUMBER(S) AFWAL-TR-88-4201			5. MONITORING ORGANIZATION REPORT NUMBER(S)	
6a. NAME OF PERFORMING ORGANIZATION Materials Lab, AFWAL, AFSC		6b. OFFICE SYMBOL (if applicable) AFWAL/MLBP	7a. NAME OF MONITORING ORGANIZATION	
6c. ADDRESS (City, State, and ZIP Code) Wright-Patterson Air Force Base, Ohio 45433			7b. ADDRESS (City, State, and ZIP Code)	
8a. NAME OF FUNDING/SPONSORING ORGANIZATION Same as 6a		8b. OFFICE SYMBOL (if applicable)	9. PROCUREMENT INSTRUMENT IDENTIFICATION NUMBER	
8c. ADDRESS (City, State, and ZIP Code)			10. SOURCE OF FUNDING NUMBERS	
			PROGRAM ELEMENT NO. 61102F	PROJECT NO. 2303
			TASK NO. 03	WORK UNIT ACCESSION NO. 07
11. TITLE (Include Security Classification) A Computational Study of the Tensile and Compressive Properties of Ordered Polymers via the Austin Model I (AM1) Semi-empirical Molecular Orbital Method				
12. PERSONAL AUTHOR(S) 1Lt S. G. Wierschke				
13a. TYPE OF REPORT Final		13b. TIME COVERED FROM Apr 87 TO Mar 88	14. DATE OF REPORT (Year, Month, Day) October 1988	15. PAGE COUNT 134
16. SUPPLEMENTARY NOTATION				
17. COSATI CODES			18. SUBJECT TERMS (Continue on reverse if necessary and identify by block number)	
FIELD	GROUP	SUB-GROUP	Polymers, Molecular Orbital, Compressive Properties, Tensile Properties, Ordered Polymers, Computational Chemistry, Molecular Modeling, Modulus, MOPAC	
07	04			
11	04			
19. ABSTRACT (Continue on reverse if necessary and identify by block number) The Austin Model 1 (AM1) semi-empirical molecular orbital method has been used to calculate tensile moduli and molecular tensile and compressive deformations for several ordered polymers and a graphite model. The calculated moduli are an improvement over previous Modified Neglect of Differential Overlap (MNDO) calculations. These moduli are the ultimate moduli for the perfectly aligned bulk systems. By analyzing the deformation of polymer molecules in tension and compression, the failure modes and weak points in the molecules can be determined. In compression, all the heterocyclic rigid rod polymers exhibit a "bending" failure mode. In tension and compression, the phenyl group in the rods is deformed more easily than the heterocyclic moiety, thus causing a lowering of the modulus. The hypothetical "ladder" polymer, polyacene, shows more tensile and compressive resistance than any of the rods, suggesting that further study into ladder polymers is warranted.				
20. DISTRIBUTION/AVAILABILITY OF ABSTRACT <input type="checkbox"/> UNCLASSIFIED/UNLIMITED <input checked="" type="checkbox"/> SAME AS RPT. <input type="checkbox"/> DTIC USERS			21. ABSTRACT SECURITY CLASSIFICATION Unclassified	
22a. NAME OF RESPONSIBLE INDIVIDUAL 1Lt S. G. Wierschke			22b. TELEPHONE (Include Area Code) 513-255-9146	22c. OFFICE SYMBOL AFWAL/MLBP

## FOREWORD

This report was prepared by the Polymer Branch, Nonmetallic Materials Division. The work was initiated under Project No. 2303, "Research to Define the Structure Property Relationships," Task No. 2303Q3, Work Unit Directive 2303Q307, "Structure Resins." During the period of April 1987 to March 1988 the work was administered under the direction of the Materials Laboratory (ML), Air Force Wright Aeronautical Laboratories (AFWAL), Air Force Systems Command (AFSC), Wright-Patterson Air Force Base, Ohio, 45433-6533 with Dr. I. J. Goldfarb as the ML Project Scientist. The report was released by the author 1Lt Scott G. Wierschke, Air Force Wright Aeronautical Laboratories, Materials Laboratory, Polymer Branch (AFWAL/MLBP) in August 1988.

## TABLE OF CONTENTS

Section	Page
I INTRODUCTION . . . . .	1
II HISTORICAL . . . . .	10
Computational Chemistry . . . . .	10
Molecular Mechanics . . . . .	12
Ab Initio Molecular Orbital Theory . . . . .	27
Semiempirical Molecular Orbital Theory . . . . .	43
Ordered Polymers . . . . .	51
Poly(p-phenylenebenzobisimidazole) (PBI) . . . . .	52
Poly(p-phenylenebenzobisoxazole) (PBO) . . . . .	54
Poly(p-phenylenebenzobisthiazole) (PBT) . . . . .	55
Poly(p-phenylenepyromellitimide) (PPPI) . . . . .	56
Poly(p-phenylene-2,6-quinoline) (PQ) . . . . .	57
Poly(p-phenylene) (PPP) . . . . .	57
Benzimidazoisquinoline (BBL) . . . . .	58
Polyacene . . . . .	59
Graphite . . . . .	60
III COMPUTATIONAL DETAILS . . . . .	61
Calculation Mechanics . . . . .	61
Geometry Input: Building a Z-Matrix . . . . .	64
Polymer Unit Cell Setup and Manipulation . . . . .	70
Tensile Modulus Calculations . . . . .	73
IV RESULTS AND DISCUSSION . . . . .	77
General . . . . .	77

## TABLE OF CONTENTS (CONTINUED)

Tensile Modulus Results . . . . .	78
Molecular Deformation Analysis . . . . .	85
Cis-Poly(p-phenylenebenzobisimidazole) (cis-PBI) . . . . .	87
Cis-Poly(p-phenylenebenzobisoxazole) (cis-PBO) . . . . .	96
Remaining Polymers (t-PBT, PPPI, PPP, PQ, Polyacene)	103
Examination of Results . . . . .	110
Conclusions . . . . .	114
 V FUTURE DIRECTIONS . . . . .	 116
Solid State Calculations . . . . .	116
Solution Phase Studies . . . . .	117
 REFERENCES . . . . .	 118

## LIST OF FIGURES

Figure	Page
1. The Rigid Rod Polymers (i) PBO and (ii) PBT . . .	8
2. Force Types . . . . .	15
3. Morse Potential curve . . . . .	16
4. Hooke's Law Potential Superimposed on Morse Curve	17
5. Comparison of Morse, Harmonic, and Cubic Curves .	18
6. Newton-Raphson Minimization of a Function . . . .	21
7. Schematic of Steric to Strain Energy Calculation	23
8. Flow Chart of Molecular Mechanics Program . . . .	25
9. Radial Dependence of STO and GTO Functions . . .	38
10. Schematic of Split Valence Orbitals . . . . .	40
11. Number of Functions per Atom per Basis Set . . .	41
12. Available MINDO/3 Parameters . . . . .	47
13. Structure of Cis- and Trans-PBI . . . . .	53
14. Cis- and Trans-PBO Structures . . . . .	54
15. Structures of Cis- and Trans-PBT . . . . .	55
16. Structure of PPPI . . . . .	56
17. Structure of PQ . . . . .	57
18. Structure of PPP . . . . .	58
19. Structure of BBL . . . . .	58
20. Structure of Polyacene . . . . .	59

# LIST OF FIGURES (CONTINUED)

21.	Graphite Structure . . . . .	60
22.	Flow Charts for (a) ab initio and (b) MOPAC . . .	63
23.	Z-Matrix Variables . . . . .	66
24.	Methanol Structure . . . . .	66
25.	Methanol after 1st three atoms . . . . .	68
26.	Neuman Projection of H5 and H6 Dihedral Angles .	69
27.	Piece of Polyethylene Cluster . . . . .	71
28.	Trans-PBT Unit Cell with Translation Vector . . .	72
29.	Polyethylene K versus True Strain [31] . . . . .	76
30.	Orientations of a Phenyl Group on a Tension Axis	83
31.	Graphite Repeat Unit . . . . .	84
32.	Cis-PBI at Four Points Along Energy-Strain Curve	87
33.	Cis-PBI Energy vs Strain (-3 to +15%) Curve . . .	88
34.	C-C Strain vs Cis-PBI Tension . . . . .	90
35.	Phenyl Strain vs Cis-PBI Tension . . . . .	90
36.	Benzimidazole Strain vs Cis-PBI Tension . . . . .	91
37.	Torsion Angle vs Cis-PBI Tension . . . . .	91
38.	C-C Length vs Cis-PBI Compression . . . . .	93
39.	Phenyl Length vs Cis-PBI Compression . . . . .	93
40.	Benzimidazole Length vs Cis-PBI Compression . . .	94
41.	Torsion Angle vs Cis-PBI Compression . . . . .	94
42.	Colinearity Angle vs Cis-PBI Compression . . . .	95
43.	Cis-PBO Four Points Along Energy-Strain Curve . .	97
44.	Cis-PBO Energy vs Strain (-3 to +15%) Curve . . .	98



# LIST OF FIGURES (CONTINUED)

45.	C-C Length vs Cis-PBO Tension . . . . .	98
46.	Phenyl Length vs Cis-PBO Tension . . . . .	99
47.	Benzoxazole Length vs Cis-PBO Tension . . . . .	99
48.	Torsion Angle vs Cis-PBO Tension . . . . .	100
49.	C-C Length vs Cis-PBO Compression . . . . .	100
50.	Phenyl Length vs Cis-PBO Compression . . . . .	101
51.	Benzoxazole Length vs Cis-PBO Compression . . . . .	101
52.	Torsion Angle vs Cis-PBO Compression . . . . .	102
53.	Colinearity Angle vs Cis-PBO Compression . . . . .	102
54.	Trans-PBT Four Points Along Energy-Strain Curve .	104
55.	PPPI Four Points Along Energy-Strain Curve . . .	105
56.	PQ Four Points Along Energy-Strain Curve . . . .	106
57.	PPP Three Points Along Energy-Strain Curve . . .	107
58.	Polyacene Three Points Along Energy-Strain Curve	108

## LIST OF TABLES

Table	Page
1. Tensile Modulus Results . . . . .	78
2. Comparison of AM1, MNDO, and Experimental Moduli	80
3. Tensile Results . . . . .	109
4. Compressive Results . . . . .	110

## SECTION I

### INTRODUCTION

The more progress physical sciences make, the more they tend to enter the domain of mathematics, which is a kind of centre to which they all converge. We may even judge the degree of perfection a science has arrived by the facility with which it may be submitted to calculation [1].

Adolphe Quetelet 1796-1874

Adolphe Quetelet's words turned out to be prophetic with regard to chemistry and physics when, in 1925, Schrödinger formulated his famous equation upon which quantum mechanics is based [2]. With the solution to this differential equation in hand, one could quantitatively predict, in principle, most, if not all, chemical phenomena using only Planck's constant, the velocity of light, and the masses and charges of nuclei and the electron [3]. This meant, experimentally useful measurements could now be made without doing the experiments! Quantities that were difficult, or impossible, to obtain experimentally could now be obtained by simply solving a differential equation.

However, as is usually the case, it didn't turn out to be quite that easy. Solving the Schrödinger equation involves extremely complex mathematics which are completely solvable only for the isolated hydrogen atom. Even after massive mathematical approximation, the computations

necessary to calculate interesting molecular properties for any system of real interest were far too complicated to do by hand.

Theoreticians tried to develop methods to make hand-worked solutions possible. The Huckel qualitative molecular orbital approximation [4], formulated in the early 1930's, provided useful information about the pi electrons of planar conjugated systems and approximate solutions that could be hand calculated for molecules as large as benzene and naphthalene (although these are a bit tedious) [5]. The first vestiges of molecular mechanics, a method which circumvents the computational problems of the Schrödinger equation by using classical mechanics instead of quantum theory, appeared in 1930 [6] and 1946 [7,8,9]. Although these methods reduced the amount of complex math needed, the computations were still too laborious and the results not quite quantitatively accurate enough to make chemistry by computation popular. It would take great advances in technology, the invention of the computer, to bring computational chemistry into its own as a science.

With the advent of computers in the 1950's, it became possible to do massive amounts of computations quickly. Naturally, those previously disgruntled quantum chemists scrambled to develop computer algorithms to obtain the elusive solution to Schrödinger's equation. Better

approximations and more terms could now be included in the calculation giving more accurate solutions and, with higher computing power, allowing work on larger, more interesting systems. One of these early algorithms, the Pariser-Parr-Pople method [10], provides quick computations of  $\pi$  electrons and is still used quite extensively in the dye industry to predict color in prospective dye molecules.

As computer hardware has advanced, so have chemical computation algorithms. There are now computer programs, running on supercomputers, that can do calculations on up to ten heavy atoms using rigorous quantum theory (*ab initio* methods), over one hundred atoms using a parameterized approximation to quantum theory (*semiempirical* methods), and into thousands of atoms using molecular mechanics. So, today the computational chemist can finally study systems of interest to the conventional chemist. The question is, what information do the calculations really provide?

Probably the most obvious results of chemical calculations are molecular structures and energies, somewhat analogous to results obtainable with nuclear magnetic resonance (NMR) spectroscopy. These results just scratch the surface of the capabilities of chemical calculations. What experiment can give the molecular structure, heat of formation, dipole moment, ionization potentials, charge densities, bond orders, orbital energies, and so on?

Experiments that can measure any one of these properties are difficult and their accuracies sometimes suspect. An experiment giving all these properties is almost inconceivable. The most exciting feature, however, is that the molecule to be studied does not have to really exist! Property predictions can be made on proposed molecules prior to their synthesis. Obviously, the accuracy of the calculations is the main objection, however the strengths and weaknesses of all the common methods are well known and documented, so good estimates of their accuracy can be made. The accuracy of computations is continually improving, so that today there are cases in which the error in the calculations is less than that of the corresponding experiment. As time goes on this will become more and more common and more and more confidence will be placed in computational results.

Today, chemical computations provide new insights into all sorts of chemical and structural problems. In most cases the calculations give data, both numerical and graphical, which would be difficult or impossible to obtain with any experimental method. The effect of silyl groups in stabilizing carbocations in positions alpha and beta to the positive charge has been studied with ab initio methods, for example [11]. The same methods have also been applied to the study and elucidation of organic reaction mechanisms [12].

where the structures and energies of reactants, intermediates, transition states, and products are determined and heats of reaction, complexation energies, and activation barriers are calculated. Semiempirical methods have been used to study processes at the active sites of enzymes [13], while molecular mechanics approaches are quite common in the study of protein structure [14], conformational analysis [15], and drug design [16]. There have even been calculations done on inorganic systems like semiconductors and metals using an extended Huckel method [17].

The scope of problems investigated with computations is large, from inorganic, analytical, and gas phase organic chemistry to biochemistry and solution phase organic chemistry [12]. One very important area that hasn't yet received sufficient attention from the computational chemistry community is organic polymer science.

There are a few reasons why organic polymers have been a relatively infrequent topic in the computational literature. First is the nature of polymer systems themselves. Typical polymer molecules are huge, with molecular weights in the millions in some cases, making computations on a complete polymer molecule impossible with quantum methods. Also, since polymers can have large molecular weight distributions [18], the complete calculation of any one molecule may not represent the molecular properties of the whole system.

Secondly, the vast majority of organic polymer work is done in industry, so although extensive computational work has been and is being done on polymers, most of that work is proprietary to industry and therefore not published in the chemical literature.

Probably the biggest reason why computational methods have not been widely applied to polymer problems is that polymer chemists need to know different things about their systems than the average chemist or biochemist, i.e. they ask different questions. For an organic chemist, a reaction's activation energy barrier is extremely useful information [12]. For the drug designer, the amount of energy required to distort a potential drug molecule to fit into an enzyme's active site is also very important [16]. These numbers are direct results of the calculations and are directly applicable to the problems at hand. Although such molecular properties are interesting to polymer scientists, they care more about the material's bulk properties. Properties like density, glass transition temperature ( $T_g$ ), and elastic tensile modulus don't come directly from chemical computations, so calculations haven't become major tools in polymer study.

There has been, of course, published computational work done on polymers. Most of it has dealt with conformational analysis of units of single polymer chains [19,20,21,22,23],



or how modifications on a chain affect the possible conformations of the chain [24,25]. Other studies have analyzed orders of protonation of polymer units [26], and theoretical electronic band structures to determine if a polymer is capable of conducting electricity or light [27,28,29]. There have been few applications of quantum theory or molecular mechanics to the prediction of bulk polymer properties, including tensile modulus and compressive strength.

Good tensile and compressive properties are very important in the development of light-weight, high-strength structural polymers. The ability to predict these properties would serve two purposes: (1) the properties could be calculated prior to the synthesis of the polymer, saving wasted preparation time if the properties are poor; and (2) the calculated properties would serve as the "ultimate" values, giving polymer processing scientists a number to shoot for while improving their processing techniques. A new technique has been developed, using semiempirical molecular orbital methods, at the F. J. Seiler Research Laboratory, U. S. Air Force Academy, for calculating energy properties of polymers, using a "cluster" method [30], and obtaining polymer elastic moduli [31]. These procedures can be modified to allow the study of polymers in compression as well as in tension.

This new technique comes at an ideal time to help solve a distressing problem in the science of high-performance ordered polymers. The ordered polymers poly(paraphenylene benzobisoxazole) (PBO) and poly(paraphenylene benzobisthiazole) (PBZT) have a rigid rod-like structures (Figure 1) and exhibit tensile moduli 50-100% higher than high performance polyethylene fibers [32]. This makes these

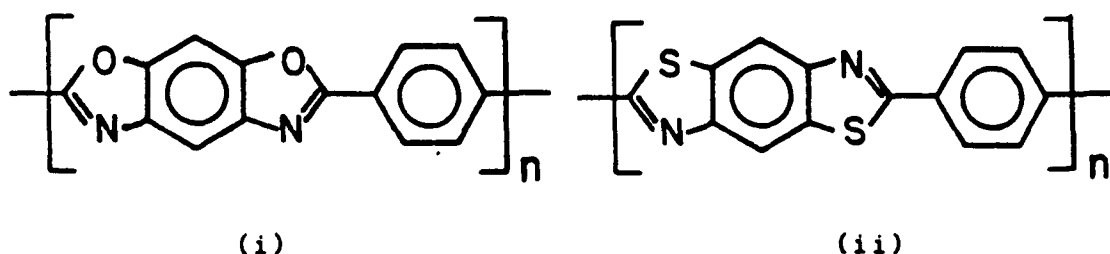


Figure 1. The rigid rod polymers (i) PBO and (ii) PBZT

polymers good candidates for use as aircraft structural materials. However, both these systems undergo failure at compressive loads too low to be useful in airframe structures [33]. This has prompted great efforts to improve the compressive strength of these polymers [34] and to develop other ordered polymers with higher compressive strengths [35]. Many routes are being examined to solve this problem including synthetic and processing approaches [36]. What is missing from all these approaches is a fundamental

understanding of what polymer tensile and compressive phenomena are and how these phenomena translate to the molecular level.

The objectives of this research are, therefore, (1) to use this newly developed, semiempirically based technique to calculate the theoretical tensile moduli of several known and unknown rigid rod and ladder type polymers; (2) to use semiempirical molecular orbital theory to analyze and understand tension in these systems; and (3) to use these methods to analyze and understand compressive phenomena in ordered polymers.

## SECTION II

### HISTORICAL

#### Computational Chemistry

The underlying physical laws necessary for the mathematical theory of a large part of physics and the whole of chemistry are thus completely known, and the difficulty is only that the exact application of these laws leads to equations much too complicated to be soluble [37].

P.A.M. Dirac 1902-1984

As stated earlier, and reiterated by Dirac, the Schrödinger differential equation is too complex to be solved exactly. So, as was also stated earlier, several mathematical techniques, and corresponding computer algorithms, have been developed to solve the equation approximately. Computational chemists are constantly developing new, faster, and more accurate algorithms for cracking the Schrödinger equation. In fact, this is what separates a purely theoretical chemist from a computational chemist. Theoretical chemists develop new ideas and models to describe chemical phenomena, they formulate equations, and develop, or modify, theories in an attempt to describe chemical and physical phenomena mathematically. Schrödinger, Bohr, Dirac, and de Broglie might be considered theoretical

chemists, although they would have probably winced at being thought of as chemists.

A computational chemist's job is not to develop new theories, but to take existing chemical theory and put it to practical use. The computationalist, being extremely well versed in theory, develops methods (computer algorithms these days) to get the best possible answers out of the stubborn theory and puts them to work on real chemical problems. Occasionally the computational chemist's work reveals deficiencies in the theory and initiates changes in the model. In a way, computational chemists might be considered "theoretical technicians."

Whether or not conventional physical or organic chemists realize that a study is computational and not theoretical is completely irrelevant if they don't understand the work itself. The work is meaningless if experimentalists can't (by reading the paper): (1) get a general understanding of the method used, along with its strengths and weaknesses; (2) understand how and why the method was applied to the problem at hand; and (3) understand and use the results obtained from the work. Many chemists are needlessly intimidated by chemical computations because the basic concepts haven't been explained to them in a clear manner. This attitude is proliferated by some computational chemists who fail to adequately explain mathematical techniques and

jargon that may be easily understood by other computationalists but make the field a confusing mystery to conventional chemists. This is inexcusable since the goal of computational chemistry is to understand the experimentally measurable world via nonexperimental methods.

To avoid this problem, the following sections provide a brief historical and technical background on the most commonly used computational methods: molecular mechanics, ab initio molecular orbital theory, and semiempirical molecular orbital theory. This is not intended to be a comprehensive review, but rather a quick guide to understanding the methods available and the reasons for the selection of the method used in this research. For a more comprehensive treatment, see [38].

### Molecular Mechanics

The molecular mechanics method for calculating molecular geometries and energies is sometimes referred to as the empirical or force field method. This technique, unlike the molecular orbital methods to be discussed later, is not based on quantum mechanics. It employs the ideas of classical mechanics and requires no complex math beyond the calculation of second derivatives. The method is a mathematical extension of accepted ideas of bonds between

atoms in molecules, and van der Waals forces between nonbonded atoms, coupled with the fundamentals of vibrational spectroscopy. "The basic idea is that bonds have 'natural' lengths and angles, and molecules will adjust their geometries so as to take up these values in simple cases. In addition, steric interactions are included using van der Waals potential (energy) functions. In more strained systems, the molecules will deform in predictable ways with 'strain' energies that can be accurately calculated [38]."

To put it very simply, molecular mechanics treats a molecule with a "ball" and "spring" model. The "balls" represent the atoms in a molecule. the "springs" connect the atoms and represent all the forces between atoms in a molecule including bonding forces, bond angle bending forces, bond torsion forces, nonbonded (or van der Waals) forces, and other forces. All of these "springs" have certain Hooke's Law-like (equation 1) force constants governing the amount of potential energy contained in the

$$V = k(r - r_0)^2/2 \quad (\text{equation 1})$$

$V$  = potential energy

$k$  = spring force constant

$r$  = spring length

$r_0$  = equilibrium spring length

'springs.' The 'springs', having different constants representing different forces, 'stretch', 'compress', 'bend', and 'twist' in such a way as to make the sum of the potential energy contained in all the 'springs' a minimum with respect to the positions of the 'balls.' The sum of all forces within the molecule is brought to zero or, in other words, a 'stationary point' is found for the molecule.

In more accurate and scientific terms, molecular mechanics treats a molecule as an array of atom types ( $sp^3$  carbon is a different type than  $sp^2$  carbon) whose atomic motions are governed by an empirically derived set of classical-mechanical potential energy functions. This set of potential energy functions, referred to as a 'force field', contains variable parameters (like force constants and equilibrium values) which are adjusted to give the best fit of experimentally determined molecular properties like geometries and heats of formation. In this model, bond lengths, bond angles, torsional angles, and nonbonded atomic distances adjust themselves during the geometry optimization procedure (this will be explained later) to minimize the total potential energy of the molecule and bring the sum of the atomic forces to near zero. From this calculation one can get good values of molecular properties for which the force field was parameterized.

The two most vital parts of any molecular mechanics



calculation are (1) the potential energy functions used, and (2) the parameters used in these functions. A potential energy function, simply called a potential function, is simply a function where potential energy rises and falls with the variation of a parameter such as bond length or bond angle. In most molecular mechanics programs there are potential functions for (Figure 2) bond, bond angle, torsion angle, 1-3 van der Waals interaction, and 1-4 van der Waals

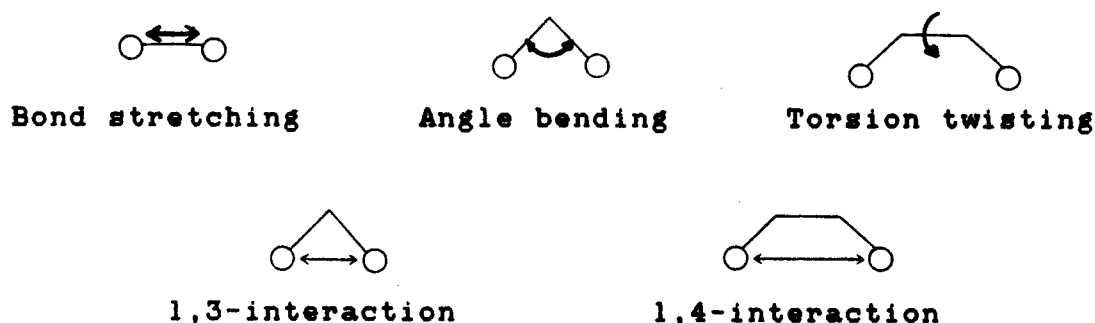


Figure 2. Force types

interaction forces. Since all of these different types of potential functions are developed in a similar manner, only the development of the bond-stretching potential function will be discussed in depth here.

The potential between any two atoms at any interatomic distance,  $r$ , is described by the familiar Morse curve (Figure 3), representing the van der Waals energy function. Energy drops rather slowly as the two atoms approach from

infinity. It falls more quickly as  $r$  gets closer to  $r_e$ , the

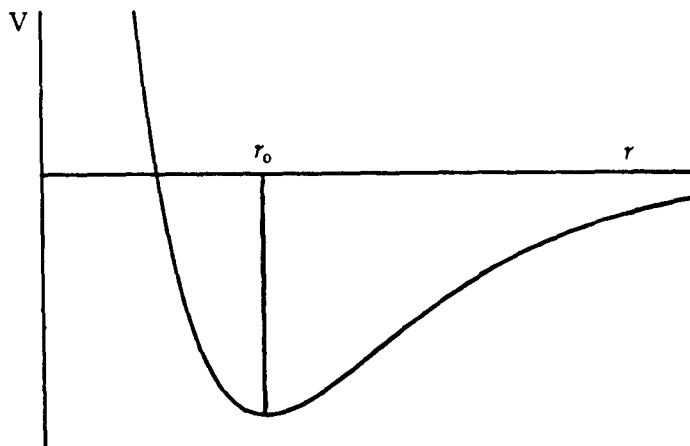


Figure 3. Morse potential curve

equilibrium bond length, where the energy minimum occurs. The potential rises rapidly as the atoms are pushed together closer than  $r_e$ . With the expression for the Morse potential in hand, the exact potential energy can be easily calculated for the bond and (if exact potentials for the other interactions are included) the exact energy minimum for the entire molecule is accessible. However, as was true for the Schrödinger equation, it's not quite that easy. The expression for a Morse curve is extremely complicated and takes too much computer time to evaluate, so, as usual, approximations must be made.

Fortunately, most molecules have bond lengths that fall within a fairly small range. Figure 4 shows the Morse curve

(solid line) with this typical bond length range shaded. Superimposed on the Morse curve is a simple Hooke's Law, or harmonic, potential (dashed line) which gives a good fit to

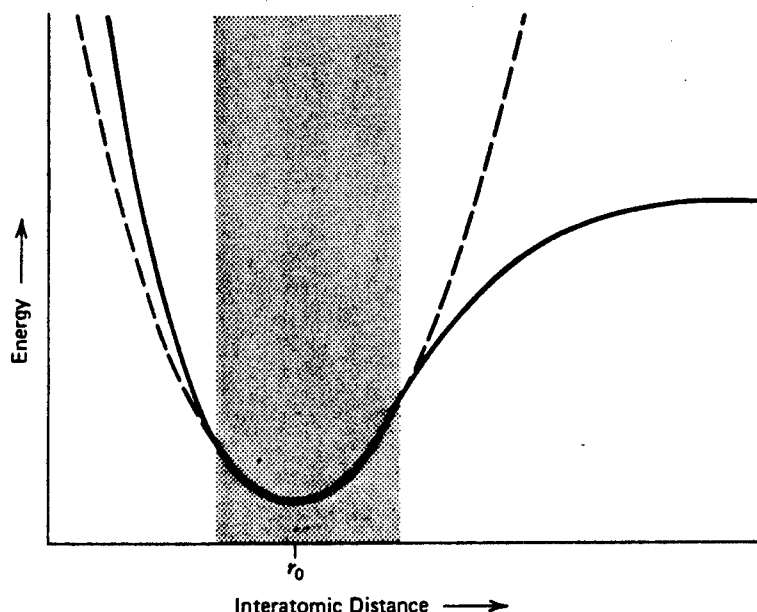


Figure 4. Hooke's law potential superimposed on Morse Curve

the realistic potential in the normal bond range. Using this potential makes the energy calculations simple and fast and allows very large molecules, i.e. proteins, to be calculated on computers. One problem that may occur is an inaccuracy of energies for molecules with unusually long bond lengths, where the harmonic potential doesn't fit the Morse curve. To give a better fit to the energy curve for moderately longer bond lengths, a cubic term is added to the potential function near the end of the geometry optimization. The potential function thus becomes:

$$V = k(r - r_0)^2/2 + k'(r - r_0)^3 \quad (\text{equation 2})$$

where  $k'$  is a constant for the cubic term. Figure 5 shows the Morse curve (solid line), the harmonic potential (long dashes), and the harmonic potential with the cubic term added (short dashes). The addition of the cubic term improves the fit in the region around  $r_0$  and broadens the

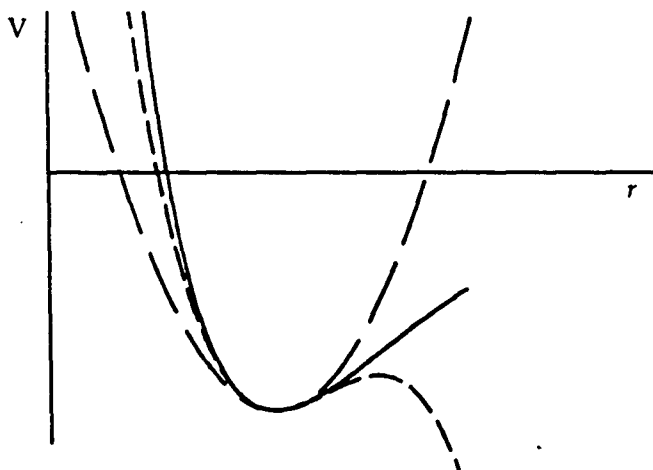


Figure 5. Comparison of Morse, harmonic, and cubic curves

region of accuracy for the energy. This term is usually not applied until the geometry is very nearly optimized. If it were applied when  $r$  is too large the final energy would be far too low since that function sinks below the real minimum at large  $r$  (figure 5), i.e. the molecule would fly apart. In essence, terms are added and/or modified to get the best fit to the real potential in a reasonable amount of computer

time. The angle bending, torsion and van der Waals potentials are approached in a similar manner. The real potentials may be a little more complicated and the approximations may differ (the 1-3, 1-4 interaction potentials use 6th, 12th and even exponentially powered terms), but the idea is to fit a computationally practical function to the chemically useful region of the real energy curve.

The parameters, i.e.  $k$ 's and  $r_e$ 's, are what really make the potential functions useful or useless. These parameters are determined from experimental data. Force constants are typically derived from vibrational spectra while bond lengths, bond angles, and torsion angles typically come from x-ray or electron diffraction studies of molecular structure. The problem here is that these different methods give different values for these variables. To combat this problem the consistent force field method [39] is used. Experimental parameters which have a mean value calculated from several compounds with the same types of bonds, angles, etc., are placed in their respective potential functions and used in a calculation. The derivatives of the properties desired (usually energy) with respect to the parameters are taken. This gives improvement factors to be added to or subtracted from the original parameters, giving new and improved parameters. These are put back into the calculation

and the procedure repeated. When the derivatives are zero (actually as near zero as one feels is necessary), the procedure is finished and a set of parameters that has been linearly least-squares fitted to the potential curve is the result. So now both the potential function and its parameters have been optimized to fit the experimental data.

Before continuing, a brief explanation of what a 'geometry optimization' entails is in order. When a molecule is 'optimized' it goes through a procedure which adjusts all of its geometric variables in such a way as to bring the molecule to a minimum energy conformation. This is done by similar methods in most all types of chemical calculations, i.e. molecular mechanics, ab initio and semiempirical; the specific formalisms may differ but the basic ideas are the same. Figure 6 explains the minimization of a function,  $f(x)$ , by one of the most common optimization methods, the Newton-Raphson technique [40]. The initial value of  $x$  is  $x_0$ . The first derivative of  $f(x)$  produces the  $f'(x)$  function. The second derivative of  $f$  at  $x_0$ ,  $f''(x_0)$ , produces a line tangent to the  $f'(x)$  curve which intersects the  $x$ -axis at  $x_1$ . This  $x$ -value is closer to the true minimum  $x$  than  $x_0$ . The procedure is repeated for  $x_1$  yielding  $x_2$ . The procedure is repeated until a value satisfactorily close to  $x$  is obtained (the exact  $x$  is never really obtained). In an energy minimization, or geometry

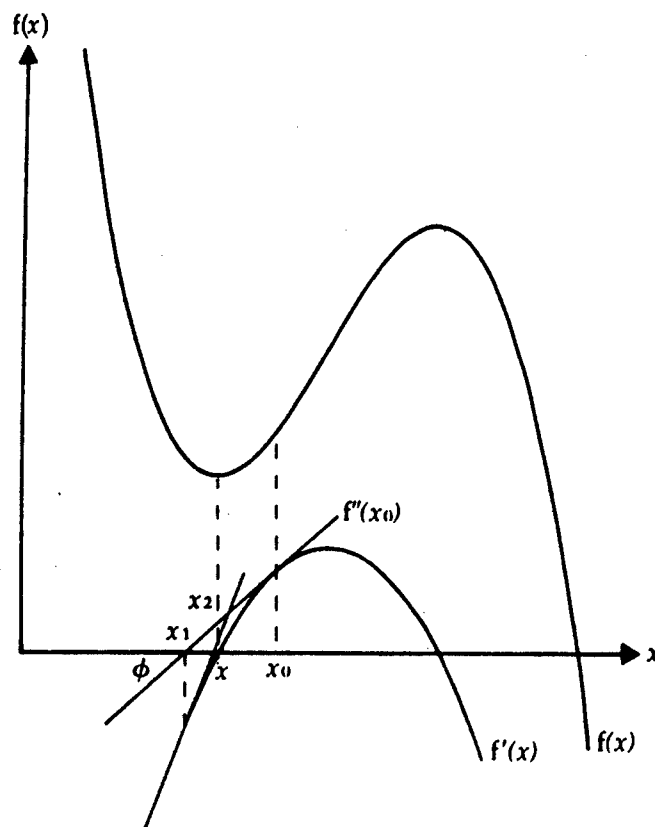


Figure 6. Newton-Raphson minimization of a function

optimization,  $f(x)$  is a potential function and the derivatives are taken of energy with respect to each geometric variable and each variable is adjusted from step to step. When the change in energy from one iteration to the next, the sum of all the variable adjustments between two successive steps, and the largest adjustment in any one variable in the molecule are all below certain specified values, the optimization criteria, the geometry is optimized. The optimization criteria can be as stringent as desired, but

too stringent criteria may give small improvements to the optimized values at a huge cost in computer time over less rigid criteria.

Up to this point only one-dimensional potential curves have been discussed in depth. The energy expression for a molecule is the sum of the potentials of all the geometric variables in the molecule:

$$V_{tot} = \Sigma V_{stretch} + \Sigma V_{bend} + \Sigma V_{torsion} + \Sigma V_{vaw} \quad (\text{equation 3})$$

This expression represents, not a curve, but a multi-dimensional potential surface.  $V_{tot}$  is referred to as the molecule's steric energy; its only usefulness by itself is in comparing the energies of geometric isomers. There are several energy minima on this potential surface, the minimum nearest the starting geometry will be found in a geometry optimization. By probing around the potential surface with carefully chosen geometries, the different minima, along with the energy barriers between them, can be found.

Since molecular mechanics is parameterized by fitting to experimental data, it can be set up to accurately reproduce any property for which there is experimental data available. The most popular molecular mechanics program, Allinger's MMP2 [41], is parameterized to give accurate geometries and energies. The molecule's dipole moment can



be calculated from its geometry and the heat of formation is computed from the steric energy and the sum of all the bond formation energies (which are also a consequence of the calculation). The molecule's strain energy can then be calculated from the heat of formation. Strain energy is the difference between the heat of formation of the molecule and that of a hypothetical strain-free molecule with the all the same groups. The heats of formation of these groups of atoms are precalculated in a strain-free environment, these are called the strain-free increments. These increments are added together to give the strain-free heat of formation for the molecule which is subtracted from the calculated heat of formation to get the strain energy. Figure 7 shows the

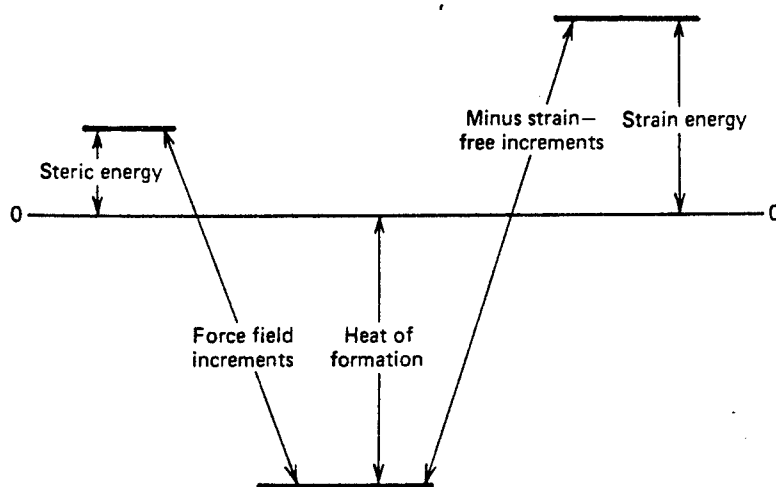


Figure 7. Schematic of steric to strain energy calculation

process to get from steric energy to strain energy schematically.

Figure 8 is a flow chart of a general molecular mechanics program. Geometric data, either internal coordinates (i.e. bond lengths, bond angles, and torsion angles), cartesian coordinates or crystal coordinates, are input into the program, along with atom connectivity information. The program goes through the input and determines what interactions occur in the molecule and selects the right potential functions to describe these interactions. The program selects the necessary parameters, which may be altered by the user if desired, and performs the geometry optimization/energy minimization. When the final geometry and energy are obtained, the thermodynamic functions, heat of formation, and any other properties that were fitted in the parameterization can be calculated.

Molecular mechanics is the best computational method for calculating geometries and heats of formation for the types of systems for which it has been parameterized. This shouldn't be surprising since the method is fit to these properties. If it didn't reproduce these values accurately the program would be reworked so that it did. Therein lies the biggest problem with the molecular mechanics technique, its dependence on experimental data. The program has been parameterized with a certain set of compounds, mainly hydrocarbons, ethers, alcohols, and some carbonyl compounds, and the parameters are assumed to be transferable to other

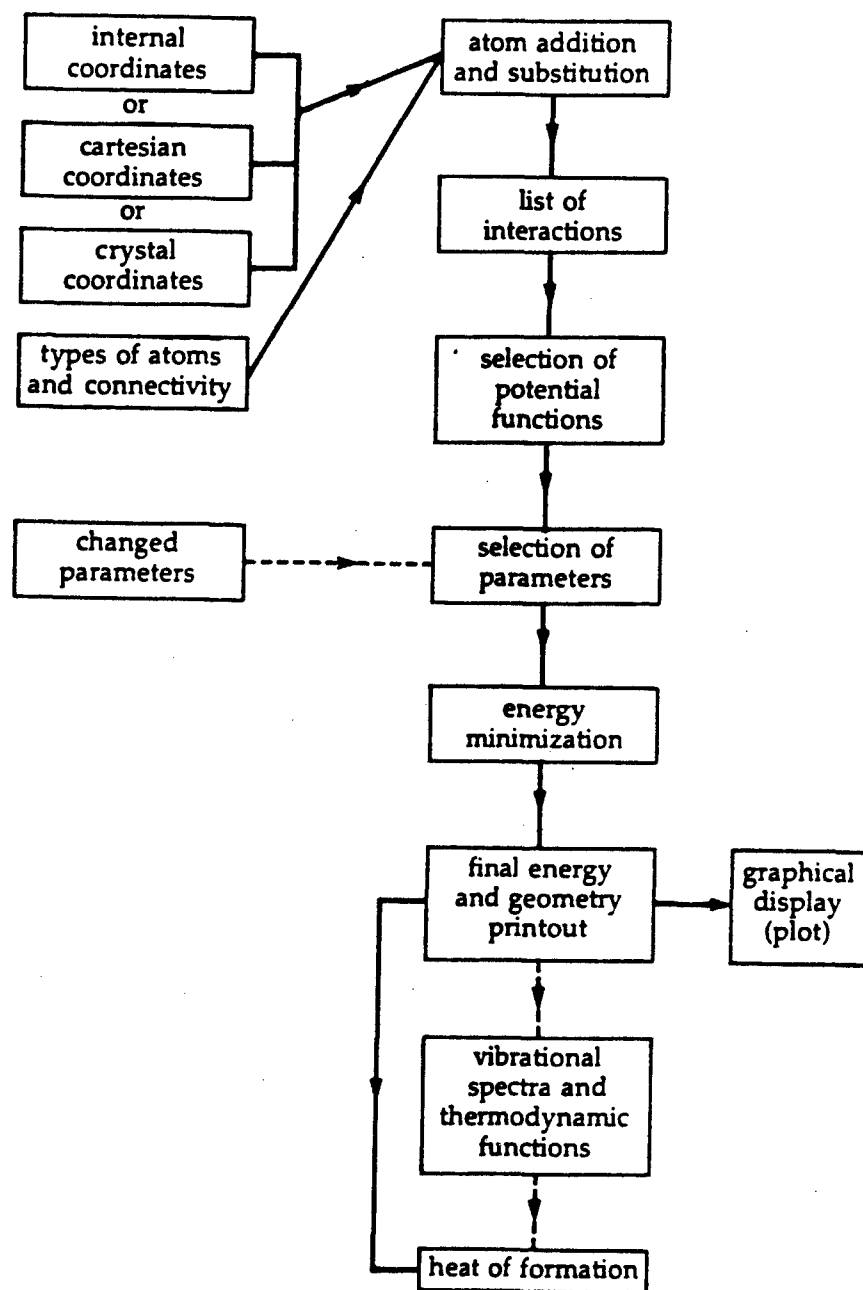


Figure 8. Flow Chart of a Molecular Mechanics Program

types of compounds. This is reasonable for compounds similar to those in the parameterizing set but may not be for more unusual compounds with the same type of bonds, angles, etc. The more critical problem is, however, the unavailability of parameters for many molecules of interest. There isn't good experimental data for many unusual sulfur and nitrogen containing compounds and therefore no good molecular mechanics parameters have been derived for them. If the compounds being studied are such that good parameters are available then molecular mechanics is the method to use, if not, something better needs to be used.

Another problem with molecular mechanics is its inability to accurately handle conjugated molecules. This is again not surprising since molecular mechanics does not treat electrons at all while conjugation in a molecule is an electronic phenomenon. A fix has been attempted by doing a quick molecular orbital calculation on the pi electron system of the starting geometry to get a set of bond orders which are used to modify the force field for the conjugated parts of the molecule only. The molecular orbital (MO) calculation is redone if the geometry varies beyond preset tolerances during the optimization and the field modified again. The electronic energy from the MO calculation has to be added into the heat of formation calculation. Even though this fix gives good results for some conjugated

molecules this difficulty in handling conjugation and the lack of parameters for heterocyclic aromatic compounds make molecular mechanics inadequate for studying the systems of interest in this research. (Most of the information in this section is from references [38] and [42])

### Ab Initio Molecular Orbital Theory

While molecular mechanics is completely empirical and parameterized, the term *ab initio*, Latin for "from the beginning", implies a rigorous, nonparameterized molecular orbital method derived from first principles, namely the Schrödinger equation. Of course, as usual, this isn't exactly the case. Although there are several assumptions made in *ab initio* theory to simplify the calculations, it is more complete and therefore more costly in computer time than any other computational method. Chemical accuracy is possible with *ab initio* methods, but only at the highest levels of theory and with huge costs in computer time (even a supercomputer can take days to calculate a four carbon molecule at the highest level of theory available). Usually calculations are performed at lower, less definitive levels of theory and the shortcomings taken into account in the analysis [43]. Terms such as "level of theory" will be explained in this section along with the other basics of *ab*

initio theory.

Of course, any comprehensive treatment of ab initio theory would entail the regurgitation of pages and pages of complex mathematical derivations and equations, not to mention a detailed rehashing of quantum mechanics. Since that is not the purpose of this section, the definitive work on ab initio molecular orbital theory by Hehre, Radom, Schleyer, and Pople [44] is recommended for those who desire the rigorous explanation. This section will concentrate on giving clear explanations of the basic principles and jargon used in practical ab initio theory. The emphasis will be on concepts not equations.

The goal of ab initio calculations is to get the best possible solution to the Schrödinger partial differential equation (equation 4):

$$HY = EY \quad (\text{equation 4})$$

where H is a differentiating operator representing the total energy of the molecule called the Hamiltonian. E is the value of the energy of the state of the molecule relative to a state where all of its nuclei and electrons are infinitely separated and at rest. Y is the wavefunction which can be represented by a mathematical function dependent on the cartesian and spin coordinates of all the particles in the

molecule. All information about the molecule, i.e. bond orders, dipole moments, valencies, etc., is contained within the wavefunction. The square of the wavefunction,  $Y^2$ , gives the probability of finding any of the molecule's particles in any given volume of cartesian space. In principle, all properties of a molecular state can be calculated from its wavefunction and its associated energy. Ab initio calculations make use of the approximations of molecular orbital (MO) theory to get the best possible wavefunction, Hamiltonian, and energy.

The Hamiltonian, like any energy expression, is composed of both kinetic and potential parts:

$$H = T + V \quad (\text{equation 5})$$

where  $T$ , the kinetic energy operator, is dependent on the velocity and mass of all the particles and  $V$ , the potential energy operator, is dependent on the electric charge and distance between particles. When the Hamiltonian operator is applied to the wavefunction,  $Y$ , the result is the wavefunction times the actual value for the energy,  $E$ .  $E$  is known as the eigenvalue of the operator and  $Y$  is the eigenfunction. The Schrödinger equation for any molecule will have several solutions corresponding to different states of the molecule. The lowest energy state is the

ground state [44]. Ab initio calculations are typically used to compute ground state properties although excited states are accessible via these methods.

The first approximation in ab initio molecular orbital (AIMO) theory is to separate the motions of nuclei from those of electrons. It is assumed that electrons move so much faster than the much larger nuclei that whenever the nuclei in a molecule move, their electrons instantaneously assume the minimum energy configuration around the nuclei. This means that the distribution of electrons depends only on the position of the nuclei not the velocity of the nuclei. In other words, only the effective electronic energy at a particular set of nuclear positions needs to be evaluated and that energy is used as a potential energy for the variation of nuclear positions (as in the geometry optimizations described earlier) and the generation of the potential surface. So, where molecular mechanics minimized the potential energy of the forces between atoms, MO theory minimizes the effective electronic energy with respect to the position of nuclei. In this way nuclear-nuclear interactions are a constant contribution to the energy for a particular nuclear configuration and are added to the energy after the electronic energy has been minimized. This is known as the Born-Oppenheimer approximation [45] and is valid where the mass of the electron is much less than that of the nuclei.



From here on it is assumed that the Hamiltonian,  $H$ , the wavefunction,  $Y$ , and the energy,  $E$ , stand for electronic motions only, which are dependent on the positions of the nuclei.

The essence of ab initio calculations consists of three distinct steps [46]:

- (1) Writing down the Hamiltonian,  $H$ , for the system.
- (2) Selecting a mathematical function,  $Y$ , as the trial wavefunction with variable parameters.
- (3) Minimizing the energy,  $E$ , with respect to variations in the parameters.

In practice, both the Hamiltonian (or a similar operator) and the wavefunction are varied in an iterative fashion to minimize energy at each set of nuclear coordinates called the self-consistent field (SCF) method. Since this approach uses the Born-Oppenheimer approximation, we must realize that the best energy obtained from the calculation is an upper bound to the actual energy of the molecular state. This is known as the variation theorem [47].

Since the many electron wavefunction,  $Y$ , is far too complicated to be expressed exactly, the molecular orbital (MO) theory is used to approximate the full wavefunction.  $Y$  is approximated by the Slater determinant [48] product of a

set of one-electron functions,  $\phi(x,y,z,\tau)$ , known as molecular spin orbitals [49]. Equation 6 shows the short hand determinant form for the closed-shell wavefunction.

$$Y_{\text{closed-shell}} = |\phi_1(1)\bar{\phi}_1(2)\dots\phi_n(2n-1)\bar{\phi}_n(2n)| \quad (\text{equation 6})$$

Each  $\phi_i$  and  $\bar{\phi}_i$  pair are two one-electron functions that differ in their spin component,  $\tau$ . The spins of the electrons in the pair are always opposite (in normal cases),  $\tau = +\frac{1}{2}$  or  $-\frac{1}{2}$ . Each pair, sometimes called an  $\alpha$ - $\beta$  spin pair, represents what is commonly known as a single molecular orbital (MO). The numbers in equation 6 represent the electrons filling the orbitals and  $n$  is the number of MO's occupied by electrons. This determinant represents a closed-shell system where all orbitals are doubly filled with electrons. The evaluation of determinants [48], the treatment of open-shell systems [49], and the complex mathematics of the variation method [50] will not be covered here. Only the results are useful to this discussion.

After the Born-Oppenheimer approximated Hamiltonian and the MO product trial wavefunction are available, the variation method can be applied to the problem. This leads to a new set of equations, one equation for each MO, in the form of equation 7:

$$F\phi_1 = e_1\phi_1 \quad (\text{equation 7})$$

where  $e_1$  is the energy eigenvalue for the MO  $\phi_1$ .  $F$  is called the Fock operator, similar to a Hamiltonian, which represents the MO's energy and these equations are sometimes called the Hartree-Fock equations. The Fock operator has within it two other operators which perform integration operations on the MO functions. When these operators are applied two types of integrals are generated which must be added to the Fock operator before it can be applied in whole to the MO functions. The first type of integral is the coulomb or two-electron repulsion integral,  $J_{1j}$ . It represents the energy of repulsion between two electrons in orbitals  $\phi_1$  and  $\phi_j$  at a distance  $r_{12}$  apart and is shown in equation 8 (in Dirac notation [51]). Equation 9 shows the other type of integral needed to evaluate the Fock operator, the two-electron exchange integral,  $K_{1j}$ . It represents the

$$J_{1j} = \langle \phi_1(1)\phi_j(2) | 1/r_{12} | \phi_1(1)\phi_j(2) \rangle \quad (\text{equation 8})$$

$$K_{1j} = \langle \phi_1(1)\phi_j(2) | 1/r_{12} | \phi_1(2)\phi_j(1) \rangle \quad (\text{equation 9})$$

energy needed to exchange two electrons in orbitals  $\phi_1$  and  $\phi_j$  at a distance  $r_{12}$  apart. The integral equations are shown simply to show how complex the mathematics is (this

will be useful in the discussion of semiempirical methods). There are  $J_{ij}$ 's and  $K_{ij}$ 's for every possible two electron pair in a molecule, so this can run into hundreds of thousands of integrals that must be evaluated.

At first glance it seems that equation 7 is similar to the Schrödinger equation and that the Fock operator is, in effect, the Hamiltonian operator. There is an important difference between  $F$  and  $H$  however. The Hamiltonian is a standard energy expression and is independent of the form of the wavefunction, while the Fock operator, as equations 8 and 9 show, has components which require the MO functions to be known before they can be evaluated. In other words,  $F$  is a function of the MO's  $\phi$ . Since  $\phi$  is an eigenfunction of  $F$ ,  $F$  is needed to get  $\phi$ . Hence, we need to know  $F$  to find  $\phi$ , and we need  $\phi$  to know  $F$ ! The problem is solved by an iterative approach. First, trial MO's are used as an initial guess to build the initial Fock operator. This  $F$  is used on the trial MO's to produce new MO's, which are used to build a new  $F$  and so on. The procedure is repeated until there is no significant change between two successive steps. At this point, the  $\phi$ 's produced by  $F$  are the same as the  $\phi$ 's that produce the coulomb-and-exchange fields in  $F$  [52]. The solutions are self-consistent and the method is termed the self-consistent field method [53]. The result is a good set of MO's,  $\phi$ , for the molecule and a set of energy eigenvalues,

$\epsilon_i$ , which correspond to the energy of an electron occupying a specific orbital.

Once the  $\phi_i$ 's and  $\epsilon_i$ 's are computed, several quantities, such as bond orders, atomic charges, and electron densities can be calculated via Mulliken Population Analysis [54] which won't be discussed here. What is more important is that  $E$ , from the Schrödinger equation, can be calculated from the MO energies,  $\epsilon_i$ .

It might seem that the total electronic energy,  $E_{elec}$ , is simply the sum of all the one electron energies for all the occupied MO's. However, a look at equations 8 and 9 shows that if  $J_{ij}$  and  $K_{ij}$  are evaluated for every permutation of electron pairs, then the coulomb and exchange energy for every electron pair is counted twice. In other words,  $J_{12} = J_{21}$  and  $K_{12} = K_{21}$  and these value should only be added into  $E_{elec}$  once. Equation 10 shows how this 'extra

$$E_{elec} = \sum_{i=1}^n [2\epsilon_i - \sum_{j=1}^n (2J_{ij} - K_{ij})] \quad (\text{equation 10})$$

energy' is subtracted to give the right  $E_{elec}$  for the closed-shell case. The  $\epsilon_i$ 's are multiplied by 2 since there are two electrons per orbital in the closed-shell case,  $n$  is the number of doubly filled MO's. The subtraction of the second summation removes one half of the electronic interaction energy added in by a straight summation of the

er's.  $E_{elec}$  must now be added to the nuclear-nuclear repulsion energy,  $V_{nn}$ , which was separated from the electronic calculation by the Born-Oppenheimer approximation, to get the total molecular energy,  $E$  from the Schrödinger equation (equation 11). This is known as the Spin Restricted Hartree-Fock (RHF) energy [55] for closed-shell

$$E = E_{elec} + V_{nn} \quad (\text{equation 11})$$

systems. For open-shell systems Spin Unrestricted Hartree-Fock (UHF) methods [56] are used.  $E$  is usually reported in atomic units (hartrees).

Geometry optimizations are handled in the same manner in ab initio calculations as in molecular mechanics. However, the electronic energy is used in ab initio techniques instead of the straight potential energy of molecular mechanics.

The Hartree-Fock energy (RHF or UHF) is higher than the exact value by a number known as the correlation energy:

$$E(\text{correlation}) = E(\text{exact}) - E(\text{Hartree-Fock}) \quad (\text{equation 12})$$

This is because the SCF procedure calculates the energy of an electron in the collective coulomb and exchange field of all the other electrons in the molecule. It doesn't take into

account the correlated motions of electrons, or the fact that if one electron moves, the others will adjust their positions (motions actually) to stay out of its way. This correlation of motion is not well described at the HF level because the electrons have been locked into one configuration by using a single determinant as the wavefunction leaving little room for movement. The two most popular methods of adding electron correlation to an HF calculation are configuration interaction (CI) [57] and Møller-Plesset perturbation theory of the 2nd, 3rd or 4th order (MP2, MP3, MP4) [58]. Both use linear combinations of several different Slater determinant wavefunctions, representing different possible electron configurations, with variable weighting factors to lower the energy to the E(exact) (see references [57 and [58] for full discussions).

The most practical consideration in ab initio calculations is the choice of a basis set. Earlier the fact that MO functions are varied during the SCF iterations to get the lowest energy was discussed. What was not discussed is how these MO functions are represented and adjusted. Each MO is described by a linear combination of N one electron functions called basis functions; this leads to equation 13,

$$\phi_i = \sum_{\mu=1}^N c_{\mu i} x_{\mu} \quad (\text{equation 13})$$

where N is the number of basis functions,  $x_{\mu}$ 's are the basis

functions and  $c_{\mu i}$ 's are molecular orbital expansion coefficients which are varied in the SCF procedure to lower energy. Atomic orbital (AO) functions of the constituent atoms are used as  $x_{\mu}$ 's, hence the name linear combination of atomic orbitals (LCAO) [59] has been given to these techniques. An AO can be represented in two ways, as Slater-type orbitals (STO) [60] or as Gaussian-type orbitals (GTO) [61]. STO's are better representations of AO's but require numerical integration techniques to evaluate repulsion integral while GTO's can be integrated using much simpler, and faster, analytical techniques [61]. GTO's have an  $\exp(-\alpha r^2)$  dependence while STO's have an  $\exp(-\alpha r)$  (Figure 9), where  $\alpha$  is a fixed coefficient for the exponent.

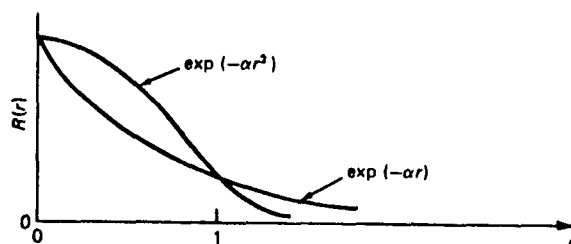


Figure 9. Radial Dependence of STO and GTO functions

Unfortunately, a single GTO doesn't represent an AO well at all. In practice, a linear combination of several GTO's with fixed exponents are used to represent an AO. The expansion coefficients,  $c_{\mu i}$ 's, of all these GTO's, called primitive gaussians [62], rise or fall during the



minimization of the MO energy. This set is termed a contracted basis function. Once this approximation is optimized the coefficients are frozen and the set is treated as a single function. A set of basis functions for each atom type's AO's is input into the calculation and optimized as parts of the minimized MO's. This leads to the most practical part of the basis set discussion, the terminology used naming a basis set, sometimes known as the 'level of theory' of the calculation.

Several approximations are made for AO's; most involving the addition of more GTO's or combining GTO's in different ways. The simplest approximation or minimal basis set is the STO-3G basis set. This means that each atomic orbital in an atom is approximated by 3 Gaussian type functions in an attempt to represent an STO. STO-3G was used extensively in early ab initio calculations but is now used mainly to get a rough idea of the energy and geometry of a molecule as it takes the least amount of computer time since it has the smallest number of basis functions.

The most common basis sets in use today are split valence basis sets. The inner or core orbitals in an atom, i.e. the 1s orbital in carbon, are represented by an STO approximated by a fixed number of GTO's while the more important valence orbitals, i.e. 2s and 2p orbitals in carbon, are represented by two or three Slater orbitals

approximated by a number of Gaussians. This allows the valence orbitals, which participate most in MO formation, more flexibility to adjust than in STO-3G (Figure 10). So,

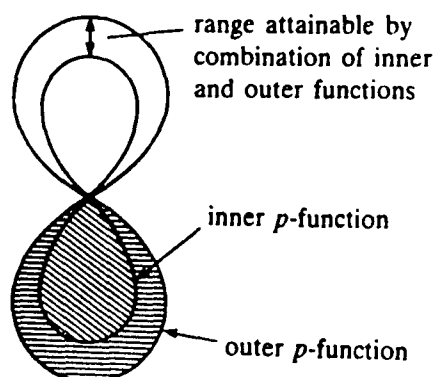


Figure 10. Schematic of Split Valence Orbitals

3-21G is a basis set where an atom's core orbitals are STO's of three Gaussians and each valence orbital is represented by two STO's, one with two GTO's and one with only one GTO.

The last two types of functions used in *ab initio* calculations are the polarization, or '\*', functions and the diffuse, or '+', functions. Polarization functions are basically atomic d-orbitals and are most useful for third row or larger atoms. Diffuse functions are exactly that, a very diffuse or 'spread out' function that adds extra flexibility to the basis set. They are most useful in anions where there are extra electrons in the system. The largest common type basis set is 6-311++G\*\*. It contains a

six Gaussian STO for all inner AO's; three STO's, one of

three GTO's and two of one GTO, for the valence orbitals; two diffuse functions, and two polarization functions.

One convention that should be addressed here is the notation used when multiple basis sets are used. Larger numbers in a basis set name implies more basis functions in the set. Figure 11 shows how the number of basis functions increases with higher levels of theory. The more basis

Atom	Basis Set						
	STO-3G	3-21G	3-21G(*)	3-21+G	6-31G*	6-31G**	6-311G*
H	1	2	2	2	2	5	3
Li-Ne	5	9	9	13	15	15	18
Na-Ar	9	13	18	17	19	19	22

Figure 11. Number of Functions per Atom per Basis Set

functions the longer the calculation; if electron correlation methods are added the calculations become completely unmanageable (a 6-31G\* calculation optimized with Møller-Plesset, 2nd order on 1,1 dichlorocyclopropane takes 24 hours of Cray supercomputer time [63]). It may be impractical to optimize a geometry at a high level of theory. So, a molecule is usually optimized with a small basis set, say 3-21G, and that geometry is used in a single point calculation with a larger basis set where no optimization is done. Electron correlation can be done on top of this

larger basis set. The correlation-larger basis set are separated by a '/' in the notation, while the larger-smaller basis set have a '//' between them. Thus, MP2/6-31G\*//3-21G means that the 3-21G basis set was used to optimize the geometry, this geometry was used for a 6-31G\* single point calculation, and 2nd order Møller-Plesset correlation was applied after the SCF calculation finished. In principle, any combination of basis sets/correlation is possible, but it would be useless to place a smaller basis set over an optimized geometry of a larger set. The most popular computer program for ab initio calculations, the Gaussian8x package (Gaussian86 [64] is the newest version), has a wide range of basis sets and electron correlation schemes internally stored in the program.

The ab initio method is the most complete and most flexible computational technique. The only parameters needed are atomic basis functions and with those any bond length, bond angle, torsion angle, and van der Waals interaction can be accounted for. Fewer parameters are needed. However, the coulomb and exchange integrals generated as a consequence can quickly run into the hundreds of thousands. Evaluating  $J_{ij}$ 's and  $K_{ij}$ 's takes enormous amounts of computer time. Although the advent of supercomputers has made much larger system accessible to ab initio calculations, there is much farther to go before this

method will be useful for the polymers to be studied here.

### Semiempirical Molecular Orbital Theory

Soon after ab initio molecular orbital theory was developed, it became obvious that it was impractical to use for all but small systems. Even after the advent of supercomputers, the computer time required to sufficiently study a system with over ten second row elements is far too great for all but the most fortunate and well-funded research groups. Molecular mechanics allows large molecules to be calculated easily but doesn't provide the kind of MO data that one might desire. It is also very restrictive as to what systems can be studied because of its "set of 4 atoms" parameterization. An approximate MO technique needed to be developed to allow larger systems to be computed. In answer to this need several MO based methods have been formulated which use experimentally derived parameters to approximate values explicitly calculated with ab initio methods. These fall under the category of semiempirical methods.

Two of the earliest and crudest semiempirical MO techniques treated only planar conjugated molecules. The Hückel MO (HMO) method [65], developed in the early 1930's by E. Hückel, treated only  $\pi$ -electrons assuming they were

the greatest contributors to the total electronic energy. The HMO method is quite simple and uses only matrix algebra. The parameters used are all relative to a carbon atom (which is given a value of 1 in all cases). Although the HMO method is a crude approximation, it gives surprisingly good qualitative results for MO's, bond orders, atomic charges and other molecular properties. Roald Hoffman formulated an Extended Hückel MO (EHMO) method in 1963 [66] which includes  $\sigma$ -electrons in the calculation, allowing any type of system to be computed. It is still used extensively today for extremely large systems which are too big for more accurate semiempirical techniques [67]. The Pariser-Parr-Pople (PPP) method [68], developed in 1953, also treats only  $\pi$ -electron conjugated systems and still finds uses today in the study of nonlinear optical phenomena in molecules [69].

The techniques listed above fall into the category of Qualitative MO theory, and although they provide vast quantities of useful qualitative information, they are not quantitatively accurate enough in their calculation of energies, geometries and other properties to satisfy most computational chemists. The obvious roadblock to quick, accurate MO computations is the enormous amount of computer time required to evaluate the thousands to hundreds of thousands of electron repulsion and exchange integrals, sometimes referred to as differential overlap (DO) integrals,

generated in the SCF procedure,  $J_{ij}$ 's and  $K_{ij}$ 's, which take the form of equations 8 and 9. The "obvious" solution is to neglect those integrals which have little impact on the final energy and find approximate values for the other integrals so they don't need to be explicitly evaluated. This is how the most popular semiempirical MO methods work, hence the name "approximate MO theory" is sometimes used for describing these techniques.

The first two of the "integral neglecting-approximating" methods use the neglect of differential overlap (NDO) approximation where some or all of the differential overlap (repulsion and exchange integrals) between different AO's ( $x_\mu$  functions) centered on atoms are neglected. They also explicitly treat only valence electrons, assuming a stable or "frozen" core of inner electrons which doesn't change much during the course of the computation. The complete neglect of differential overlap (CNDO) method [70], developed in 1964, neglects all differential overlap between different  $x_\mu$  functions. Only the one electron resonance integrals,  $J_{ii}$ 's and  $K_{ii}$ 's, are retained and parameterized values are input for them. This essentially means that all AO's around atoms are spherical. The intermediate neglect of differential overlap (INDO) method [71], formulated in 1966, differs from CNDO only in that it evaluates all exchange integrals between AO's on the same atom, known as one-center exchange

integrals. This helps to give some directionality to the AO's, i.e. p-orbitals which are along the x, y, or z-axis. CNDO and INDO give nearly the same results for closed-shell systems, but INDO is far superior in calculating electron spin density in radicals.

Although CNDO and INDO were more accurate than previous semiempirical attempts, they didn't give the accuracy that was hoped for, so their inventor, J. A. Pople, abandoned further work in semiempirical methods and continued advancing ab initio theory. The big problem with CNDO and INDO was that they had been parameterized to reproduce the results of available ab initio calculations on diatomics and other small molecules [72]. The best ab initio computations in the mid-1960's were minimal basis set (STO-3G) runs which are recognized today as not being especially accurate. When CNDO and INDO didn't give as good results as STO-3G, semiempirical methods were marked as only marginally useful and abandoned.

A different approach to semiempirical MO theory, taken by Dewar [73], has resulted in the three most popular semiempirical techniques in use today. Instead of giving the overlap integrals values to reproduce energies and geometries from ab initio calculations, Dewar's techniques are parameterized to reproduce experimental data. This gives much better and more usable results than previous



semiempirical methods. It eliminates the need for post-SCF electron correlation since the experimental energies that are the basis for the integral parameters already include correlation. The first such approach was the modified intermediate neglect of differential overlap (MINDO/3) method, developed in 1975 [74]. MINDO/3 is basically the INDO method described previously except all included integrals are approximated to reproduce molecular geometries and heats of formation. MINDO/3 is parameterized by atom pairs, i.e. in order to have parameters for a compound with a Li-N bond pair experimental data on compounds with Li-N bonds must be available. A "\*" in Figure 12 denotes the bond pairs for which the newest version of MINDO/3 is

	H	B	C	N	O	F	Si	P	S	Cl
H	*	*	*	*	*	*	*	*	*	*
B	*	*	*	*	*	*				
C	*	*	*	*	*	*	*	*	*	*
N	*	*	*	*	*	*			*	*
O	*	*	*	*	*	*			*	*
F	*	*	*	*	*	*			*	
Si	*		*				*			
P	*		*					*		*
S	*		*	*	*	*			*	*
Cl	*		*	*	*			*	*	*

Figure 12. Available MINDO/3 Parameters

parameterized [75]. Although MINDO/3 is not perfect (its strong points and shortcomings are extremely well documented [76]) it was a breakthrough in computational

chemistry. Suddenly there was a way to get good energies and optimized geometries quickly for a 50-atom molecule [77], something unthinkable with ab initio calculations. The method has received much criticism from the ab initio school [78] but its importance in getting useful computational information into the hands of non-specialists cannot be denied.

MINDO/3 does as good a job at calculating energies and geometries as an INDO-based formalism can do. In order to do better all one-center electron repulsion integrals must be included in the calculation. It has been shown that it is not correct to neglect repulsion integrals involving overlap if the overlap is between two AO's of the same atom [79]. The inclusion of all the electron repulsion and exchange integrals between AO's on the same atom and neglect of those between AO's on different atoms is known as the neglect of diatomic differential overlap (NDDO) approximation [80]. Dewar and Thiele used the NDDO approximation to formulate the modified neglect of diatomic differential overlap (MNDO) semiempirical Hamiltonian in 1977 [81]. It is parameterized to reproduce experimental ionization potentials, dipole moments, and heats of formation and was developed to avoid the weaknesses of MINDO/3.

MNDO handles most problems better than MINDO/3 with the notable exceptions of treating carbocations and silanes. It

handles the effects of lone-pair electron repulsions much better than MINDO/3 [81]. MNDO calculations usually take 1.5 times longer than corresponding MINDO/3 computations but the improvement in results is usually worth the extra time. Probably the biggest advantage of MNDO over MINDO/3 is that it works for a larger range of compounds because it uses an atom-by-atom parameterization instead of bonded atom pairs. I.e., to have parameters for a compound with a Li-N bond pair, experimental data on nitrogen-containing compounds and lithium-containing compounds are needed not compounds with Li-N bonds which may be hard to come by. MNDO presently handles any molecule containing H, Li, B, C, N, O, F, Na, Al, Si, P, S, Cl, K, Cr, Ge, Br, Sn, I, Hg, and Pb [82]. MNDO is the most widely used semiempirical method today.

A brief word on semiempirical parameters is appropriate here. When the "overlap" integrals,  $J_{ij}$ 's and  $K_{ij}$ 's, are approximated several different parameters are used for each integral (see the original papers for MINDO/3 [74], MNDO [81], and AM1 [83] for details on the different parameters). Guesses at these parameters are made and calculations are run on several compounds for which there is experimental data. The calculated values are compared to the experimental numbers and a mean error is calculated for the set of compounds. The parameters are then adjusted and the calculations run again, the values compared and the

parameters adjusted. The procedure is repeated until the mean error over the set of compounds is below a deemed acceptable value and the 'optimized' parameters are input into the computer program. The procedure is quite similar to that involved in parameterizing molecular mechanics.

Probably the biggest problem with MNDO (and MINDO/3) is its tendency to overestimate repulsions between atoms when they are near their van der Waals radius apart. This leads to energies that are too positive for crowded molecules and too negative for four-membered rings, and the failure to reproduce hydrogen bonds. Dewar and Thiele recognized this problem in the original MNDO paper [81] but it was not successfully corrected until 1985 with the introduction of the Austin Model 1 (AM1) Hamiltonian [83]. AM1 is basically the MNDO method with the core-core repulsion terms (or functions) 'softened up.' The core (nucleus and inner non-valence electrons) repulsion function (CRF) was modified from MNDO to AM1, then a new set of parameters was made to make the new method self consistent. There are not yet as many parameters for AM1 as there are for MNDO. At present AM1 can handle H, C, N, O, F, Cl, Si, and I. AM1 reproduces heats of formation, dipole moments, and ionization potentials better than MNDO or MINDO/3 in most cases. It also gives more realistic geometries in cases where there is high steric crowding [81] or where aromatic rings are connected

via single bonds [84]. AM1 is the newest available semiempirical method and as such its shortcomings are not as well documented as MNDO or MINDO/3, but its popularity is growing and as it does more data will become available. AM1 represents the best results that can be achieved using the NDDO approximation and is the method of choice for this work because of its ability to give good energies and geometries for connected heteroaromatic rings [84].

The MINDO/3, MNDO, and AM1 methods are contained in two computer program packages: AMPAC by Dewar [85], and MOPAC by Stewart [86]. The two programs are quite similar and allow many different computation options, from the addition of configuration interaction to the calculation of various thermodynamic properties to the calculation of nonlinear hyperpolarizabilities (see the program manuals for details). These packages allow great flexibility in how a calculation can be run and are easy to use. The MOPAC program is used in this research.

#### Ordered Polymers

Most organic polymers, due to their long and flexible chain structures, assume random molecular conformations and, barring crystallization, random intermolecular orientations in the solid form and solution [87]. There is a class of

organic polymers which, due to their more rigid molecular structure, tend to aggregate and orient themselves into much more ordered solutions (liquid crystalline solutions), films and fibers than typical polymers. These are termed ordered polymers [88] and have shown the highest tensile and compressive properties of any organic material outside of graphite [32].

The ordered polymers that have been studied so far show tensile properties high enough to make them candidates for incorporation into aerospace structures. However, they undergo compressive failure at loads much lower than those experienced by an airframe. The purpose here is to examine the tension and compression of several of these ordered polymers in an attempt to understand the tensile and compressive phenomena of these systems, predict their tensile moduli, and get insight into solving the problem of insufficient compressive strength in these materials.

The following sections describe the systems to be studied, including the structure, a brief history where applicable, and the reason for studying each system.

#### Poly(p-phenylenebenzobisimidazole (PBI)

Cis- and trans-PBI (Figure 13), synthesized in 1976, [89] are of the class of ordered polymers known as 'rigid

rods'. The reason for the name is obvious from the polymer

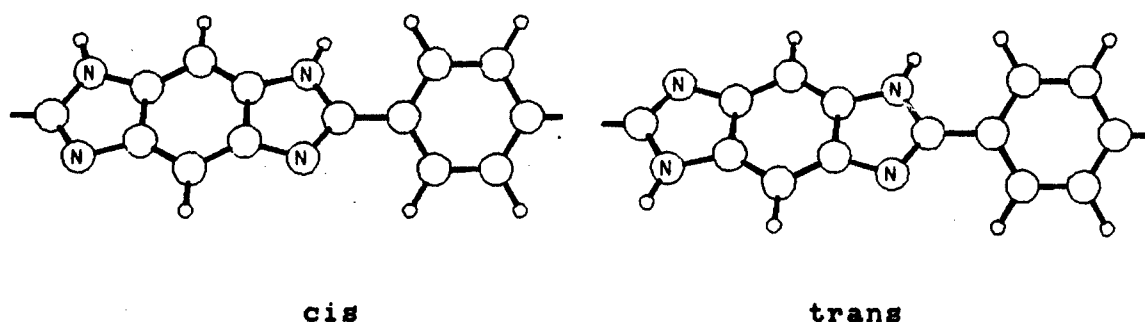


Figure 13. Structure of Cis- and Trans-PBI

structure, the polymer chain is extended and rigid as there are no tetrahedral centers where coiling bond rotations can occur. The rigid rods were synthesized under the assumption that a stiff extended chain molecule, like uncooked spaghetti in a box, would line up in a highly linear fashion giving high strength and modulus. In reality, the cis- and trans- don't appear separately as the polymer is made in polyphosphoric acid (PPA) and all nitrogens are protonated. There would probably be a random distribution of cis- and trans- along a chain of the solid state polymer. However, the computer allows us to study the two isomers independently and make observations on these two different structures that wouldn't be possible experimentally. PBI has not been synthesized in sufficiently high molecular weight

for the determination of any of its mechanical properties. The tensile moduli of both cis- and trans-PBI will be calculated and an extensive molecular tensile and compressive analysis will be done on the cis- isomer.

Poly(p-phenylenebenzobisoxazole) (PBO)

Cis- and trans-PBO (Figure 14), first synthesized in 1975 [90,91,92], are also rigid rods. Cis-PBO is presently

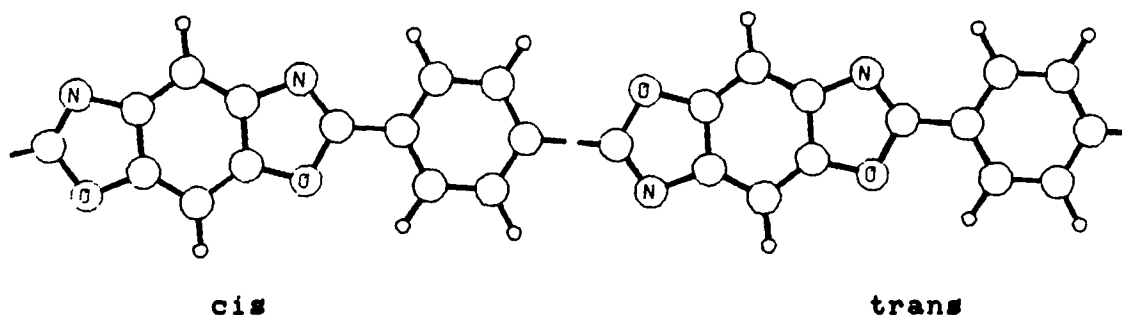


Figure 14. Cis- and Trans-PBO Structures

under study by Dow Chemical and others for use as a structural polymer. Trans-PBO is difficult to synthesize in high molecular weights due to quinone formation in the para-OH monomer. Computational study of cis- and trans-PBO will give information on the difference in properties of the cis- and trans- isomers and allow comparison to the other



rigid rods. The tensile and compressive deformations of cis-PBO and the theoretical moduli of both polymers will be studied here.

### **Poly(p-phenylenebenzobisthiazole) (PBT)**

Cis- and Trans-PBT (Figure 15), first made in 1978 [93,94], are the sulfur analogs to cis- and trans-PBO. They both have been studied as structural materials and are now drawing interest in the area of nonlinear optics. Model

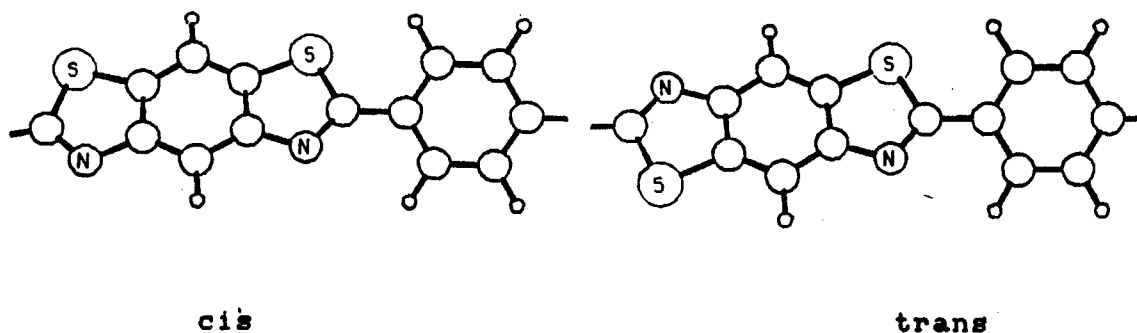


**Figure 15. Structures of Cis- and Trans-PBT**

compounds of cis- and trans-PBT have been studied by x-ray crystallography [95]. Cis-PBT shows a bowed, less extended structure than trans-PBT. A comparison of the two structures to each other and to other rigid rods will provide information on the effect of large atoms, like sulfur, on the

tensile and compressive properties of rigid rod ordered polymers. Theoretical moduli for cis- and trans-PBT and the molecular deformations of trans-PBT in tension and compression will be calculated.

Poly(p-phenylenepyromellitimide) (PPPI)

PPPI (Figure 16) is a rigid rod with C-N bonds along the chain axis instead of C-C bonds. PPPI has been synthesized [96], but not in very high molecular weights. As a consequence no mechanical property data is available for PPPI. This study will provide the theoretical

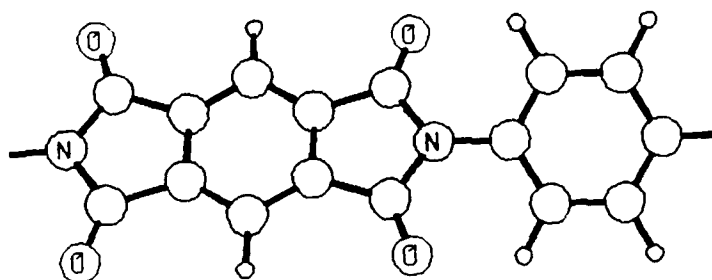


Figure 16. Structure of PPPI

maximum tensile modulus for this material and allow observations of the effect of axial non-C-C bonds on rod properties and molecular tensile and compressive deformations.

Poly(p-phenylene-2,6-quinoline) (PQ)

PQ (Figure 17) is the one of the simplest types of

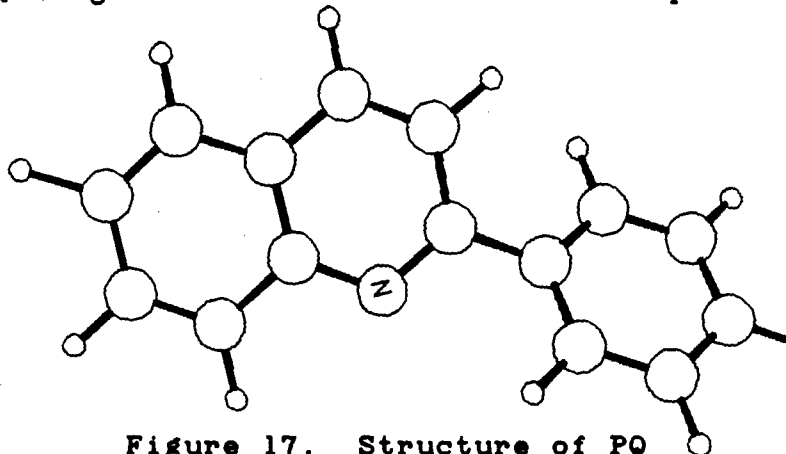


Figure 17. Structure of PQ

polyquinoline. It is a different type of rigid rod with a "crankshaft" structure. This particular polyquinoline has not been made but variations of it are being studied as possible high-performance fibers [97]. Computational studies on this simple polyquinoline will provide information on the effect of "crankshaft" structure on rigid rod behavior and give an idea of the mechanical properties to be expected from this type of material.

Poly(p-phenylene) (PPP)

PPP (Figure 18) is the simplest rigid rod polymer, a string of benzene rings hooked together. It is not a heterocyclic polymer like the previous rigid rods. PPP is

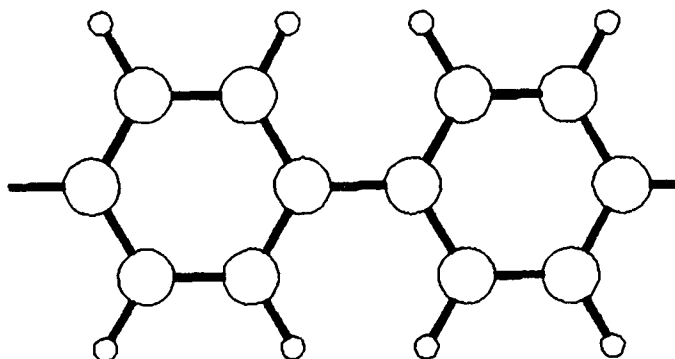


Figure 18. Structure of PPP

being studied by several groups [98,99]. Calculations on this rod will shed some light on basic rod properties, prior to the introduction of heteroatoms. PPP's tensile modulus and molecular deformations will be calculated.

#### Benzimidazoisquinoline (BBL)

BBL (Figure 19), first made in 1971 [100], is a completely different type of ordered polymer. It contains at

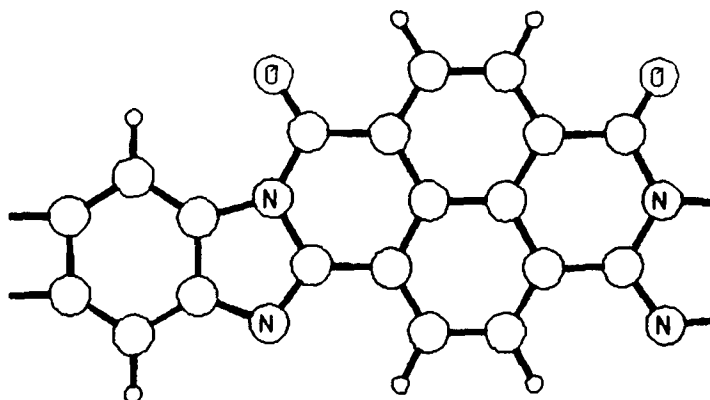


Figure 19. Structure of BBL

least two parallel chemical bonds at all points along the polymer chain. This type of structure constitutes a "ladder polymer." BBL showed some promising properties but could not be made in sufficiently high molecular weights for extensive tests. Seeing how BBL compares to the rigid rods computationally will help in deciding whether or not further pursuit of this material is warranted. BBL's theoretical modulus will be determined here.

### Polyacene

Polyacene (Figure 20) is an hypothetical polymer which

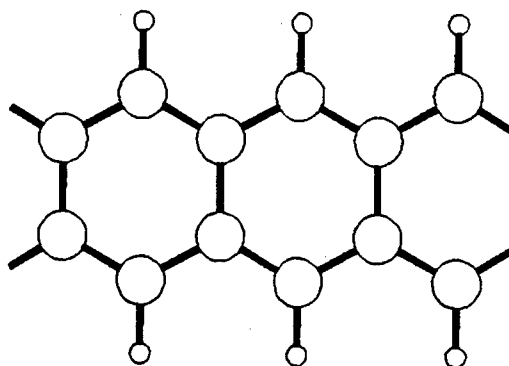


Figure 20. Structure of Polyacene

represents the simplest possible aromatic ladder polymer, a chain of fused benzene rings. This polymer has not been made yet, but this theoretical study of its tensile and compressive responses will give insights into the inherent strengths and weaknesses of the ladder-type structure.

## Graphite

Graphite (Figure 21) has an infinite two-dimensional

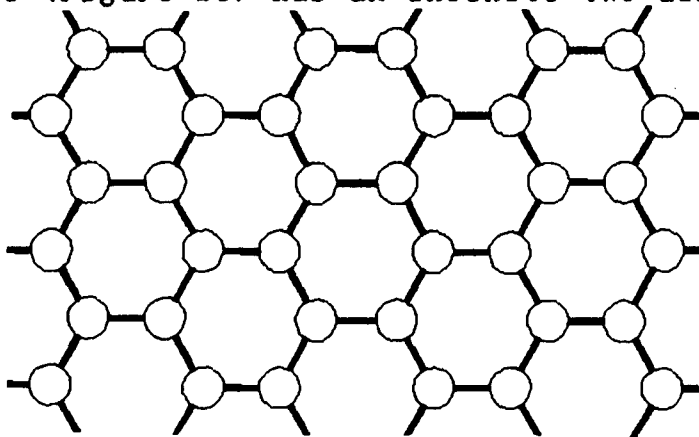


Figure 21. Graphite Structure

sheet structure of fused benzene rings. Graphite has the highest tensile modulus, tensile strength, and compressive strength of any known 'organic' material [32]. Its mechanical properties set the standards to which all organic polymers are compared. Studying graphite's response to compression and tension will help in the design of structures to reproduce these high properties. Only graphite's theoretical modulus will be determined here.

The theoretical study of all the above systems will help to explain compressive and tensile phenomena on a molecular level giving insights into the corresponding bulk phenomena. The scope of systems to be studied will allow some correlation between structure and mechanical properties.

### SECTION III

#### COMPUTATIONAL DETAILS

##### Calculation Mechanics

When you get some free time, could you run the second orientation of graphite? [101]

W.W. Adams 1946-Tomorrow

The MOPAC program [86], version 3.11, from the Frank J. Seiler Research Laboratory, U.S. Air Force Academy was used in this work. MOPAC contains within it the MINDO/3, MNDO, and AM1 semiempirical methods along with other features for manipulating input and calculating different molecular properties from the achieved semiempirical wavefunction (all of these features are documented in the MOPAC manual which comes with the program). MOPAC is public domain software and can be easily obtained from the Quantum Chemistry Program Exchange (QCPE).

Most of the calculations were done on a Cray XMP/12 supercomputer (the polyacene computations were performed on a Digital MicroVAX II). This allowed the calculation of these large systems to be done more quickly than is usually possible. It also made it possible to calculate a larger number of tension and compression points for each system, making the study more thorough than would have been possible with conventional computers. The complete study took over

600 hours of Cray CPU time.

It is important to understand what is actually going on inside a computer program so it does not become a mysterious 'black box' where data goes in and answers magically come out. Figure 22 shows typical flow charts for (a) an ab initio program and (b) MOPAC and other semiempirical programs. First MOPAC reads in the geometric input data and sets up the initial molecular geometry. It also reads the options chosen for the calculation which include: time limit, method to be used, optimization criteria desired, etc. Here the AM1 method is used with a 100-fold shrinking of the geometry optimization criteria. Next, the program assigns the proper parameters to all the atoms in the molecule and enters the SCF energy calculation procedure. Once the SCF calculation has converged, MOPAC calculates the first and second energy derivatives and determines all the atomic forces (i.e. the Newton-Raphson technique described earlier). If the optimization criteria are satisfied, the optimized geometry and wavefunction are used in population analysis and the calculation of properties. If the criteria are not satisfied, the geometry is adjusted and the SCF procedure reentered. The cycle repeats until the criteria are reached and the optimized geometry is written out. This repeating cycle is where MOPAC gains its tremendous





computational speed advantage over ab initio techniques. At the beginning of each optimization cycle, the ab initio program has to assign the basis set and set up all the resulting integrals for the new geometry, explicitly evaluate all the integrals, perform the SCF calculation, and then calculate the atomic forces. This takes an enormous amount of time. MOPAC calculations can be several orders of magnitude faster, depending on the size of the system.

One more block needs to be added to the flow chart to incorporate the tensile and compressive analysis processes into figure 22. For each tension or compressive point calculated, a full geometry optimization and energy calculation must be run. MOPAC allows this to be done in one massive run instead of several small ones (one for each tension or compression configuration). This will be explained in the following sections along with an explanation of MOPAC geometry input and details of the tensile modulus calculation.

#### Geometry Input: Building a Z-Matrix

One of the biggest roadblocks to successful molecular orbital calculations, both semiempirical and ab initio, is setting up the initial molecular geometry for input into the program. A mistake in the geometric input may result in the

calculation of an entirely different molecule than was desired and waste large amounts of computer time. While molecular mechanics usually uses atomic cartesian coordinates, most MO programs use the molecule's internal set of bond lengths (defined by two atoms), bond angles (defined by three atoms), and dihedral angles (defined by four atoms) to define the positions of its atoms in space. Defining a molecule using these 'internal' coordinates, though it may seem strange initially, is easier than using x, y, and z coordinates, especially when there is no graphical input device to assist in the molecule building process.

The set of internal coordinates is known as a Z-matrix. The Z-matrix contains all the bond lengths, bond angles, dihedral angles and atomic connectivity data needed to define the positions of all the atoms in a molecule. Atom A's bond length is defined as the distance between atom A and atom B (AB). The bond angle is the angle measured from A to atom C with B as the vertex (ABC). The dihedral angle is defined as the angle formed between the two planes formed by atoms A, B, C and B, C, D (ABCD). In many cases, the dihedral angle is the same as a torsional angle but this is not necessarily the case. Dihedral angles are the hardest of the variables to understand and define properly; the example will help to clarify this variable. Figure 23 shows these three different variables pictorially.

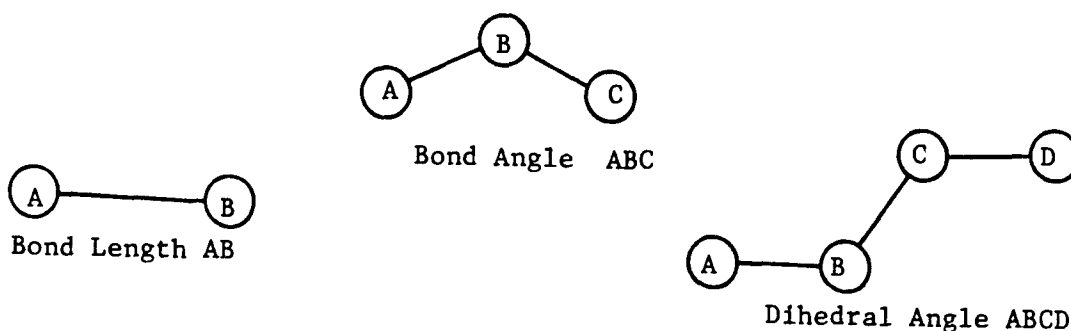


Figure 23. Z-Matrix Variables

The best way to explain MOPAC Z-matrix input and clarify the defining of the variables is to build an example molecule. Methanol,  $\text{CH}_4\text{O}$  (Figure 24) is a ideal choice since it contains both torsional and non-torsional type dihedral angles. The numbers give the order in which the atoms will be defined. MOPAC allows any variable in a Z-matrix to be either fixed or optimized. This is done by marking the variable with a '1' to allow it to optimize or a '0' to hold it fixed. This can be useful if only a certain variable is of interest.

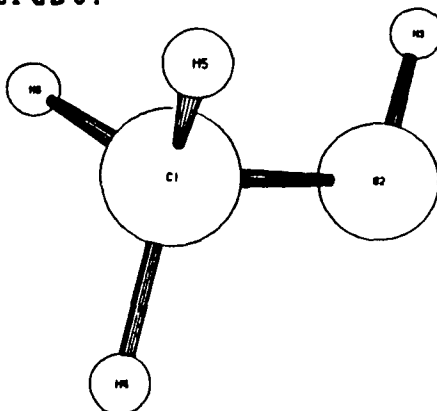


Figure 24. Methanol Structure

A Z-matrix consists of rows, one for each atom, with ten columns. The columns contain the following information:

- (1) Atom A's atomic symbol
- (2) The bond length (AB)
- (3) Optimization marker for bond length (0 or 1)
- (4) The bond angle (ABC)
- (5) Optimization marker for bond angle (0 or 1)
- (6) The dihedral angle (ABCD)
- (7) Optimization marker for dihedral angle (0 or 1)
- (8) Atom number of B, defining bond length
- (9) Atom number of C, defining bond angle
- (10) Atom number of D, defining dihedral angle

Atom #1, the carbon, sets the origin for the molecule and therefore has zero values for all the columns:

```
C      0.00  0  0.00   0  0.00   0  0 0 0
```

Atom #2, the oxygen, has only a bond length to atom #1 and no other variables. A typical C-O bond length is 1.40Å, this variable will be optimized (1 in column 3), and a 1 goes in column 8 to define the length to the carbon:

```
O      1.40  1  0.00   0  0.00   0  1 0 0
```

Atom #3, the hydrogen attached to the oxygen, has a bond length to #2 (about 0.95Å), and a bond angle to #1 (107°), but no dihedral angle, both variables are optimized:

```
H      0.95  1 107.0   1  0.00   0  2 1 0
```

Figure 25 shows the molecule so far.

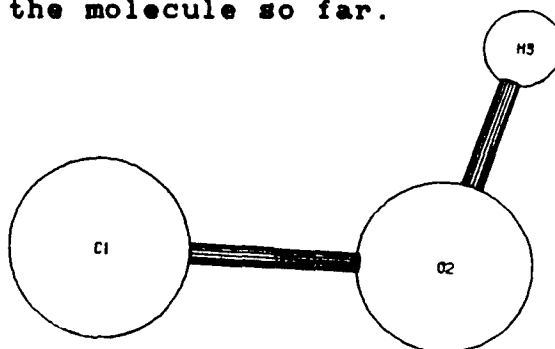


Figure 25. Methanol after 1st three atoms

The next atom, #4, is a hydrogen attached to the carbon, #1, by about 1.12Å. It has a bond angle with #2 of 105° and a torsion-like dihedral angle with hydrogen #3 of 180°. Here the planes defined by 412 and 123 form an angle of 180° (see Figure 24). The row of the Z-matrix is:

```
H      1.12  1  105.0  1  180.0  1  1 2 3
```

Atoms #5 and #6, the last two hydrogens, are nearly identical. They have bond lengths (1.12Å) to the carbon, #1, and bond angles (111°) to the oxygen, #2, but their dihedral angles are shown in a Neuman projection (Figure 26) as opposites of each other (+120 and -120) and not as torsion angles. This is because the dihedrals are defined to the hydrogen, #4, that is bound to the same carbon atom as #5 and #6 are bound to (check the angle formed by planes 512 and 124 or 612 and 124 to be sure). The Z-matrix rows are:

```
H      1.12  1  111.0  1  120.0  1  1 2 4
```

```
H      1.12  1  111.0  1 -120.0  1  1 2 4
```

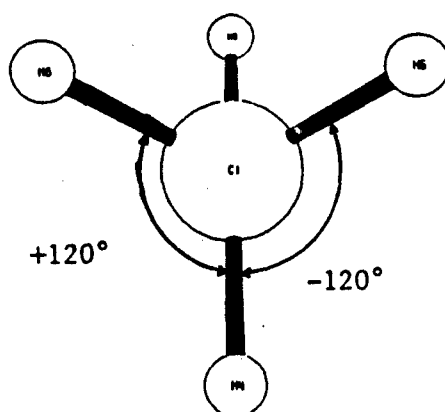


Figure 26. Neuman projection of H5 and H6 Dihedral angles

The complete Z-matrix is below:

C	0.00	0	0.00	0	0.00	0	0	0	0
O	1.40	1	0.00	0	0.00	0	1	0	0
H	0.95	1	107.0	1	0.00	0	2	1	0
H	1.12	1	105.0	1	180.0	1	1	2	3
H	1.12	1	111.0	1	120.0	1	1	2	4
H	1.12	1	111.0	1	-120.0	1	1	2	4

With this Z-matrix and the appropriate input keywords (see the MOPAC manual), the program will do a full geometry optimization of methanol. This is not the only possible Z-matrix for methanol but it gives the best contrasting examples of the two different dihedral angles. Other input examples are available in the MOPAC manual. The input for the systems studied in this work are far more complicated than that for methanol, but this input gives the basic knowledge needed to understand more complex molecular input.

Two final side notes should be made: (1) *ab initio* (Gaussian86 [64]) Z-matrices are slightly different than

those for MOPAC; the G86 manual explains the input procedure. (2) The input of molecules into MOPAC can be greatly simplified by using the DRAW program [102]. DRAW is a graphics program that draws a molecule atom by atom on a computer terminal as its Z-matrix is typed in. It cuts down on input errors and generates MOPAC input files on command. DRAW also reads MOPAC output allowing graphic visualization of results. All molecules studied in this work were input with DRAW.

#### Polymer Unit Cell Setup and Manipulation

The polymer calculations possible in MOPAC are not done on infinite polymer chains explicitly, but use what is termed the "cluster" method [30] to calculate the properties of a single polymer repeat unit or unit cell within an "infinite" chain. The program uses the geometry for the polymer unit cell and its unit cell length, called the translation vector (TV). It takes this data and repeats the cell several times, using the Born-von Karman cyclic boundary conditions [103], to create a cyclic molecule or "cluster" of repeat units which approximates an infinite polymer chain. There are no "end effects" which are present when an oligomer is used to estimate polymer properties. The resulting MOPAC calculation gives an optimized unit cell



length and a heat of formation for the repeat unit within a polymer chain. This method gives good agreement with experimentally determined repeat unit lengths and heats of formation [30,31]. The one major problem with this method is that the unit cell length needs to be at least 10Å long so the overlap of atomic orbitals between atoms at opposite ends of the cell is indeed negligible. This is no problem for the systems studied here (they all have repeat units longer than 10Å). For something like polyethylene, however, several repeat units must be calculated as the 'unit cell' to make a unit longer than 10Å. The resulting  $H_f$  for the cell would have to be divided by the number of repeat units in the cell to get the heat of formation per repeat unit. Figure 27 shows a piece of a cluster for polyethylene. The input cell has six repeat units in it and to either side of

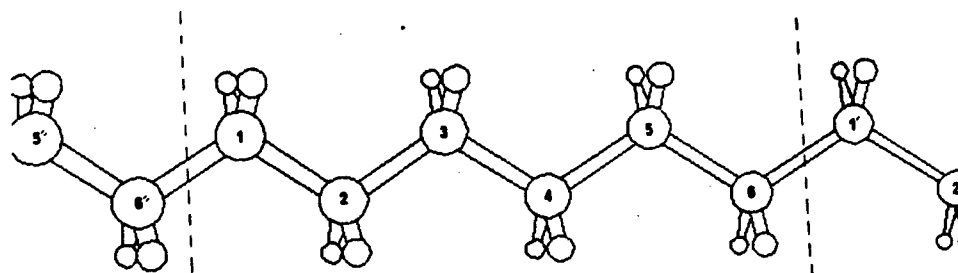


Figure 27. Piece of a Polyethylene Cluster

the input cell are cells translated into position by the program using the translation vector. By this technique each atom in the primary input cell 'sees' the same

environment as it would if it were in an infinite polymer chain. Figure 28 shows a trans-PBT unit cell with the translation vector marker being the seemingly unattached atom on the far left of the cell. This is where the carbon marked 'X' translates to begin the next cell.

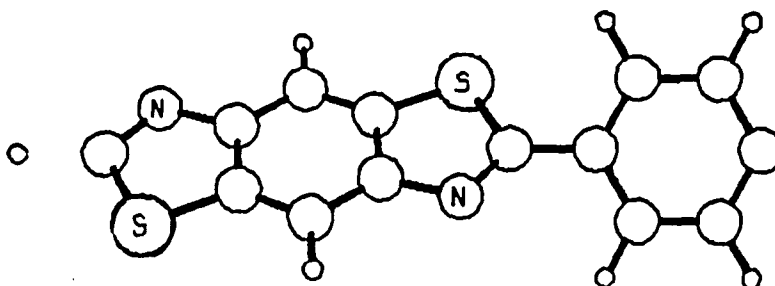


Figure 28. Trans-PBT Unit Cell with Translation Vector

When the polymer calculation is finished, the equilibrium length of the unit cell, the translation vector (TV), is a result. This TV represents the length of the repeat unit in its lowest energy geometry. The unit cell can now be 'stretched' or 'squeezed' by increasing or decreasing the translation vector away from its equilibrium value. This represents molecular tension or compression. When the translation vector is changed, the unit is reoptimized to the lowest energy geometry for the new cell length. The heat of formation will be higher for this new configuration than for the equilibrium length. So, by optimizing the geometry at several different values of TV, a

curve of heat of formation versus molecular tension and/or compression can be generated.

MOPAC allows incremental variations of any variable, including the translation vector, simply by using a '-1' as the optimization marker and adding a list of desired values for the variable to the bottom of the input file (see MOPAC manual). An entire geometry optimization is done for each value of TV and each optimized geometry is output along with its heat of formation. From the geometric data, molecular deformations, i.e. bond stretching, angle bending or twisting, can be monitored as a function of tensile or compressive strain, showing how the unit reacts to the input of compressive or tensile force. Force constants can be calculated from the second derivative of the heat of formation versus strain curve. Analyzing molecular deformation helps to explain tensile and compressive phenomena while force constants are used in the calculation of tensile moduli as described in the next section.

#### Tensile Modulus Calculations

Once the heat of formation versus strain data is generated, it can be used to determine the polymer's tensile modulus by the method described by Klei and Stewart [31]. The data is plotted as a curve and the curve is fitted to a

third order polynomial (equation 14),

$$\Delta H_{f,r}(\Delta L) = A(\Delta L)^3 + K/2(\Delta L)^2 + B(\Delta L) + C \quad (\text{equation 14})$$

where  $\Delta L$  is the change in translation vector length,  $K$  is the molecular force constant,  $\Delta H_{f,r}$  is the change in the heat of formation, and  $A$ ,  $B$ ,  $C$  and  $K/2$  are the coefficients of the polynomial. Once the curve is fitted, the force constant can be calculated for any point on the energy-strain curve.

The elastic modulus of a polymer is equal to the stress,  $\sigma$ , divided by the strain,  $\epsilon$ ; i.e. the slope of the stress-strain curve. The stress is a force per unit area ( $F/A$ ) and the strain is the change in length divided by the equilibrium length ( $\Delta L/L_{eq}$ ). Equation 15 shows the derivation of the modulus expression used in this program (note that  $K = F/\Delta L$ ).

$$E = \sigma/\epsilon = (F/A)/(\Delta L/L_{eq}) = F \cdot L_{eq}/\Delta L \cdot A = K(L_{eq}/A) \quad (\text{equat. 15})$$

The only parameter in equation 15 that doesn't fall out of the semiempirical MO calculations is the cross-sectional area,  $A$ . The easiest way to get a cross-sectional area is to input an experimental or estimated density,  $d$ , for the bulk material and use equation 16 to get equation 17, where

$$d = m/v = m/A_{eq}L_{eq} = nM_w/A_{eq}L_{eq} \quad (\text{equation 16})$$

$$A_{eq} = M_w/dN_A L_{eq} \quad (\text{equation 17})$$

$A_{eq}$  is the net cross-sectional area of the polymer chain at its equilibrium length,  $M_w$  is the molecular weight of the cluster,  $n$  is the number of moles,  $v$  is the volume, and  $N_A$  is Avogadro's number ( $n = 1/N_A$ ). The introduction of the experimental density (crystal density when available) builds the average chain environment into the calculation, so this method calculates the tensile modulus of a 'perfect polymer system' where all chains are horizontally aligned and of infinite molecular weight. There are no imperfections in the system, such as chain ends or voids, so there are no failure modes possible in the system except the breaking of chemical bonds. This is the ultimate modulus possible for the uniaxially oriented material.

In all the calculations performed here the repeat units were stretched from  $\Delta L/L_{eq} = 0$  to  $\Delta L/L_{eq} = 0.15$  or 15% strain. The Poisson ratio was made zero so the cross-sectional area remained constant at  $A_{eq}$  throughout the modulus calculation. Since the modulus program refits the curve for each new point added, a different force constant and modulus ( $E = KL_{eq}/A$ ) is calculated for every point on the energy versus strain curve. This is done to show the region

where  $K$  really becomes computationally constant (Figure 29). The reported modulus is calculated from the force constant in this region. Experimental crystal densities are used when available and density estimates where necessary. The calculated moduli are compared to experimentally determined moduli when they are available.

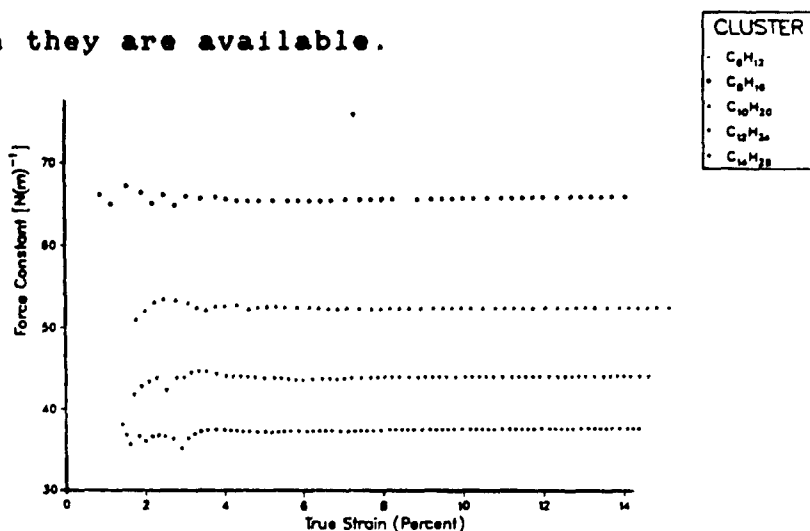


Figure 29. Polyethylene  $K$  versus True Strain [31]

## SECTION IV

### RESULTS AND DISCUSSION

#### General

Every attempt to employ mathematical methods in the study of chemical questions must be considered profoundly irrational and contrary to the spirit of chemistry. If mathematical analysis should ever hold a prominent place in chemistry-an aberration which is happily almost impossible-it would occasion a rapid and widespread degeneration of that science [104].

A. Compté 1798-1857

Each polymer studied in this research was stretched by +15% of its equilibrium length and compressed by -3% of its equilibrium length. The tensile moduli were calculated for each system and compared to experimentally determined values when available. Detailed molecular deformation analyses were performed for cis-PBI, cis-PBO, trans-PBT, PPPI, PPP, PQ and polyacene. The heat of formation versus percent strain curve is shown for each of these seven systems along with plots revealing the tensile and compressive deformation patterns for these molecules. Geometries are shown for each system at equilibrium, at the onset of tensile failure (when it occurs), at the brink of compressive failure (when it occurs), and at high compression. The results for these ordered polymers are tabulated and correlations between molecular structure are attempted.

# Tensile Modulus Results

	$L_{eq}$ (Å)	$M_w$ (g/mol)	$d$ (g/cc)	$A_{eq}$ (Å <sup>2</sup> )	$K$ (N/M)	Modulus (GPa)
cis-PBI	12.31	232.24	1.50*	20.89	113.8	670
trans-PBI	12.30	232.24	1.50*	20.90	113.0	665
cis-PBO	12.22	234.21	1.65*	19.29	115.3	730
trans-PBO	12.20	234.21	1.65*	19.33	112.1	707
cis-PBT	12.51	266.35	1.69*	20.92	102.1	610
trans-PBT	12.56	266.35	1.69*	20.84	100.4	605
PPPI	12.49	290.23	1.50*	25.72	107.1	520
PQ	10.71	203.24	1.50*	21.01	100.3	511
PPP	8.54	152.20	1.35*	21.92	117.0	456
Polyacene	7.34	150.18	1.50*	22.65	291.7	945
BBL	12.33	334.29	1.65*	27.29	159-165	720-745
Graphite	7.34	438.44	2.26*	43.87	881-911	1475-1525

\* = estimated density [105]  
 \* = x-ray calculated density [106]

Table 1. Tensile Modulus Results

Table 1 contains the results of the tensile modulus calculations for all twelve systems studied.  $L_{eq}$  is the calculated equilibrium length for the polymer repeat unit, in angstroms;  $M_w$  is the molecular weight of the repeat unit used, in grams/mole;  $d$  is the density input into the computation, in grams/cm<sup>3</sup>;  $A_{eq}$  is the equilibrium cross-sectional area calculated from the density by equation 17, in square angstroms;  $K$  is the force constant from the energy-vs-strain curve fit, in Newtons/meter; and modulus is the elastic modulus calculated from  $K$ ,  $L_{eq}$ , and  $A_{eq}$  using equation 15, in 10<sup>9</sup> Newtons/meter<sup>2</sup> (GPa). The densities used were obtained from x-ray diffraction data for PBO, PBT, BBL and graphite and estimated from available model compound data



for PBI, PPPI, PPP, and PQ. Since polyacene has never been made, the density used here is an educated guess. Should the estimated densities be too high or too low the correct modulus,  $E_{cor}$ , can be easily calculated by multiplying the estimated modulus reported here,  $E_{est}$ , by the ratio of the correct density,  $d_{cor}$ , over the estimated density,  $d_{est}$ :

$$E_{cor} = E_{est}(d_{cor}/d_{est}) \quad (\text{equation 18})$$

This works because the modulus is inversely proportional to the cross-sectional area (equation 15) and cross-sectional area is inversely proportional to the density (equation 17), therefore the modulus is directly proportional to the density. This correction may have to be made for those systems whose densities were estimated as better density values become available.

Table 2 shows a comparison of the AM1 calculated modulus, the Stewart and Klei MNDO calculated modulus [31], the x-ray diffraction modulus, and the experimental tensile modulus from a polymer fiber for systems where some or all of these numbers are available. Stewart's moduli have been adjusted to account for the more accurate densities of PBO, PBT, and PPP reported in this work. This way the modulus obtained from the two different semiempirical methods can be fairly compared. The Stewart calculated modulus of

polyethylene is also compared with experimental and x-ray moduli to show the validity of the modulus calculation technique; other examples are available in [31].

	AM1 (GPa)	MNDO <sup>31</sup> (GPa)	X-ray <sup>106</sup> (GPa)	Experimental <sup>106</sup> (GPa)
Cis-PBO	730	670	475	330
Trans-PBO	707	619	-	-
Cis-PBT	610	602	-	-
Trans-PBT	605	528	400	300
PPP	456	448	-	-
Graphite	1475-1525	-	830	770
Polyethylene	-	362	235-358 <sup>107</sup>	

Table 2. Comparison of AM1, MNDO, and Experimental Moduli

The differences in the AM1 and MNDO moduli can be accounted for by considering the inherent differences in the two MO methods. The MNDO Hamiltonian is known to overestimate nuclear-nuclear repulsions and, as a consequence, it predicts a minimum energy geometry for the PBO and PBT rods where the phenyl and heterocyclic rings in the polymer are perpendicular to each other. AM1 predicts, more correctly, that the rings are planar or near planar to each other [108]. This difference in calculating energy minima causes different energy vs strain curves to be generated, thus giving a different force constant and corresponding modulus.

This accounts for the significant difference in the PBO results but not for the similarity in the PBT and PPP moduli. Unfortunately there are no AM1 parameters for

sulfur at present, so the PBT calculations were done with MNDO parameters for sulfur and AM1 parameters for all other atoms. This results in a minimum energy geometry where the heterocycle and phenyl are at  $40^\circ$  angle to each other instead of near planar [108]. The 'semi' AM1 treatment produces an energy vs strain curve more similar to that produced by MNDO than in the PBO case. Therefore the force constants and the moduli are similar. One would expect the AM1 modulus to be higher if sulfur parameters were available. In the PPP case the minimum energy geometry is nearly the same for both AM1 and MNDO, the phenyl rings being perpendicular to each other. This is due to the presence of hydrogens at all positions ortho- to the ring junction, while in PBO and PBT only two of the four positions are occupied. The energy vs strain curves are thus quite similar, along with the force constant and modulus. The AM1 values are better than the MNDO values due to its better treatment of the energies and geometries. Both methods give reasonable agreement to the experimental numbers available. AM1 gives the highest potential modulus for each material.

Turning back to the results in Table 1, there are some interesting points to note besides the direct comparison of the moduli for the different materials (the table clearly shows which materials are predicted to have higher moduli). First, in the all the PBx polymers the cis- isomers have

higher moduli than their trans- counterparts (Stewart saw this also). The reason for this is still unclear. Secondly, the PBO polymers show significantly higher moduli than the PBI and PBT systems. Remember, however, that the 1.50 g/cc density for the PBI's is a conservative estimate and if the true density is near that of the PBO's, which is not unreasonable, the moduli would be 737 GPa for cis-PBI and 732 GPa for trans-PBI, both higher than their PBO counterparts. In this case there is some evidence of a trend of decreasing modulus with increasing size of the x-atoms in the PBx systems. To confirm this a better density for the PBI's and studies on different atoms in the x-positions of PBx systems are needed.

It also appears from Table 1 that systems with phenyl moieties aligned only horizontally along the tension axis (PPP,PQ) have lower moduli than those having phenyl moieties aligned only vertically on the tension axis (polyacene), with those systems having phenyls with both orientations (PBI, PBO, PBT, PPPI and BBL) have moduli intermediate between the two extremes (Figure 30 defines the vertical and horizontal orientations of a phenyl ring). This suggests that it is easier to stretch a phenyl ring in the horizontal direction than in the vertical direction. This is an exciting new insight into the designing of new high modulus materials. It explains the large difference in the moduli of

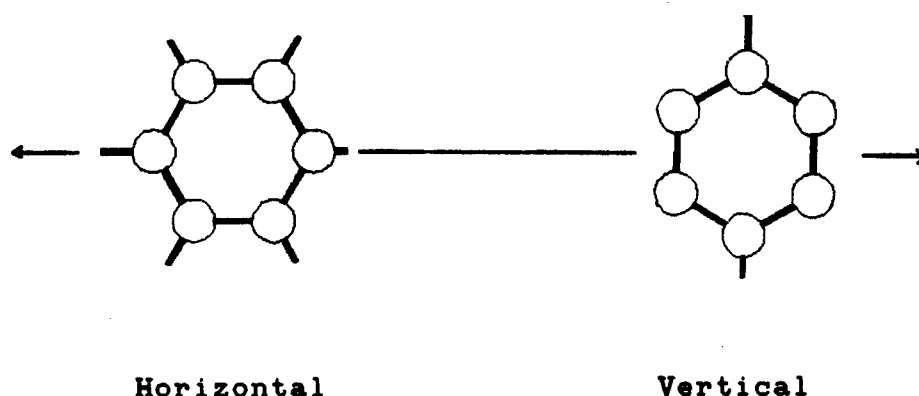


Figure 30. Orientations of a Phenyl Group on Tension Axis

the two ladder polymers, polyacene and BBL, BBL containing four horizontally oriented phenyls along the tension axis. Studies on other systems with phenyl moieties need to be made to show that this is universally true. The graphite model studied here contains all vertically oriented phenyls, if the other orientation were studied and the above postulated is true, that orientation of graphite should have a modulus significantly lower than 1475 GPa. This study is still pending. This phenomenon will be discussed in more detail in the molecular deformation analysis.

Comparing polyacene and graphite in Table 1 yields another interesting insight. It is not possible, with MOPAC as it stands now, to make a polymer system 'infinite' in more than one direction, which is what would be needed to correctly model graphite. Therefore, an approximate 'graphite cluster' was built that is five phenyls wide and two and a half phenyls long with the translation

vector along the length direction as usual (Figure 31). This is essentially five polyacene clusters (Figure 20) fused together widthwise. The equilibrium lengths of the polyacene and graphite clusters are both 7.34 angstroms. Noting that the graphite modulus of 1475-1525 GPa is not five times that of the polyacene, 945 GPa, and remembering that

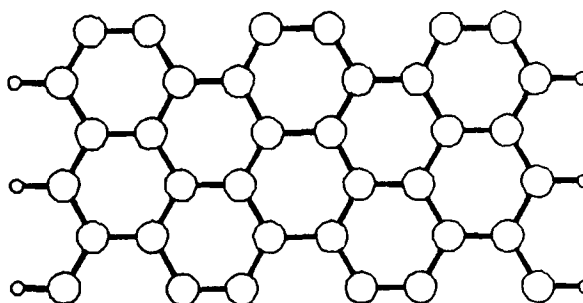


Figure 31. Graphite Repeat Unit

the density of 1.50 g/cc is a conservative guess for the density of polyacene (if the true density were 1.65, for example, the modulus would be 1040 GPa), one would assume that there is an asymptotic limit to the modulus in one direction with increase in the width of the "graphite chain." Studies on several different repeat unit widths will have to be done to confirm this, the limiting factor being the availability of massive amounts of computer time and space.

These moduli are the theoretical maximum moduli for these materials and are, as expected, higher than those moduli obtained from x-ray diffraction which are in turn

higher than the moduli obtained from the tensile testing of fibers. These calculated moduli are reasonable values for the perfectly aligned, infinite polymer solid that cannot yet be produced by today's fiber or crystal processing technology. As these technologies improve, moduli approaching these calculated maxima may well be possible.

### Molecular Deformation Analysis

Although the calculation of ultimate tensile moduli gives quantitative information on the relative strength of different materials and what types of structure give high strengths, it does not provide an explanation of why different molecular structures exhibit different moduli and strengths. In order to explain why one structure is stiffer or stronger than another, the structure's responses to molecular tension and compression must be examined. This examination will give insights into why different structures exhibit the tensile and compressive properties they do.

A molecular deformation analysis can be performed by examining changes in all of the bond lengths, bond angles, and dihedral angles in a polymer repeat unit with tension or compression of the unit. However, that would give more information than necessary to examine the problem and the huge amount of data would be difficult to effectively

digest. An easier approach is to choose certain distances and angles within the unit that have incorporated in them several of the unit's bond lengths and angles so that changes in bonds lengths or angles result in a change in the value of the distance. An example is the length of the benzothiazole moiety in PBT along the tension/compressive axis. Changes in the bond lengths, bond angles, and dihedral angles within the benzothiazole moiety manifest themselves in a change of the overall benzothiazole length. This way all of the geometric variables in the repeat unit can be indirectly monitored by keeping track of only a few values.

For the rigid rod polymers studied here, five values are monitored: the length of the heterocyclic moiety, the length of the phenyl moiety, the length of the carbon-carbon bond connecting the two groups, the torsion angle between the heterocycle and the phenyl, and an angle defining the coplanarity (or colinearity) of the two groups. The lengths are plotted as a percentage change from their equilibrium values versus the percent strain, compressive or tensile, on the unit as a whole. The absolute values of the angles are plotted versus percent unit strain. From these plots, the effects of the different pieces of the repeat unit on the molecule's modulus, tensile strength, and compressive strength can be examined.



**Cis-Poly(p-phenylenebenzobisimidazole) (cis-PBI)**

Figure 32 shows the cis-PBI repeat unit in four stages:  
at equilibrium, right before tensile failure where the bond

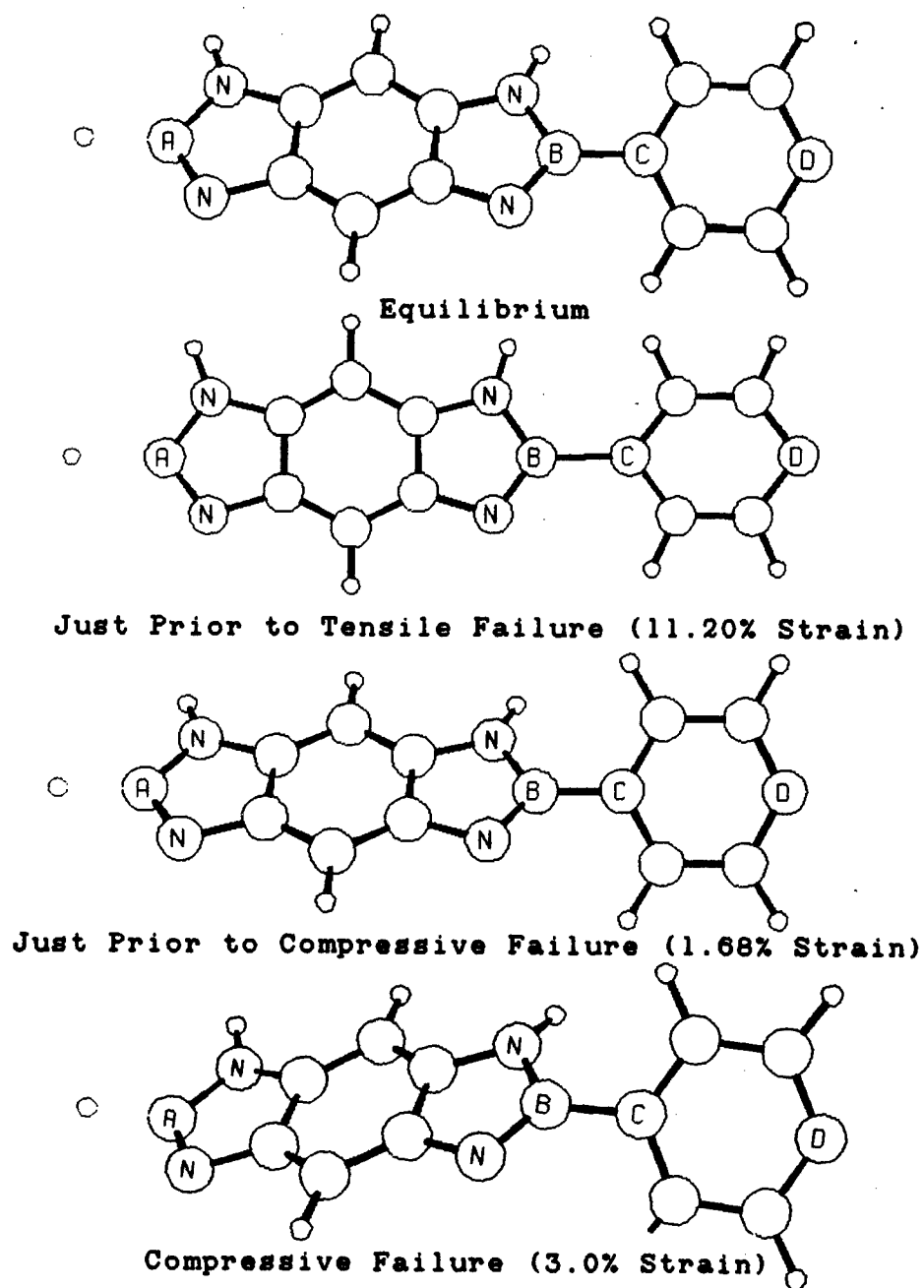


**Figure 32. Cis-PBI at Four Points Along Energy-Strain Curve**

between atoms B and C breaks, right before compressive failure where the angle between atoms A, B, and D becomes nonlinear, and long after compressive failure has occurred. These are the geometric points of interest along the energy versus strain curve (Figure 33) as they illustrate the

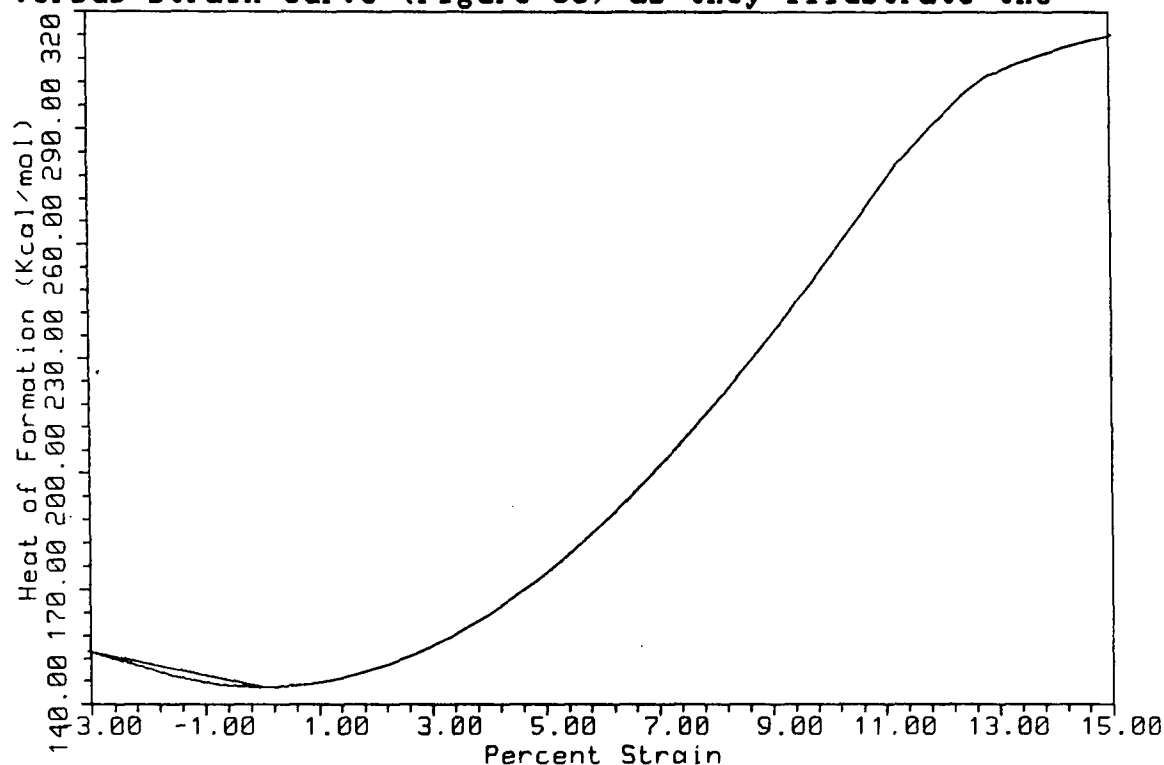


Figure 33. Cis-PBI Energy vs Strain (-3 to +15%) Curve

cumulative deformation of the molecule from tension and compression. In order to fully understand the tensile and compressive phenomena the deformations of the different pieces of the molecule must be examined, as stated earlier. The values used to monitor deformation in the cis-PBI repeat unit can be best explained by looking back to figure 32.

The length of the heterocyclic piece is the distance between atoms A and B (AB). BC is the carbon-carbon bond length connecting the heterocycle and the phenyl moiety. The phenyl length is represented by the distance between atoms C and D (CD). The torsion angle is the twist angle around the carbon-carbon bond, BC, and the angle between atoms A, B, and D is monitored as a measure of the coplanarity of the phenyl and heterocyclic groups. The other rigid rods are monitored in the same manner with the same lettering scheme for the atoms, lengths, and angles so this explanation will be assumed when discussing those systems (PQ is slightly different and will be explained later).

Figures 34-37 show the variation of the C-C bond (BC), the phenyl length (CD), the benzimidazole length (AB), and the torsion angle respectively versus tension of the cis-PBI unit (the lengths are plotted as percent strain from equilibrium values). As the unit is stretched all three lengths increase. The benzimidazole length begins at 6.576Å and increases to a maximum of 7.009Å, +6.58%, before tensile failure occurs at 11.20% strain of the polymer. The phenyl length starts at 2.797Å and rises to 3.182Å, +13.77%, before falling at tensile failure. The C-C begins at 1.467Å and increases slowly to 1.763Å, +20.20%, then the bond breaks and the distance increases dramatically (tensile failure). The torsion angle starts out at 35° and decreases to zero,

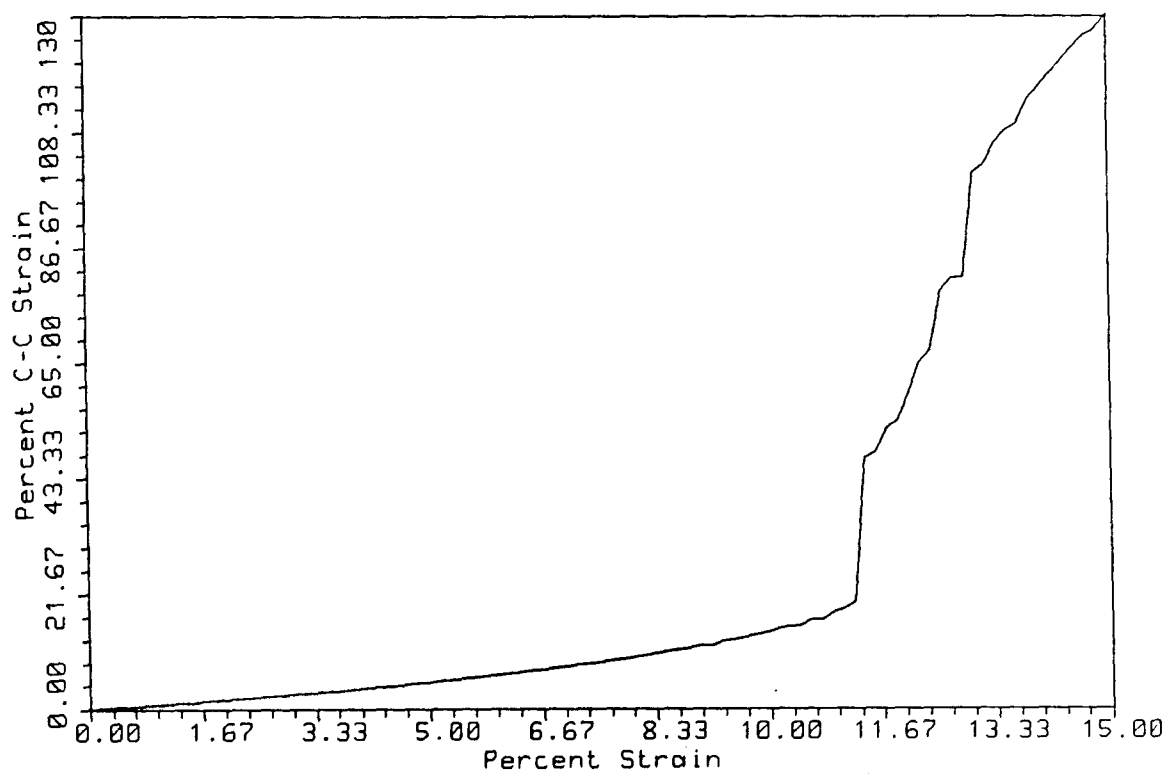


Figure 34. C-C Strain vs Cis-PBI Tension

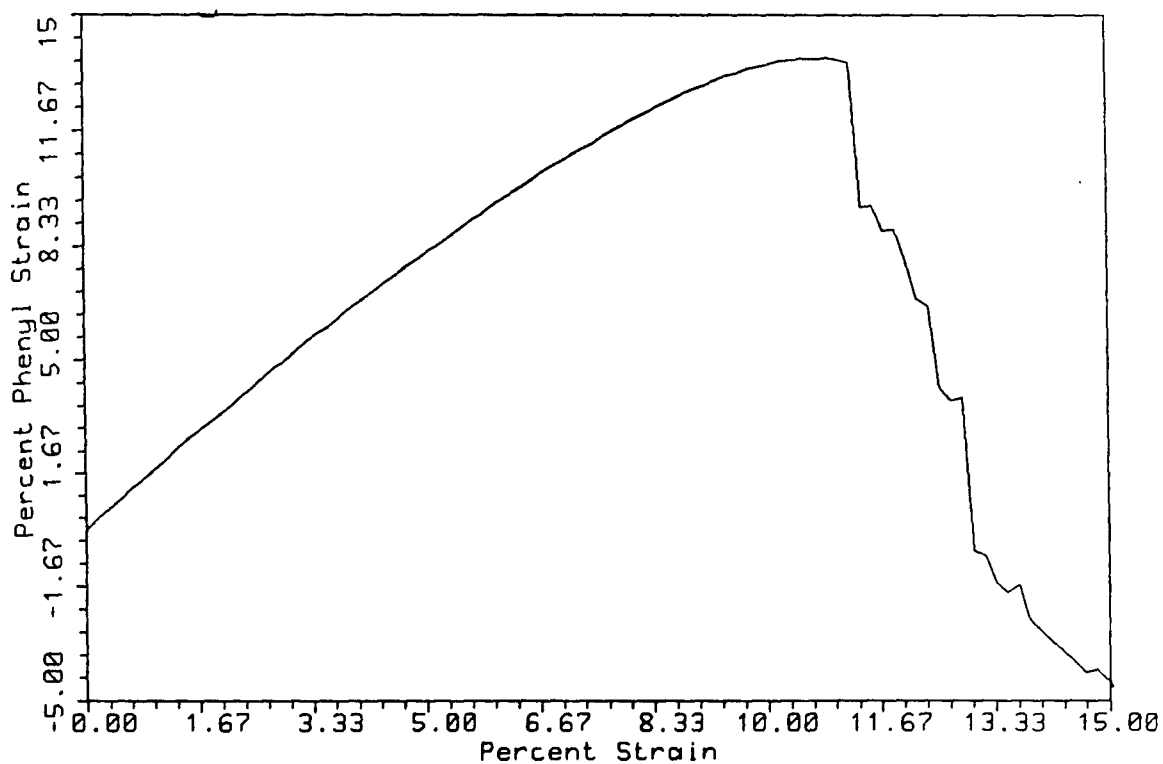


Figure 35. Phenyl Strain vs Cis-PBI Tension

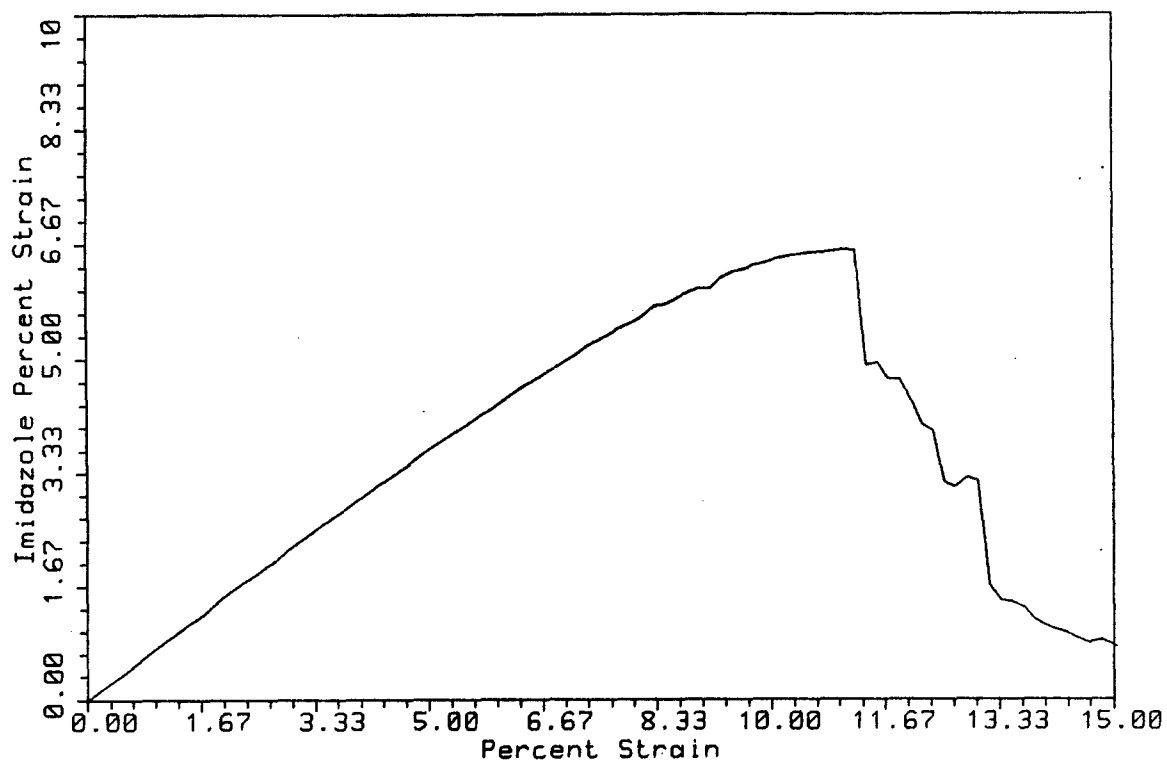


Figure 36. Benzimidazole Strain vs Cis-PBI Tension

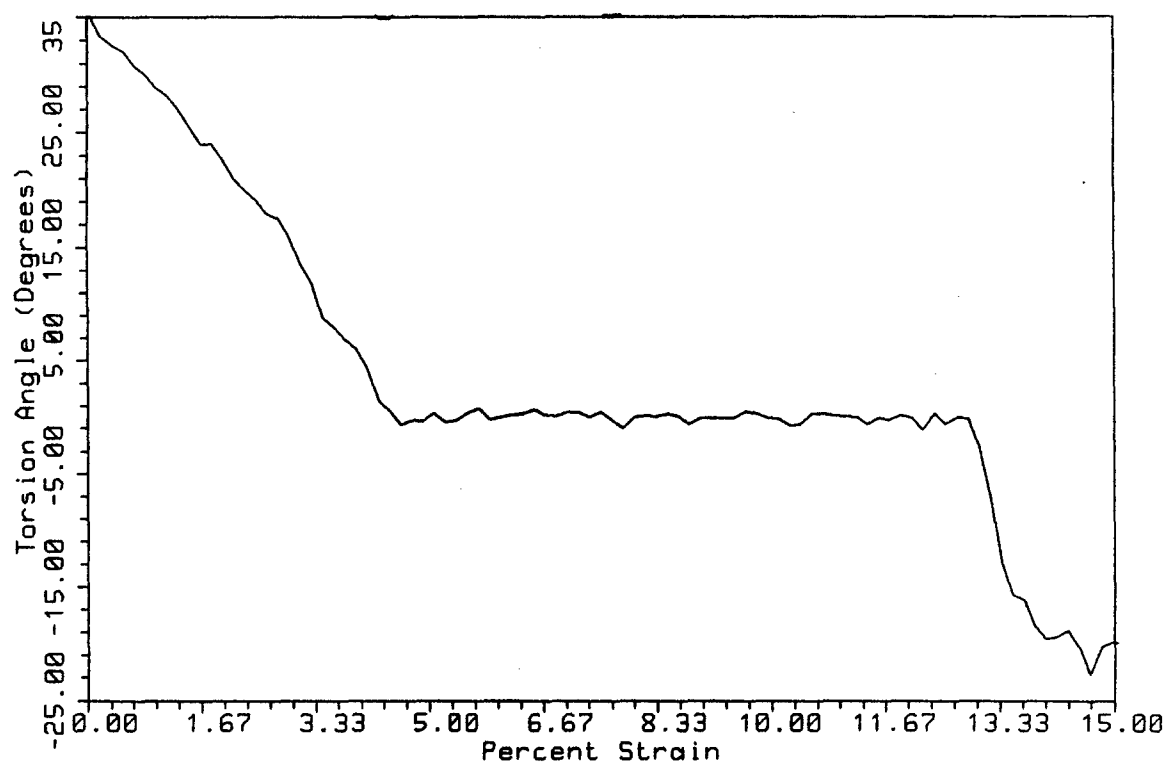


Figure 37. Torsion Angle vs Cis-PBI Tension

indicating planarity, at 4.5% strain. Interestingly, the phenyl ring is deformed more than twice as much as the benzimidazole and the two groups become planar with tension. The colinearity of the groups does not change with tension. The tensile strain, 11.20%, needed to break the repeat unit is very high compared to the strains that break bulk rigid rod materials [109]. This is not surprising as the only possible mode of failure here is bond breakage while imperfections in bulk materials can cause premature failure. It takes 136.8 kcal/mole of energy (from the energy curve) to bring the cis-PBI to tensile failure.

Figures 38-42 show the variations in C-C length, phenyl length, benzimidazole length, torsion angle, and colinearity angle respectively with percent cis-PBI compressive strain. The most interesting point here is that the colinearity angle (ABD) remains relatively constant ( $\pm$  or  $- 2^\circ$ ) until 1.93% compressive strain on the unit where it increases dramatically meaning the unit bends or "kinks." The typical mode of compressive failure in rigid rod polymer fibers is kinking [110], so for our purposes this molecular bending will be termed compressive failure. As the cis-PBI unit is compressed the C-C length shrinks almost linearly to 1.447Å, -1.38% from equilibrium, before it rises sharply as the polymer starts to bend. The phenyl group shrinks to 2.701Å, -3.44%, almost linearly before it also increases

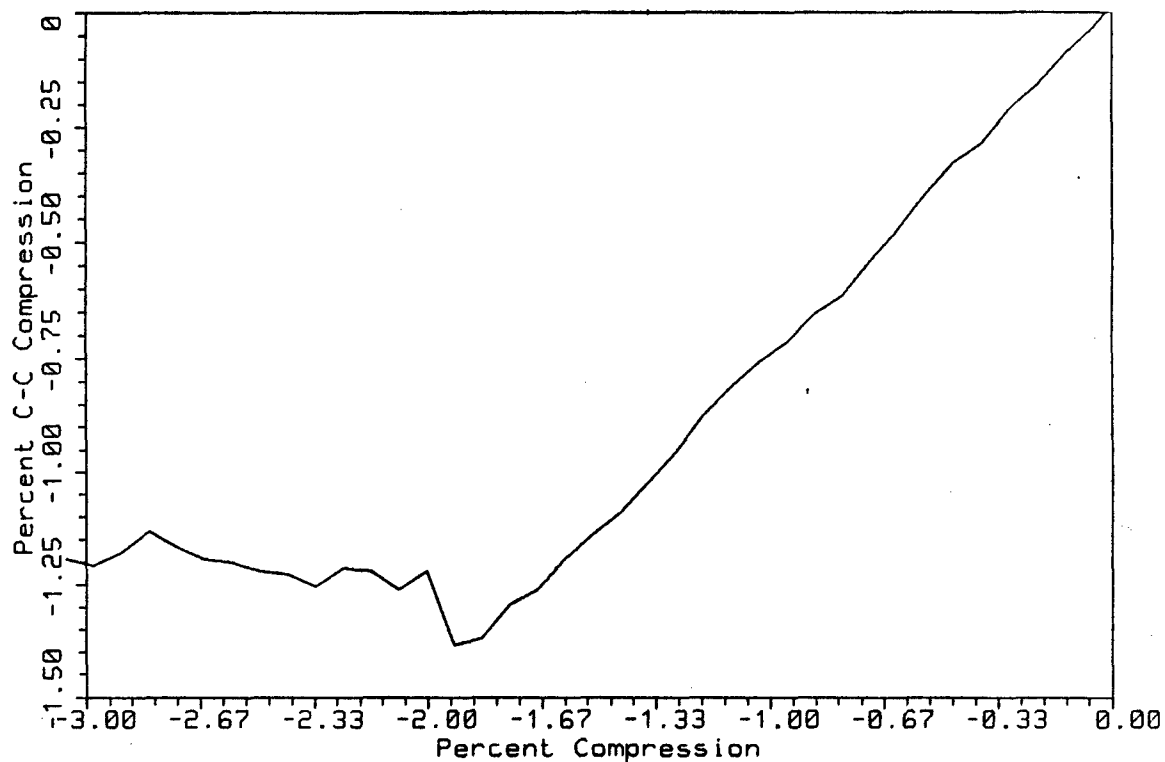


Figure 38. C-C Length vs Cis-PBI Compression

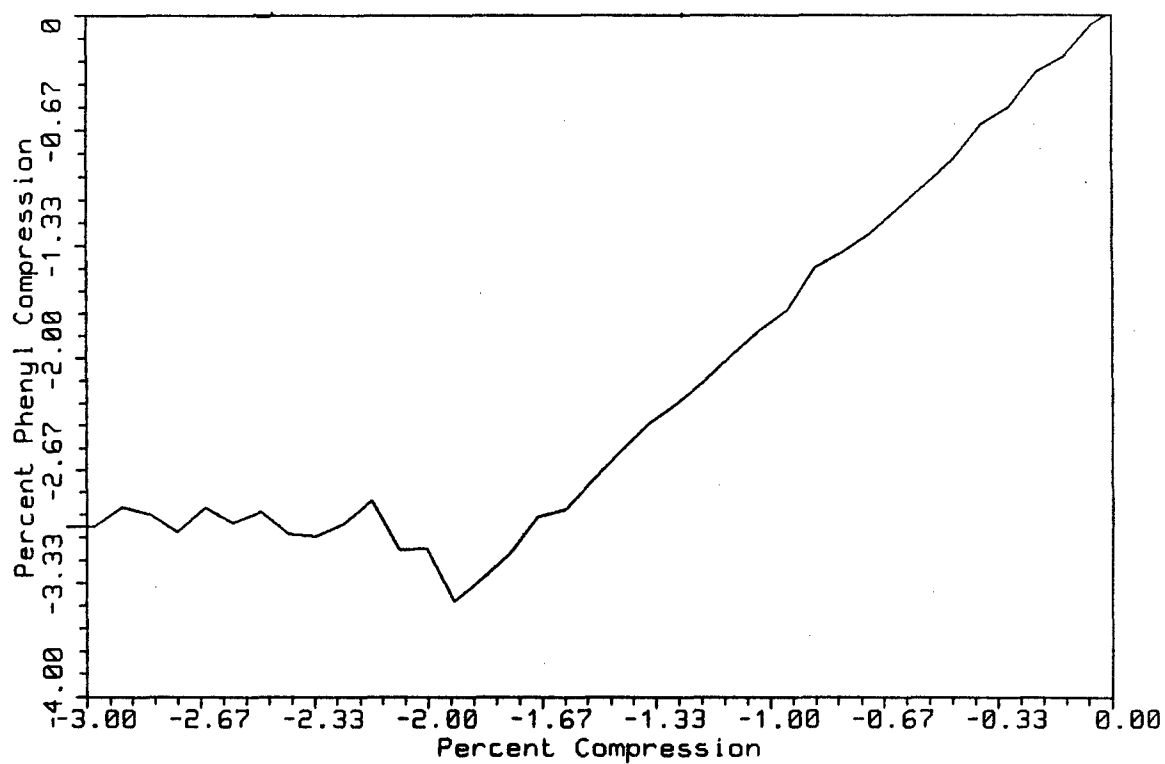


Figure 39. Phenyl Length vs Cis-PBI Compression

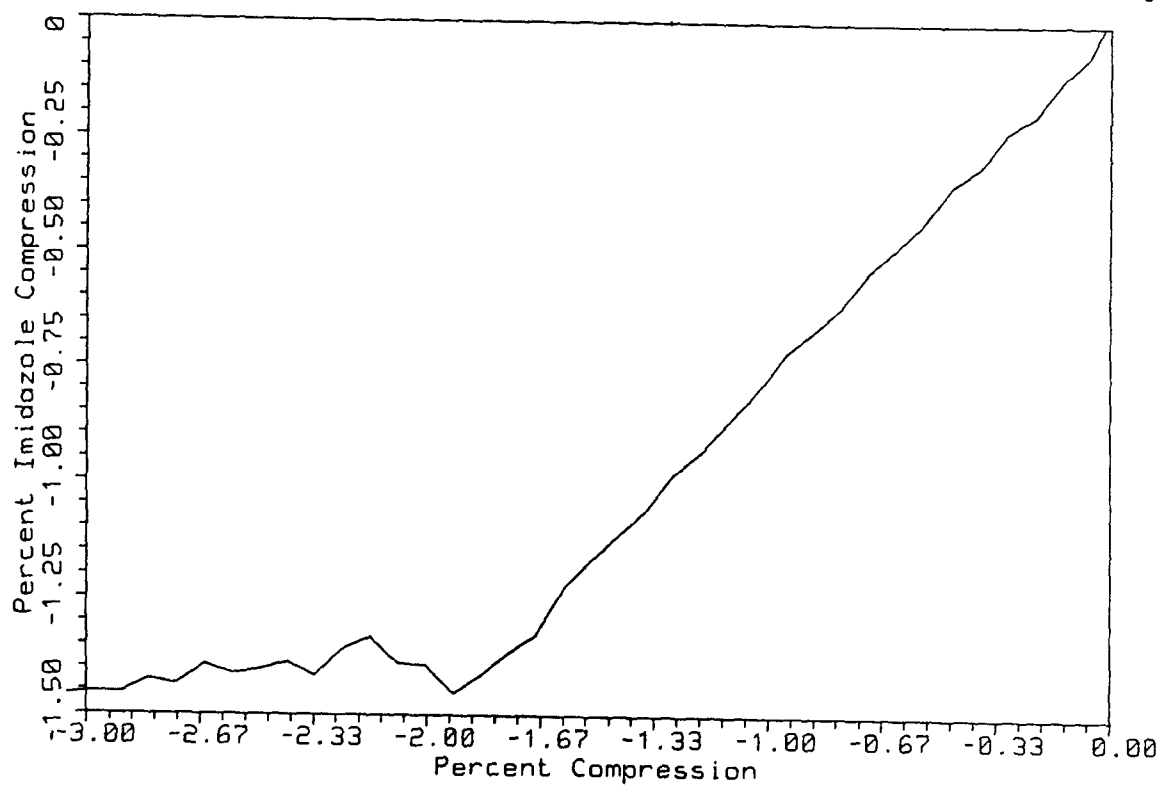


Figure 40. Benzimidazole Length vs Cis-PBI Compression

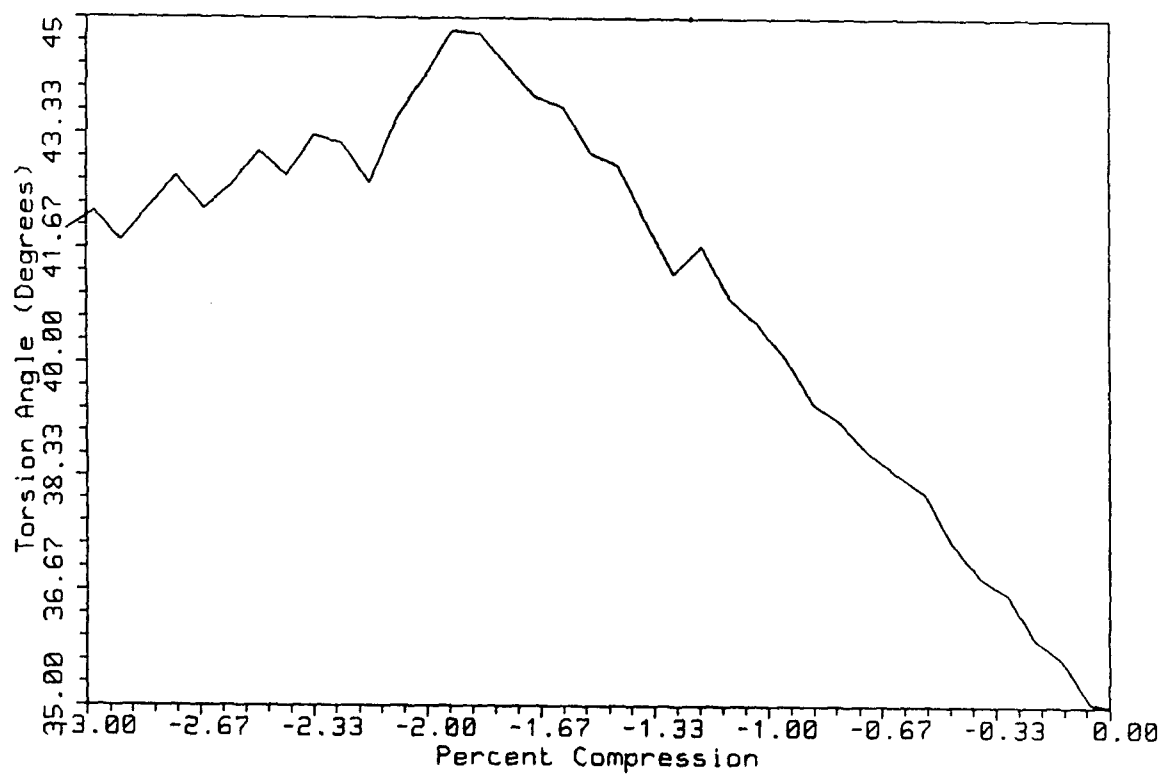


Figure 41. Torsion Angle vs Cis-PBI Compression



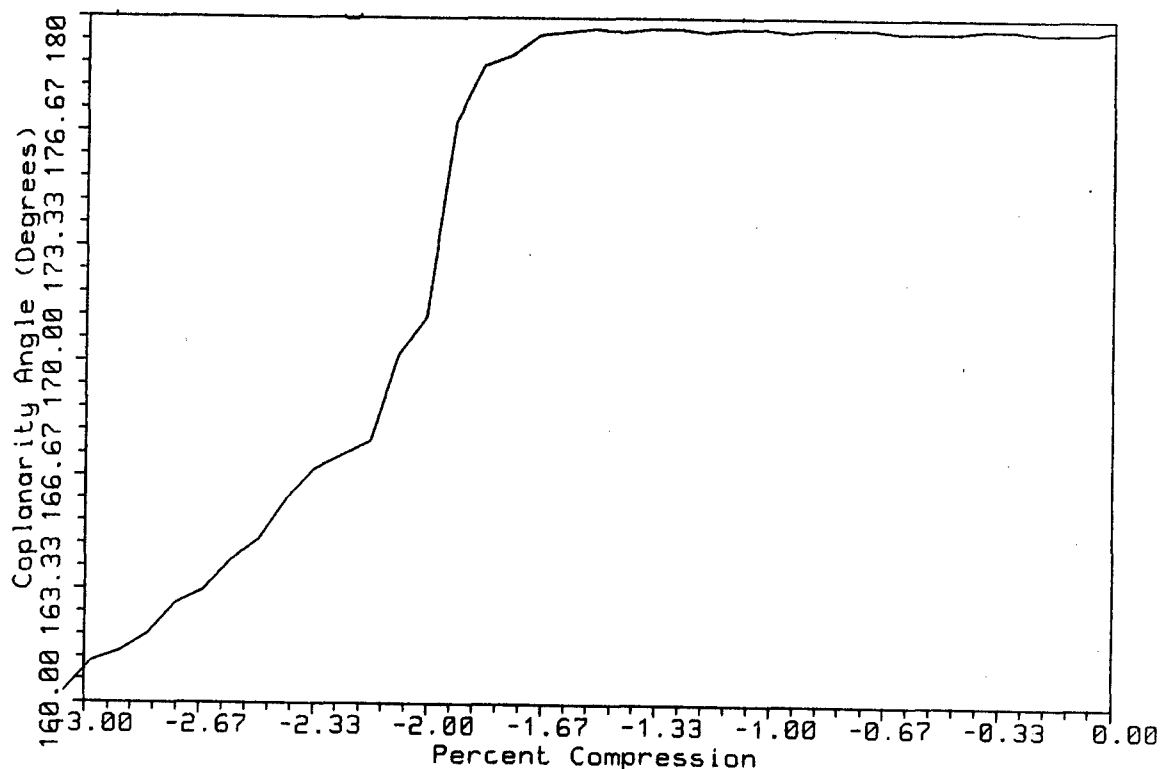


Figure 42. Colinearity Angle vs Cis-PBI Compression

after compressive failure. The benzimidazole exhibits similar behavior, shrinking to 6.480Å, -1.46%, before increasing at 1.93% cis-PBI compressive strain. The torsion angle increases in a linear fashion from 35° to 45° and begins to decrease at the compressive failure point. It should be noted here that the phenyl ring deforms more than twice as much as the benzimidazole, just as it did in tension. Also, the torsion angle increases with compression while it decreases with tension. The plots show that the compression is absorbed completely by the C-C bond length and the rings until enough energy is put into the system to force the molecule to bend, 4.62 kcal/mole in this case.

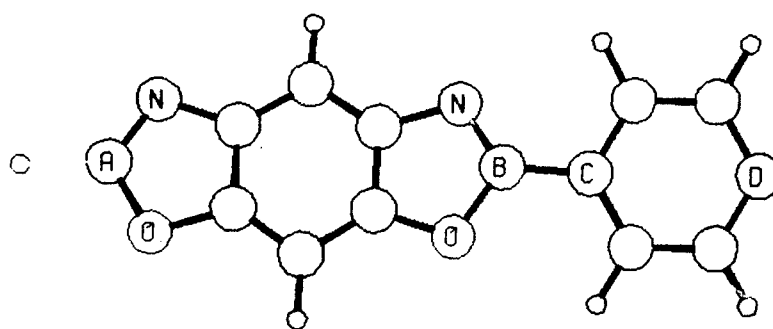
After bending starts, more compression results in more bending with the monitored lengths increasing back towards their equilibrium values.

This type tensile and compressive behavior is seen in all of the heterocyclic rigid rods studied here. So, the in depth explanations given above will not be necessary for the other systems. The plots of the deformation pattern will be given for PBO and the pertinent results highlighted for each polymer. The results will be tabulated for all the systems.

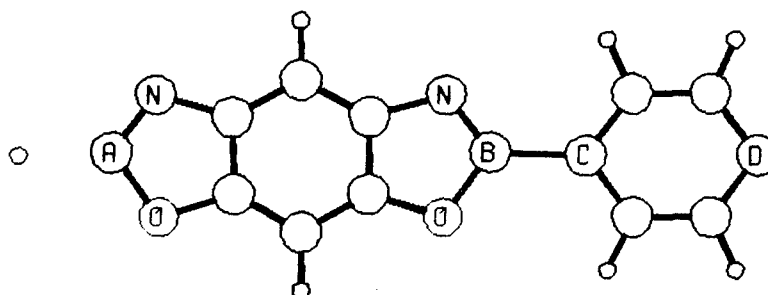
Cis-Poly(p-phenylenebenzobisoxazole) (cis-PBO)

Figure 43 shows the cis-PBO repeat unit at equilibrium, just prior to tensile failure, just prior to compressive failure, and after compressive failure. Figures 44-53 show the energy vs strain curve and deformation patterns for cis-PBO. Cis-PBO behaves much like cis-PBI.

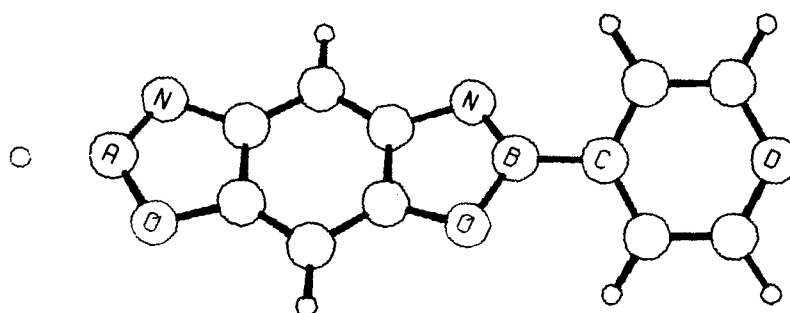
In tension, the C-C bond stretches 20.42% before breaking at 11.81% unit strain where tensile failure occurs. The phenyl ring stretches by 13.64% and the benzoxazole by 7.21% before they both recoil after failure. The torsion angle is 16° at equilibrium and goes to zero at 1.33% unit strain. 140.22 kcal/mole of energy is required to bring cis-PBO to tensile failure.



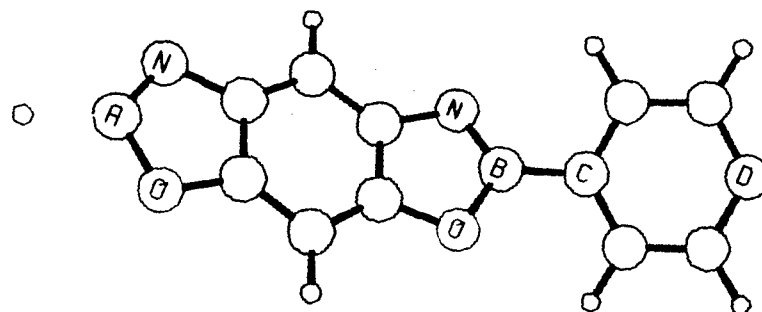
Equilibrium



Just Prior to Tensile Failure (11.81% Strain)



Just Prior to Compressive Failure (2.10% Strain)



Compressive Failure (3.0% Strain)

Figure 43. Cis-PBO Four Points Along Energy-Strain Curve

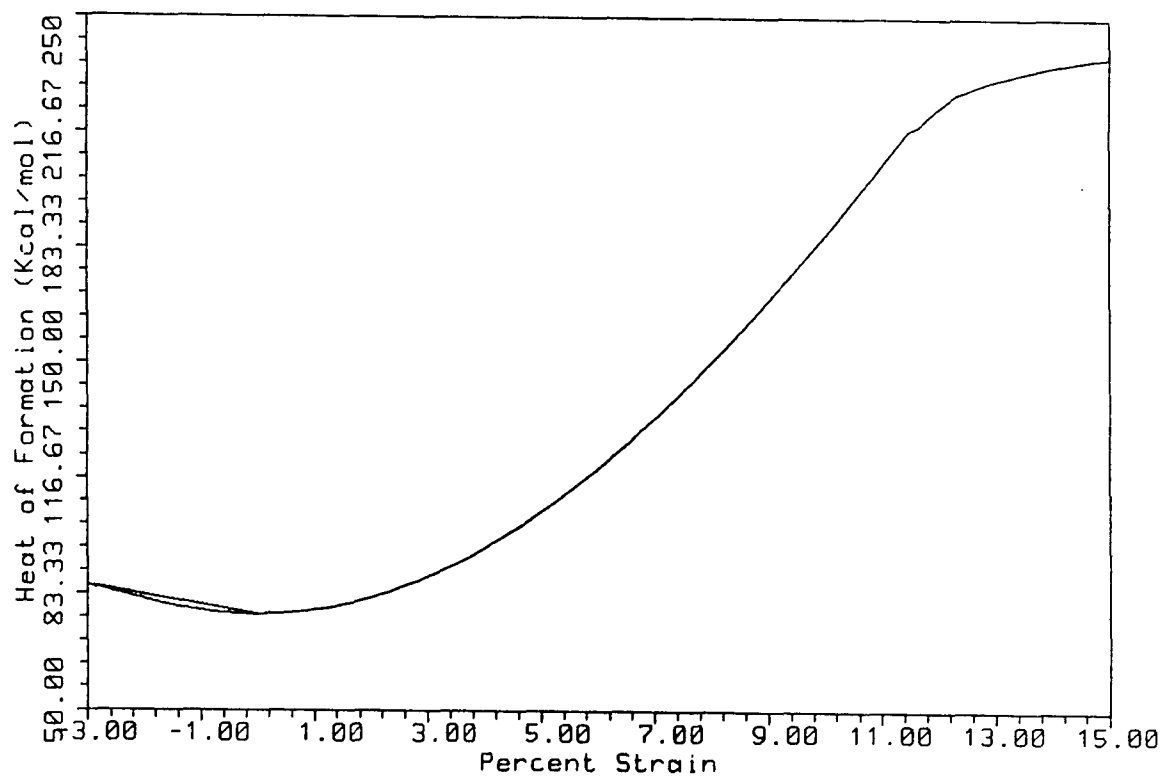


Figure 44. Cis-PBO Energy vs Strain (-3 to +15%) Curve

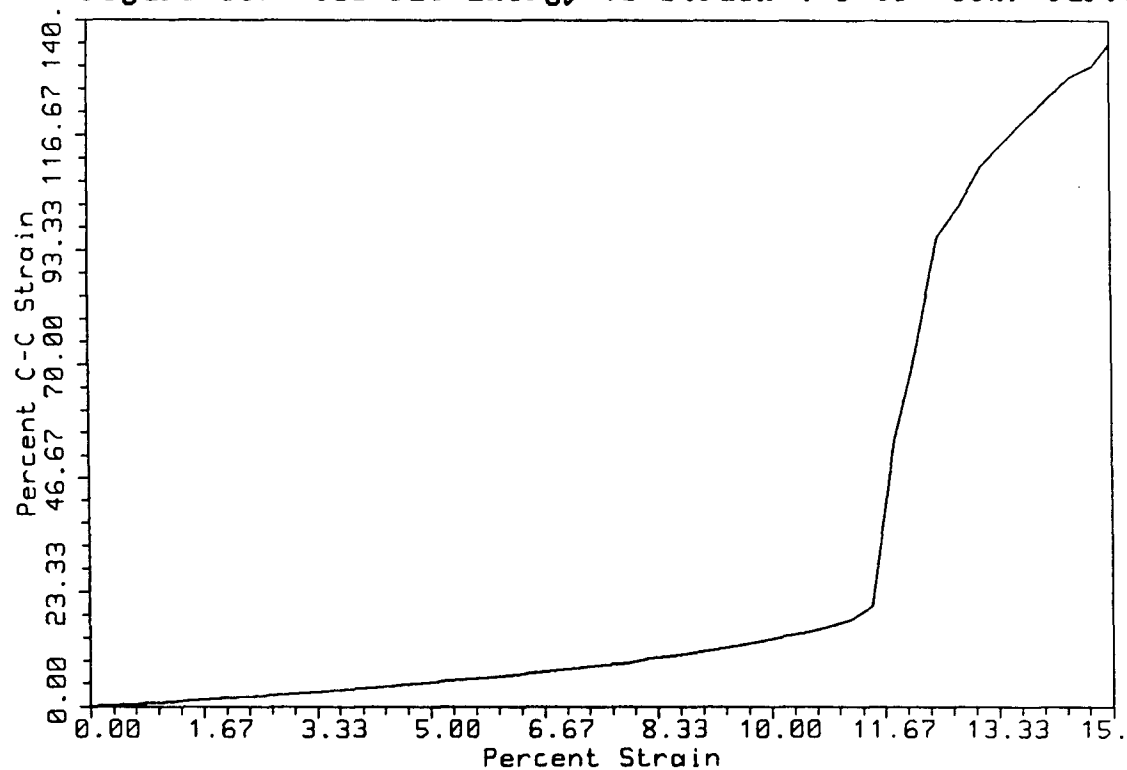


Figure 45. C-C Length vs Cis-PBO Tension

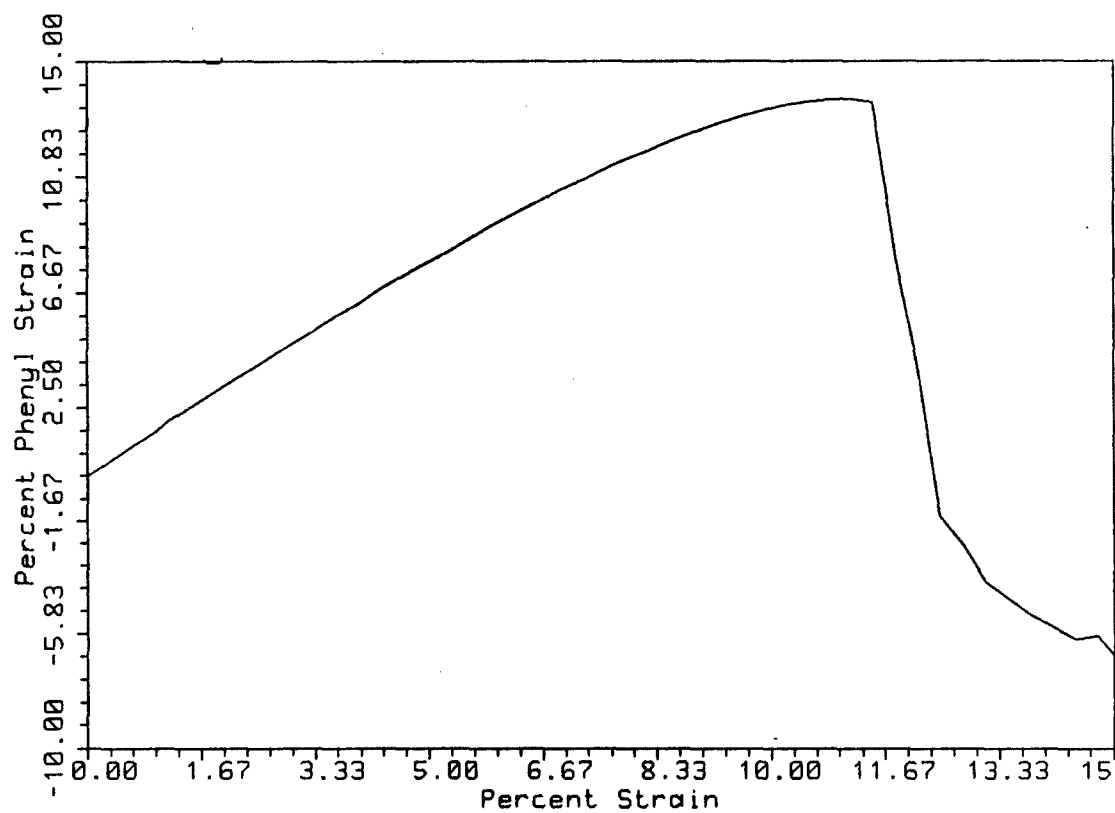


Figure 46. Phenyl Length vs Cis-PBO Tension

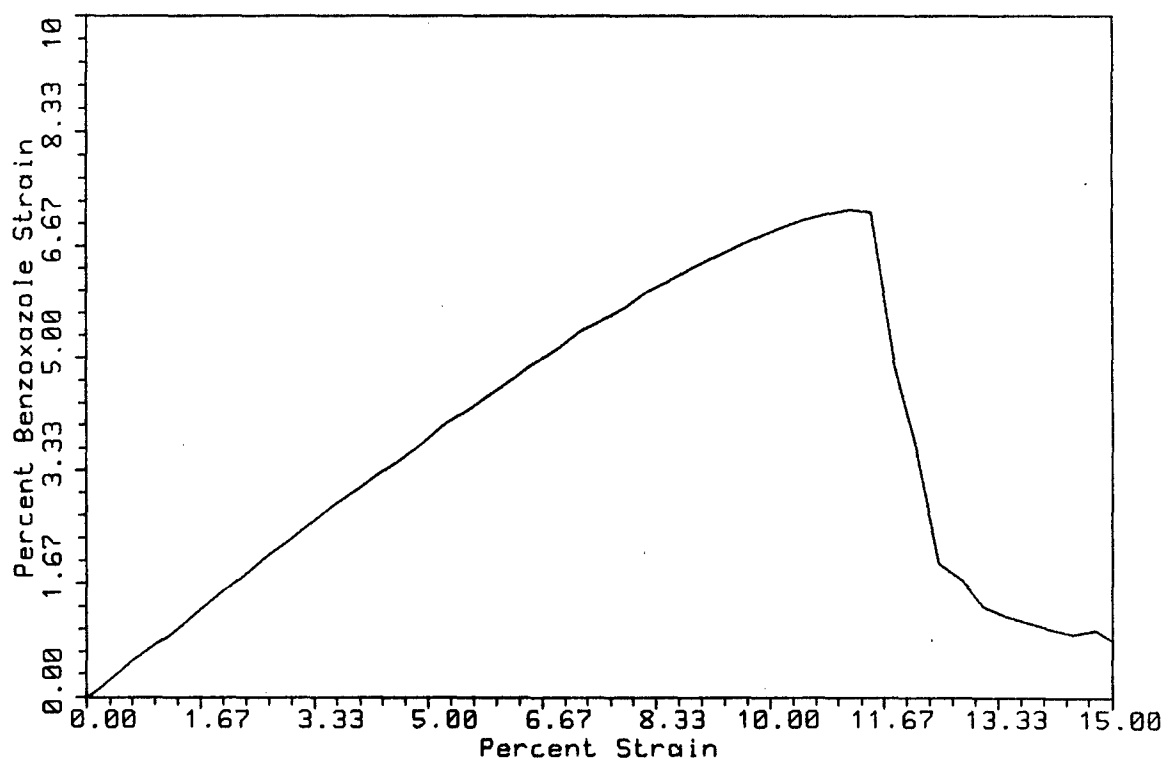


Figure 47. Benzoxazole Length vs Cis-PBO Tension

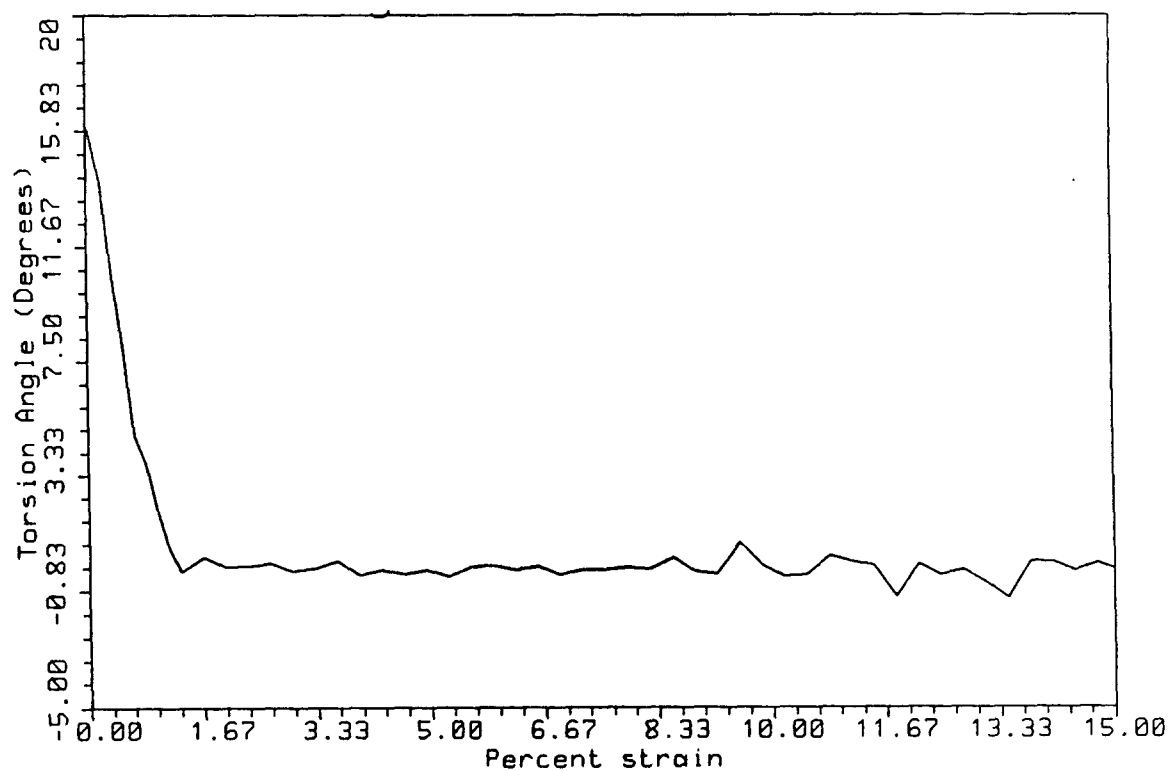


Figure 48. Torsion Angle vs Cis-PBO Tension

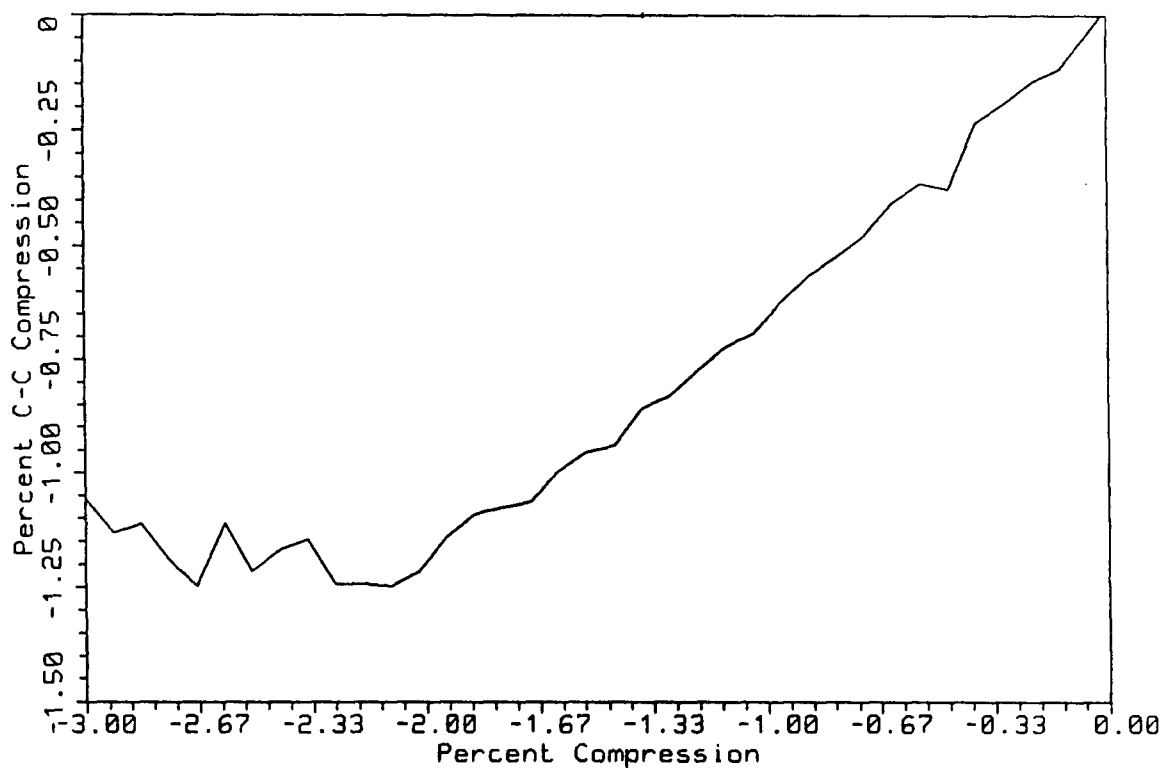


Figure 49. C-C Length vs Cis-PBO Compression

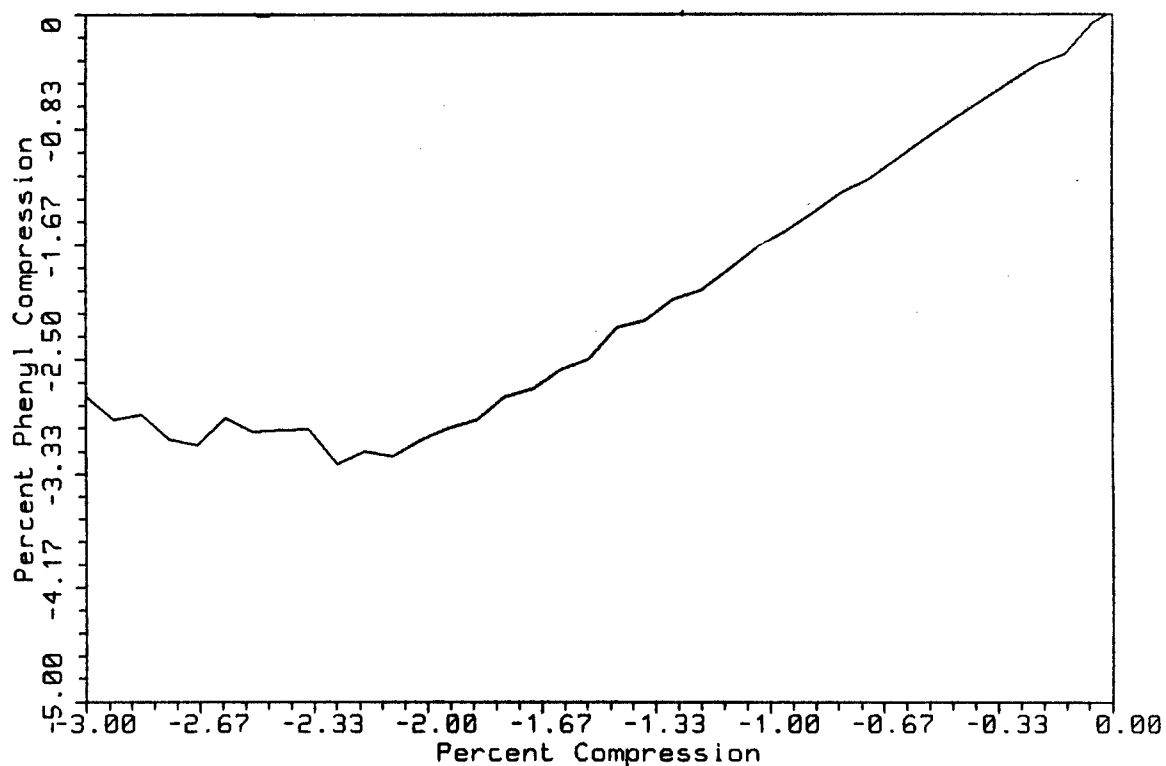


Figure 50. Phenyl Length vs Cis-PBO Compression

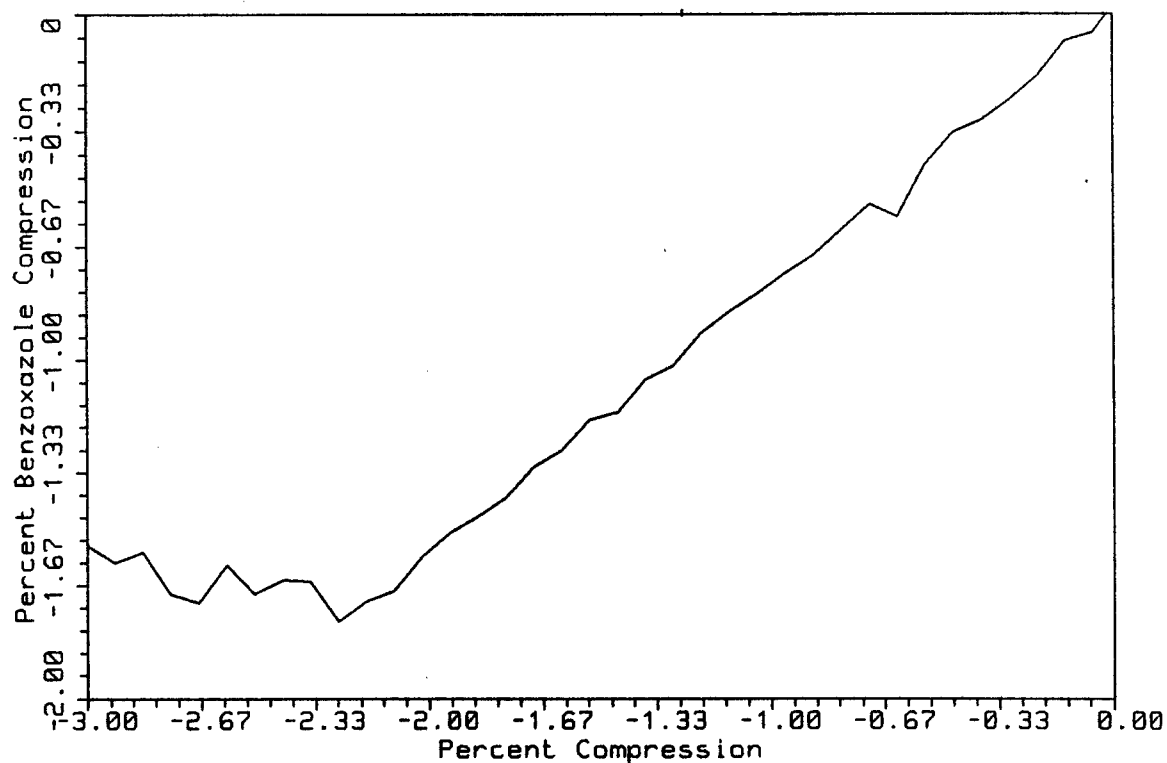


Figure 51. Benzoxazole Length vs Cis-PBO Compression

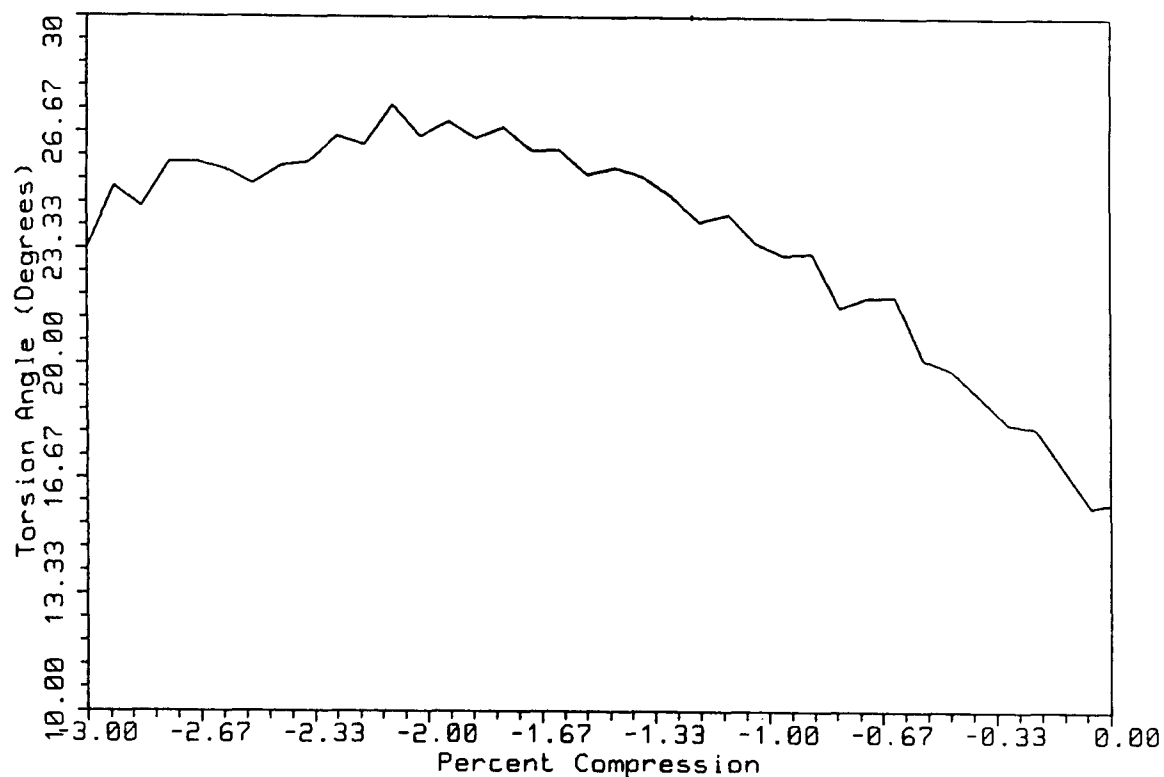


Figure 52. Torsion Angle vs Cis-PBO Compression

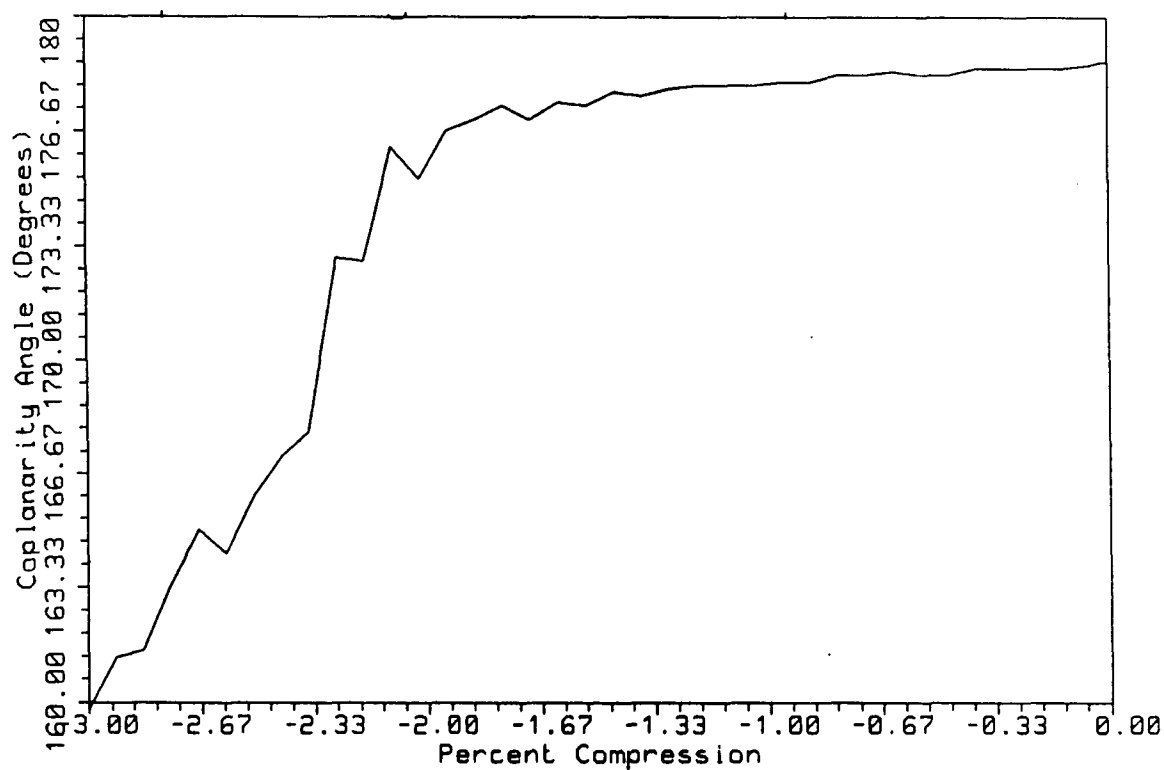


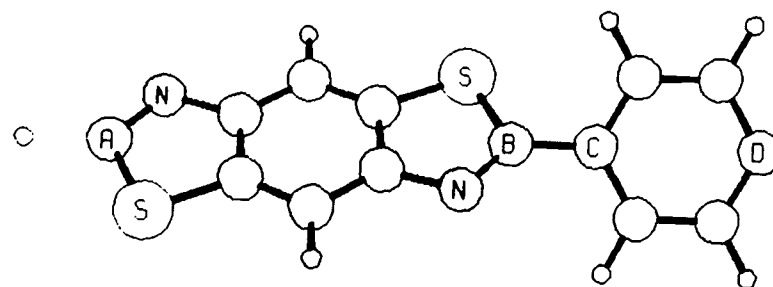
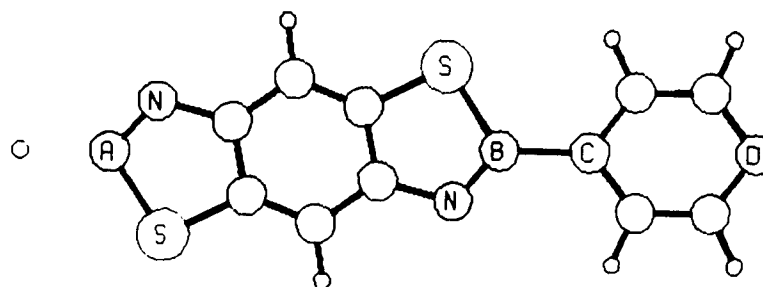
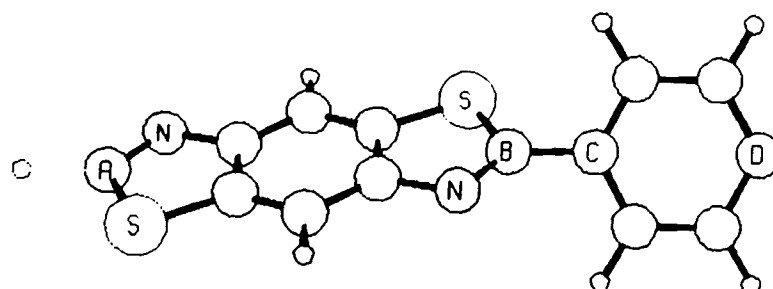
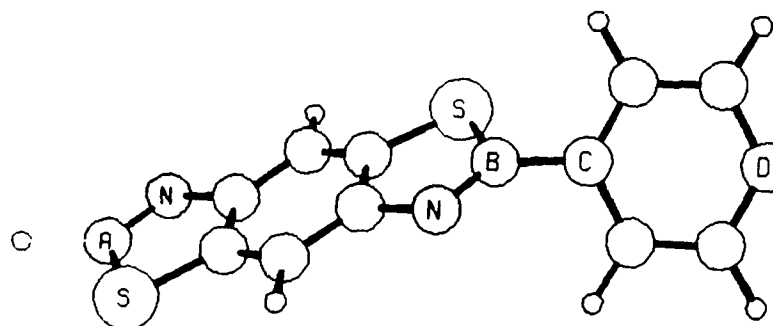
Figure 53. Colinearity Angle vs Cis-PBO Compression

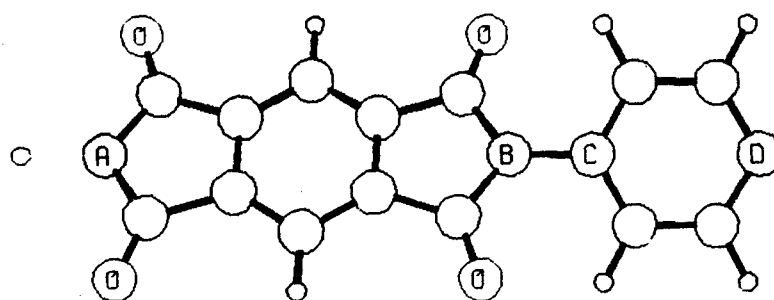


In compression, the C-C bond shrinks by 1.25%, the phenyl ring by 3.21%, and the benzoxazole by 1.68% before the polymer bends and they begin to lengthen again. The torsion angle starts at 16° and climbs to 27.5° before dropping at compressive failure. The repeat unit begins to bend, signifying compressive failure, at 2.10% compressive strain. It takes 4.69 kcal/mole of energy to bring cis-PBO to compressive failure.

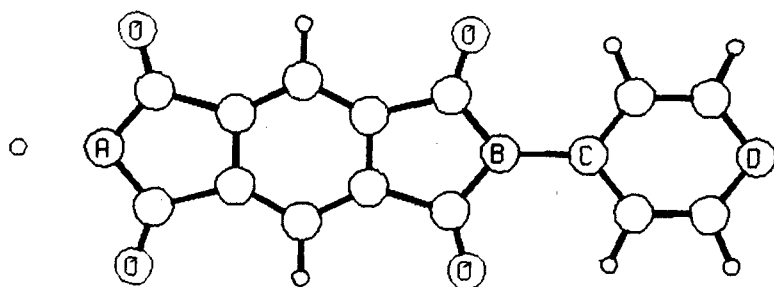
Remaining Polymers (Trans-PBT, PPPI, PPP, PQ, Polyacene)

Figures 54-58 show trans-PBT, PPPI, PQ, PPP, and polyacene respectively at important points in their energy curves. Since the remaining rods behave similarly to cis-PBI and cis-PBO and polyacene does not break or bend in the tension or compression ranges studied, there is no need to duplicate their deformation plots or energy curves here (these plots are available on request). The pertinent results for these polymers are collated, along with cis-PBI and cis-PBO into Tables 3 and 4. Table 3 shows the tension results while Table 4 deals with the compression results. It should be noted that since neither PPP nor polyacene failed in the tension or compression ranges studied, the values in Tables 3 and 4 reflect those at 15% tension and 3% compression respectively. Note also that PQ, with its

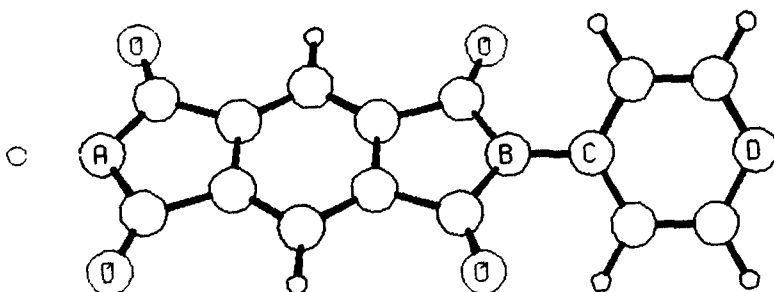
**Equilibrium****Just Before Tensile Failure (12.33% Strain)****Just Before Compressive Failure (1.74% Strain)****Compressive Failure (3% Strain)****Figure 54. Trans-PBT Four Points Along Energy-Strain Curve**



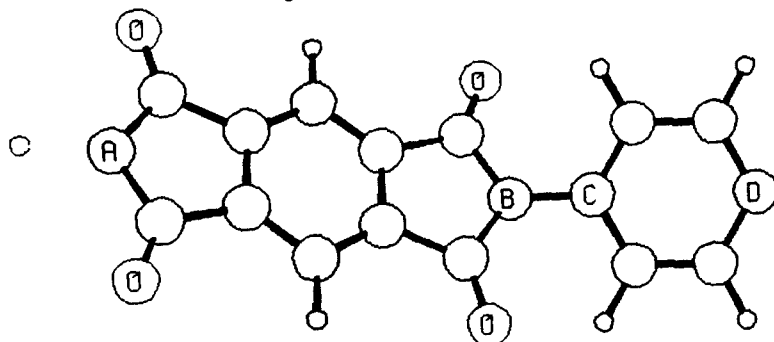
Equilibrium



Just Before Tensile Failure (13.32% Strain)

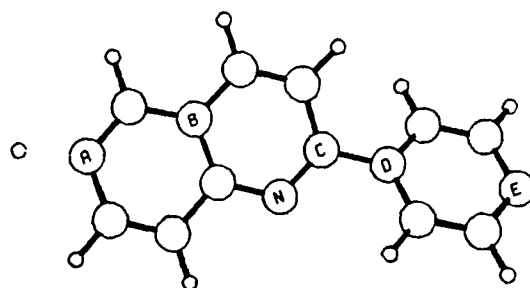


Just Before Compressive Failure (1.97% Strain)

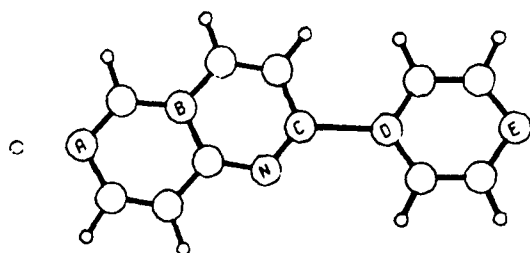


Compressive Failure (3.0% Strain)

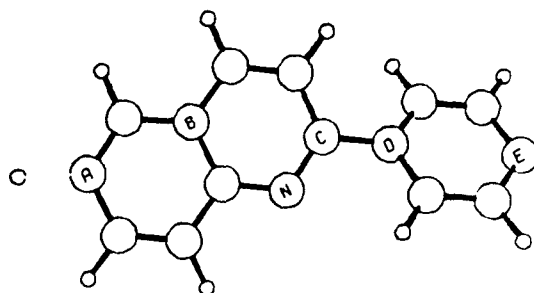
Figure 55. PPPI Four Points Along Energy-Strain Curve



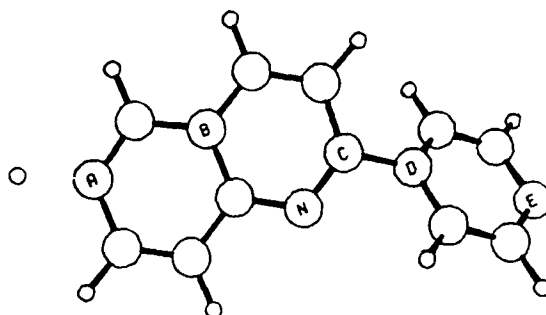
**Equilibrium**



**Just Before Tensile Failure (13.06% Strain)**

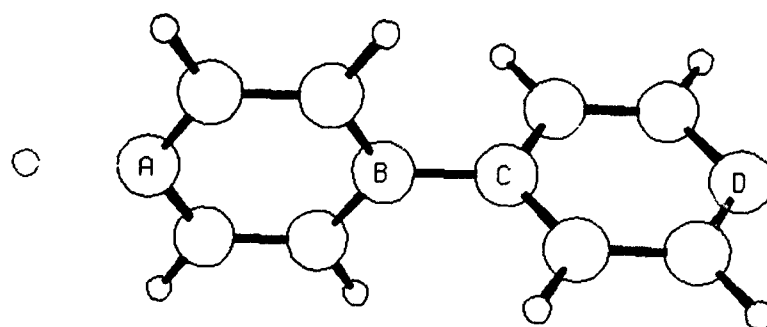


**Just Before Compressive Failure (0.85% Strain)**

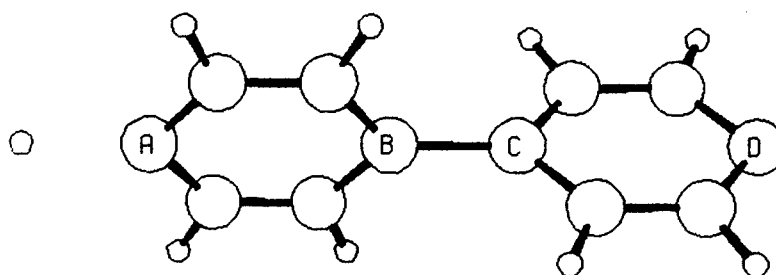


**Compressive Failure (3.0% Strain)**

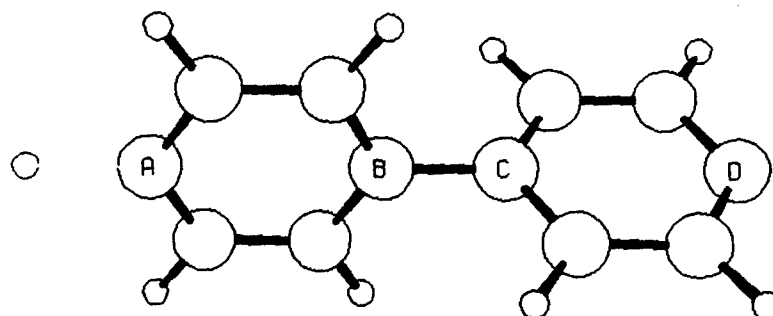
**Figure 56. PQ Four Points Along Energy-Strain Curve**



Equilibrium

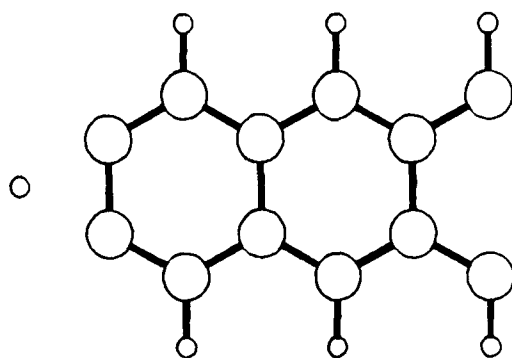


15% Tensile Strain

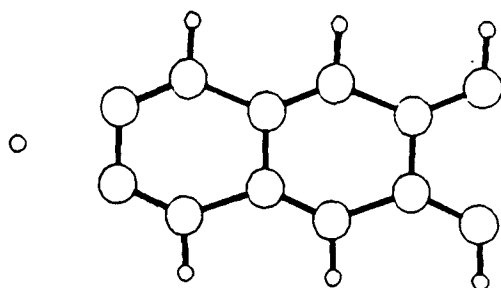


3% Compressive Strain

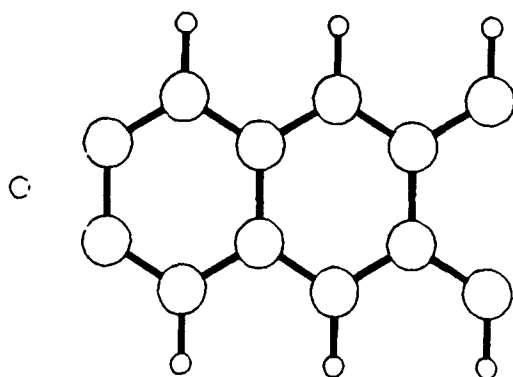
Figure 57. PPP Three Points Along Energy-Strain Curve



Equilibrium



15% Tensile Strain



3% Compressive Strain

Figure 58. Polyacene Three Points Along Energy-Strain Curve

crankshaft structure had to be defined differently than the other rigid rods (Figure 56). The heterocycle length is AC, the C-C length is CD, the phenyl length is DE, and the colinearity angle is BCE.

In Table 3, Strain is the percent strain where tensile failure occurs,  $E_T$  is the energy input to bring the polymer to tensile failure, C-C is the percent change in C-C bond length up to tensile failure, Phenyl is the percent change in the phenyl length up to tensile failure, Hetero is the percent change in the heterocycle length up to tensile failure, and Torsion shows the change in torsion angle up to tensile failure (zero degrees denotes planarity).

	Strain (%)	$E_T$ (kcal/mol)	C-C (%)	Phenyl (%)	Hetero (%)	Torsion (°)
Cis-PBI	11.20	136.79	20.20	13.77	6.58	35-0
Cis-PBO	11.49	140.22	20.42	13.64	7.21	16-0
Trans-PBT	12.27	151.28	18.75	13.65	9.20	42-0
PPPI	13.32	193.53	17.92	14.56	11.20	28-0
PQ	13.06	136.09	20.59	13.12	9.38	33-0
PPP*	-	121.73	16.47	14.18	-	90-90
Polyacene+	-	336.45	-	-	-	-

\*did not fail up to 15% strain

+did not fail up to 20% strain

Table 3. Tensile Results

In Table 4, Strain is the percent compressive strain where compressive failure occurs,  $E_C$  is the amount of energy input to bring the polymer to compressive failure, C-C is the percent shrinkage of the C-C bond length up to

compressive failure, Phenyl is the percent change in the phenyl length up to compressive failure, Hetero is the percent shortening of the heterocyclic length up to compressive failure, and Torsion shows the change in torsion angle up to compressive failure (zero degrees denotes planarity).

	Strain (%)	E <sub>c</sub> (kcal/mol)	C-C (%)	Phenyl (%)	Hetero (%)	Torsion (°)
Cis-PBI	1.93	4.62	1.38	3.44	1.46	35-45
Cis-PBO	2.10	4.68	1.25	3.21	1.68	16-28
Trans-PBT	1.93	4.03	1.24	3.01	1.61	42-56
PPPI	1.97	5.04	1.18	3.18	1.77	28-35
PQ	0.85	0.38	0.25	1.35	0.78	33-35
PPP*	-	5.84	1.40	3.91	-	90-90
Polyacene*	-	10.88	-	-	-	-

\*did not fail up to 3% compressive strain

Table 4. Compressive Results

#### Examination of Results

In tension, all the rigid rod polymers behave in the same manner. From the start of tension up to tensile failure, the C-C bond, phenyl, and heterocycle all stretch in concert with the phenyl ring deforming more, by percentage, than the heterocycle, twice as much in some cases. The C-C bond stretches by nearly 20% in most cases, a stiffer heterocycle causing it to be strained more (cis-PBI, cis-PBO) while a less stiff heterocyclic moiety



takes more of the tension itself, leaving the C-C bond less strained (trans-PBT, PPPI). The torsion angle between the groups goes to zero in tension, meaning the polymers become planar with tension. Energy rises with tension until a threshold is reached,  $E_r$ , where the C-C bond breaks and the phenyl and heterocyclic group shrink in recoil.

From Table 3, it is clear that the phenyl group is less stiff than the heterocycle in all cases. Since the phenyl group stretches nearly the same amount in all the rods, the differences in modulus can be attributed to the different stiffnesses of the heterocyclic moieties. The energy,  $E_r$ , represents the amount of tensile energy needed to break the polymer. This energy should be proportional to the ultimate tensile strength for the polymer; the higher  $E_r$ , the higher the tensile strength. By this token, the tensile strength order (highest to lowest) would be PPPI, trans-PBT, cis-PBO, cis-PBI, and PQ. This is nearly opposite of the modulus order.

PPP and polyacene did not undergo tensile failure in the tension range studied (15% for PPP, 20% for polyacene). PPP lacks a heterocycle and therefore more of the tension is absorbed by the less stiff phenyl rings relieving some of the strain from the C-C bond. C-C strain is only 16.47% in PPP at 15% unit strain, lower than all the other polymers at their tensile failures. Although PPP's strain at failure, or

elongation to break, is higher than the other polymers, its modulus is much lower than the other rods so its  $E_T$ , and corresponding tensile strength, will probably be lower than the other rods. PPP is also the only rod that doesn't become planar with tension.

Polyacene showed no tensile failure up to 20% strain. 336.45 kcal/mole of tensile energy was put in to strain it that far, this is more than double the energy required to break most of the rigid rods. This suggests that polyacene will have an enormous ultimate tensile strength (further tests of polyacene are underway to determine this). This result, along with the fact that polyacene has a modulus 200 GPa higher than BBL, suggests that ladder polymers with all vertically oriented phenyl moieties have a higher potential than the rigid rods as high modulus-high tensile strength polymers.

In compression, all the rigid rods act in a similar way, except PQ. Initially the C-C bond, phenyl group, and the heterocycle compress with the phenyl group deforming nearly twice as much, on a percentage basis, as the heterocycle. The torsion angle increases, twisting the two groups farther out of planarity. When enough compressive energy has been input, the molecule begins to bend and the measured lengths begin to increase and the torsion angle begins to decrease. This is termed the point of compressive

failure. PQ begins to bend almost immediately upon compression, only 0.85% strain starts the bend. Its lengths never increase and its torsion angle never decreases. This must have something to do with its "crankshaft" structure.

It is obvious from Table 4 that the phenyl group is easier to compress than the heterocyclic moiety in all cases. The energy put in to make the polymer bend,  $E_c$ , should be proportional to the compressive force required to bring about this failure (it is not yet clear whether or not molecular bending is the compressive failure mode in bulk materials). Assuming this to be true, the compressive strength order of the rigid rods, highest to lowest, is PPP, PPPI, cis-PBO, cis-PBI, trans-PBT, and PQ (cis-PBO fibers do exhibit higher compressive strength than trans-PBT fibers [110]).

PPP does not exhibit "kinking" up to 3% compressive strain. This is probably due to the fact that it is the only rod studied with hydrogens at all position ortho- to the C-C link. This causes the phenyl rings to stay perpendicular to each other throughout the compression (and the 15% tension for that matter) due to van der Waals repulsions. Both the C-C bond and the phenyl length compress linearly with unit compression up to 3%. Further work will be done to find the compressive failure point for PPP but at 3% compression its  $E_c$  is higher than all the

other rigid rods at compressive failure. Thus a high compressive strength is predicted.

Polyacene also shows no compressive failure up to 3% compression. It has an  $E_c$ , at 3%, that is more than twice as high as any of the rigid rods at compressive failure. A compressive strength much larger than the rigid rods is predicted. Both the compressive and tensile results on polyacene suggest that ladder polymers with all vertically oriented phenyls should be examined as possible high-performance organic materials.

### Conclusions

The AM1 semiempirical MO method can be used successfully to calculate the theoretical ultimate modulus of polymers. AM1 gives improvements over previous MNDO moduli due to the improvements in approach from MNDO to AM1. The calculated values are significantly higher than experimental or x-ray moduli. This is to be expected since the calculations model the perfectly aligned system which is not yet possible via present processing techniques. The calculated moduli will serve as standards against which future experiments will be compared.

Through analysis of molecular deformations in tension and compression of rigid rod polymers, some insights have

been gained into tensile and compressive processes at the molecular level. First, horizontally oriented phenyl rings are easier to deform than heterocyclic moieties in rigid rods, which means eliminating them should increase modulus. Second, in compression, rigid rods tend to bend or 'kink' at the C-C linkage at a certain percent strain, around 2%. Third a critical energy value can be assigned to a compressive or tensile failure which should be proportional to the force required to cause the failure. This allows a relative ordering of polymers by theoretical tensile and/or compressive strength. Finally, the hypothetical ladder polymer, polyacene, shows higher tensile and compressive properties than the rigid rods. This suggests that further study of ladder-type polymers as high-performance materials is warranted.

This study has taken no account of the intermolecular forces between different polymer chains which occur in real materials. These forces are obviously important in the determination of bulk properties, especially compressive properties. The work simply documents the tensile and compressive potential inherent in the polymer molecules by themselves. Other forces may serve to improve or decrease the properties in real materials.

## SECTION V

### FUTURE DIRECTIONS

#### Solid State Calculations

Aside from the other work noted in the text, there are a few important topics that will have to be considered if the modeling of organic polymers is to become useful as a scientific tool.

Although this study provides fresh insights into polymer tensile and compressive properties, it is still only a model of a single polymer chain with no others around it. Since polymers are used and tested in their solid state, this model is limited in what properties it can predict accurately. The model gives definitive information of the compressive and tensile potential of a certain polymer chain, but does not take into account the intermolecular interactions that are important in determining bulk properties, especially compressive properties. The AM1 formalism can be used to make approximations to the intermolecular interactions of two or possibly three polymer chains. However, remember that this work took nearly 600 Cray supercomputer hours and adding more chains would take much longer and would not be practical. Another approach is needed to calculate the polymer solid-state.

Work is presently being done on a solid state semiempirical MO method, using the AM1 and MNDO Hamiltonians. It is called MOSOL [111] and promises to provide solid state data and direct calculation of densities, Poisson Ratios, and mechanical properties. At present it is still impractical to use but improvements are constantly being made.

#### Solution Phase Studies

Since many polymers are processed out of solutions, a solution modeling capability is also necessary. Solution modeling is even more difficult than a solid model because there is little periodicity in the liquid phase and there is more than one component in the system. Work is being done on modeling solutions, but this is mostly on small molecules [112] or ions [113]. The effective modeling of polymer solutions with computational chemistry techniques is still in the future.

## REFERENCES

1. A. Quetelet, Instructions Populaires sur le Calcul des Probabilités, Tarlier, Brussels, 1828.
2. E Schrödinger, Ann. Phys., 79, 361 (1926).
3. E. Merzbacher, Quantum Mechanics, Wiley, New York (1961).
4. A. Streitwieser, Molecular Orbital Theory for Organic Chemists, Wiley, New York (1961).
5. L.J. Schaad, B.A. Hess, J. Am. Chem. Soc., 94, 3068 (1972).
6. D.H. Andrews, Phys. Rev., 36, 544 (1930).
7. T.L. Hill, J. Chem. Phys., 14, 465 (1946).
8. I. Dostrovsky, E.D. Hughes, C.K. Ingold, J. Chem. Soc., 173 (1946).
9. P. de la Mare, L. Fowden, E.D. Hughes, C.K. Ingold, J. Mackie, J. Chem. Soc., 3200 (1955).
10. R.G. Parr, Quantum Theory of Molecular Electronic Structure, Benjamin, New York (1963).
11. S.G. Wierschke, J. Chandrasekhar, W.L. Jorgensen, J. AM. Chem. Soc., 107, 1496 (1985).
12. W.L. Jorgensen, J.F. Blake, J.D. Madura, S.G. Wierschke, Supercomputer Research in Chemistry and Chemical Engineering, ACS Symposium Series #353, 1987.
13. D. Storch, L. Strausser, U.S. Air Force Academy, unpublished results (1987).
14. H.A. Scheraga, F.R. Maxfield, Biochemistry, 15, 5138, (1976).
15. A.J. Hopfinger, Conformational Properties of Macromolecules, Academic, New York, (1975).



16. G.M. Schwenzer, J. Org. Chem., 43, 1079, (1978).
17. R. Hoffman, J. Am. Chem. Soc., 108, 3078, (1986).
18. F.W. Billmeyer, Textbook of Polymer Science, 3rd, Wiley, New York (1984) p. 16.
19. W.J. Welsh, D. Bhaumik, H.H. Jaffe, J.E. Mark, Polym. Eng. Sci., 24, 218 (1984).
20. W.J. Welsh, D. Bhaumik, J.E. Mark, Macromolecules, 14, 947 (1981).
21. W.J. Welsh, J.E. Mark, Polym. Eng. Sci., 23, 140 (1983).
22. W.J. Welsh, J.E. Mark, J. Mat. Sci., 18, 1119, (1983).
23. D. Bhaumik, W.J. Welsh, H.H. Jaffe, J.E. Mark, Macromolecules, 14, 951 (1981).
24. W.J. Welsh, D. Bhaumik, J.E. Mark, J. Polym. Sci., 20, 59 (1981).
25. W.J. Welsh, H.H. Jaffe, M. Kondo, J.E. Mark, Makromol. Chem., 183, 801 (1982).
26. W.J. Welsh, J.E. Mark, Polym. Bull., 8, 21 (1982).
27. D. Bhaumik, H.H. Jaffe, J.E. Mark, Macromolecules, 14, 1125 (1981).
28. D. Bhaumik, J.E. Mark, J. Polym. Sci., Phys. Ed., 21, 1111 (1983).
29. D. Bhaumik, J.E. Mark, J. Polym. Sci., Phys. Ed., 21, 1130 (1983).
30. J.J.P. Stewart, New Polym. Materials, 1, 53 (1987).
31. H.E. Klei, J.J.P. Stewart, Int. J. Quant. Chem., Quant. Chem. Symp., 20, 529 (1986).
32. W.W. Adams, R.K. Eby, Mat. Res. Soc. Bull., 5 (Nov 1987).
33. S.J. DeTeresa, AFWAL-TR-85-401 (March 1985).

34. S. Kumar, W.W. Adams, T.E. Helminiak, J. Reinforced Plact. and Composites, in press (1987).
35. W.W Adams, T.E. Helminiak, Science of Ceramic Chemical Processing, Wiley, New York (1986) p. 444.
36. S. Kumar, W.W. Adams (to be published).
37. P.A.M. Dirac, Proc. Roy. Soc. (London), 123, 714 (1929).
38. T. Clark, A Handbook of Computational Chemistry, Wiley, New York, (1985).
39. S. Lifson, A.J. Warshel, J. Chem. Phys., 49, 5116 (1968).
40. D.H. Faber, C. Altona, Comput. Chem, 1, 203 (1977).
41. N.L. Allinger, MMP2(85), QCPE Program #MMP2(85).
42. U. Burkert, N.L. Allinger, Molecular Mechanics, ACS Monograph #177 (1982).
43. [38], Introduction.
44. W.J. Hehre, L. Radom, P.v.R. Schleyer, J.A. Pople, Ab Initio Molecular Orbital Theory, Wiley, New York, (1986).
45. M. Born, J.R. Oppenheimer, Ann. Physik, 84, 457 (1927).
46. J.P. Lowe, Quantum Chemistry, Academic, Orlando (1978).
47. J.N. Murrel, S.F. Kettle, J.M. Tedder, The Chemical Bond, Wiley, New York (1981).
48. J.C. Slater, Phys. Rev., 36, 57 (1930).
49. R.S. Mulliken, J. Chim. Phys., 46, 497 (1949).
50. [46], Appendix 4.
51. [46], Appendix 11.
52. [46], Appendix, 7.
53. S.M. Blinder, Am. J. Phys., 33, 431 (1965).

54. R.S. Mulliken, J. Chem. Phys., 23, 1833, 1841, 2338, 2343, (1955).
55. C.C.J. Roothan, Rev. Mod. Phys., 23, 69 (1951).
56. J.A. Pople, R.K. Nesbet, J. Chem. Phys., 22, 571 (1954).
57. J.A. Pople, R. Seeger, R. Krishnan, Int. J. Quant. Chem., 11, 149 (1977).
58. C. Møller, M.S. Plesset, Phys. Rev., 46, 618 (1934).
59. W.J. Hehre, R.F. Stewart, J.A. Pople, J. Chem. Phys., 51, 2657 (1969).
60. J.C. Slater, Phys. Rev., 35, 210 (1930).
61. S.F. Boys, Proc. Roy. Soc (London), A200, 542 (1950).
62. [44], p. 19.
63. Computed at Air Force Materials Laboratory.
64. Gaussian 86, Carnegie-Mellon Quantum Chemistry Publishing Unit, Pittsburgh (1984).
65. E. Hückel, Z. Physik, 70, 204 (1931).
66. R. Hoffman, J. Chem. Phys., 39, 1397 (1963).
67. R. Hoffman, J. Am. Chem. Soc., 108, 1876 (1986)
68. R.G. Parr, R. Pariser, J. Chem. Phys., 21, 466, 767 (1953).
69. M. Ratner, unpublished results.
70. J.A. Pople, D.P. Santry, G.A. Segal, J. Chem. Phys., 43, 5129 (1965).
71. J.A. Pople, D.L. Beveridge, Approximate Molecular Orbital Theory, McGraw Hill, New York (1970).
72. [71], Appendix.
73. M.J.S. Dewar, Science, 187, 1037 (1975).

74. R.C. Bingham, M.J.S. Dewar, D.H. Lo, J. Am. Chem. Soc., 97, 1285 (1975).
75. p. 39, MOPAC Manual (4th Ed.) A General Molecular Orbital Package, (1987).
76. [38], p. 144.
77. [73], p. 1043 (LSD molecule).
78. [38], p. 141.
79. [73], p. 1040.
80. [71] NDDO approximation.
81. M.J.S. Dewar, W. Thiel, J. Am. Chem. Soc., 99, 4899 (1977).
82. [75], p. 38.
83. M.J.S. Dewar, E.G. Zoebisch, E.F. Healy, J.J.P. Stewart, J. Am. Chem. Soc., 107, 3902 (1985).
84. S.G. Wierschke, AFWAL-TR-87-4034 (July 1987)
85. M.J.S. Dewar, AMPAC, QCPE Program #506.
86. J.J.P. Stewart, MOPAC, QCPE Program #455.
87. [18], p. 6.
88. W.W Adams, T.E. Helminiak, "Ordered Polymers and Molecular Composites," (1984).
89. R.F. Kovar, F.E. Arnold, J. Poly. Sci., Poly. Chem. Ed., 14, 2807 (1976).
90. T.E. Helminiak, F.E. Arnold, C.L. Benner, Polymer Preprints, ACS Poly. Div., 16(2), 659 (1975).
91. J.F. Wolfe, F.E. Arnold, Macromolecules, 14, 909 (1981).
92. E.W. Choe, S.N. Kim, Macromolecules, 14, 920 (1981).
93. J.F. Wolfe, B.H. Loo, F.E. Arnold, Polymer Preprints, ACS Poly. Div., 19(2), 1 (1978).

94. J.F. Wolfe, B.H. Loo, F.E. Arnold, Macromolecules, 14, 915 (1981).
95. A.V. Fratini, E.M. Cross, J.F. O'Brien, W.W. Adams, J. Macromol. Sci.-Phys, B24, 159 (1985).
96. C.E. Sroog, A.L. Endrey, S.V. Abramo, C.E. Berr, W.M. Edwards, K.L. Oliver, J. Polym. Sci., A3, 1374 (1965).
97. J.K. Stille, Macromolecules, 14, 870 (1981).
98. P. Pradere, A. Boudet, J. Mat. Sci., 22, 4240 (1987).
99. M.R. Unroe, B.A. Reinhardt, Polymer Preprints, ACS Poly. Div., 28(1), 183 (1987).
100. F.E. Arnold, R.L. Van Deusen, J. Appl. Polym. Sci., 15, 2035 (1971).
101. W.W. Adams, private communication (1986-1988).
102. D. Storch, DRAW, QCPE Program #493.
103. P.G. Perkins, J.J.P. Stewart, J. Chem. Soc. Faraday Trans II, 76, 520 (1980).
104. A. Compte, Philosophie Positive, (1830).
105. W.W. Adams, S. Kumar, A.V. Fratini, private communication, (1988).
106. W.W. Adams, S. Kumar, P. Arsinovic, private communication, (1988).
107. 235-255 by x-ray diffraction, 239 by inelastic neutron scattering, 358, 290 by Raman Spectroscopy, 257-340 by IR, see [31].
108. S.G. Wierschke, AFWAL-TR-88-0, in press.
109. W.W. Adams, S. Kumar, private communication (1988).
110. W.W. Adams, S. Kumar, private communication (1988) and [32].
111. J.J.P. Stewart, MOSOL, QCPE Program #495.
112. W.L. Jorgensen, J. Gao, C. Ravimohan, J. Phys. Chem., 89, 3470 (1985).

113. J. Chandrasekhar, W.L. Jorgensen, J. Chem. Phys., 77, 5080 (1982).